
Electronic Thesis and Dissertation Repository

6-20-2013 12:00 AM

Multiple approaches for assessing mangrove biophysical and biochemical variables using in situ and remote sensing techniques

Francisco Javier Flores de Santiago
The University of Western Ontario

Supervisor

Jinfei Wang

The University of Western Ontario Joint Supervisor

John M. Kovacs

The University of Western Ontario

Graduate Program in Geography

A thesis submitted in partial fulfillment of the requirements for the degree in Doctor of Philosophy

© Francisco Javier Flores de Santiago 2013

Follow this and additional works at: <https://ir.lib.uwo.ca/etd>



Part of the [Biodiversity Commons](#), [Botany Commons](#), [Environmental Monitoring Commons](#), [Forest Biology Commons](#), and the [Marine Biology Commons](#)

Recommended Citation

Flores de Santiago, Francisco Javier, "Multiple approaches for assessing mangrove biophysical and biochemical variables using in situ and remote sensing techniques" (2013). *Electronic Thesis and Dissertation Repository*. 1345.

<https://ir.lib.uwo.ca/etd/1345>

This Dissertation/Thesis is brought to you for free and open access by Scholarship@Western. It has been accepted for inclusion in Electronic Thesis and Dissertation Repository by an authorized administrator of Scholarship@Western. For more information, please contact wlsadmin@uwo.ca.

**MULTIPLE APPROACHES FOR ASSESSING MANGROVE BIOPHYSICAL AND
BIOCHEMICAL VARIABLES USING IN SITU AND REMOTE SENSING
TECHNIQUES**

(Thesis format: Integrated Article)

by

Francisco Javier Flores de Santiago

Graduate Program in Geography

A thesis submitted in partial fulfillment
of the requirements for the degree of
Doctor of Philosophy

The School of Graduate and Postdoctoral Studies
The University of Western Ontario
London, Ontario, Canada

© Francisco Javier Flores de Santiago 2013

Abstract

Mangrove forests are important ecosystems and play a key role in maintaining the equilibrium in coastal lagoons and estuaries. However, in recent years, there has been a considerable loss of mangrove extension due to anthropogenic activities. Recent studies suggest that multiple *in situ* and remote sensing approaches must be carried out to understand the dynamics in these complex ecosystems. Therefore, the objective for this PhD dissertation is to develop multiple techniques for monitoring the seasonal biophysical and biochemical conditions of the mangrove forests. Particular objectives will include: *i.* Test the feasibility of using a Chlorophyll Content Index from a CCM-200 unit as an estimator of the variation of leaf pigments (chlorophyll-a, chlorophyll-b) content for a range of mangrove species. *ii.* Assess changes in chlorophyll-a, leaf area, leaf length, and Leaf Area Index between the dry and rainy seasons in a variety of mangrove classes. *iii.* Assess the seasonal importance of *in situ* hyperspectral measurements (e.g. 450-1000 nm) for chlorophyll-a determination in a variety of mangrove species. And finally, *iv.* Determine whether an object-based image analysis approach can provide an accurate classification of mangroves from spaceborne Synthetic Aperture Radar data. The results from these studies could provide reliable information regarding seasonal ecological assessments of mangrove forests using *in situ* and remote sensing methods.

Keywords: mangrove, pigments, hyperspectral, SAR, Mexico.

Co-Authorship Statement

The following thesis is presented in manuscript format. All chapters have been published. Francisco Flores de Santiago was the principal and corresponding author for the manuscripts. J.M. Kovacs was the second author providing constant guidance, financial assistance through the Natural Sciences and Engineering Council of Canada, and significant editing on manuscripts. F.F. Verdugo was the third author for chapters 2, 3, and 4 providing fieldwork assistance, methodological supervision, and financial support thorough Universidad Nacional Autónoma de México. P. Lafrance was the third author for chapter 5 providing fieldwork funding and logistics assistance.

Acknowledgments

This thesis would not have been possible without the support of many people and organizations. Special thanks to my joint supervisors Jinfei Wang at the University of Western Ontario and John M. Kovacs at Nipissing University for financial support through their Natural Sciences and Engineering Research Council of Canada (NSERC) discovery grants, help with the field work, comments regarding manuscript editing and constant guidance throughout my degree.

I would like to thank Dr. Francisco Flores Verdugo for his financial and logistical support during the fieldwork campaigns, as well as for the information regarding mangrove ecology.

I thank Consejo Nacional de Ciencia y Tecnología from Mexico (CONACYT) for the full grant provided during my four years of PhD studies.

I would like to thank my thesis examiners Dr. Jacek Malczewski, Dr. Adam Yates, Dr. Norman P.A. Hüner, and Dr. Yuhong He.

I am also grateful for the students in the GITA laboratory, Department of Geography, The University of Western Ontario, Chuiqing, Xinyang, Qin, Wenfeng, Xue, Ting, and Peng.

I would like to acknowledge Professor Marco Van De Wiel for many useful comments regarding methodological aspects of this dissertation. I also would like to acknowledge UWO staff Lori Johnson for the significant advice during my PhD application process. I also appreciated the friendship of John Osborne, Idowu Ajibade, Nathaniel Bergman, Mohammadreza Jelokhani, Vincent Kuuire, Yannick Rousseau, Autumn Gambles, Salvador Escobedo, Rafael Alarcon, Cristina Salome, Cynthia Nava, and Patricio Valadez.

I extremely appreciate the support from my wife Monserrat Santiago during my PhD studies and for the great time we spent together in Canada.

Table of Contents

Abstract.....	ii
Co-Authorship Statement.....	iii
Table of Contents.....	v
List of Tables.....	viii
List of Figures.....	xi
List of Appendices.....	xv
Chapter 1.....	1
1 Mangroves.....	1
1.1 Mangrove species classification.....	2
1.2 Physiognomic classification and mangrove zonation.....	5
1.3 Mangrove worldwide distribution.....	6
1.4 Mangrove pigments.....	8
1.5 Mangrove hyperspectral data assessment.....	11
1.6 Remote Sensing of mangrove areas.....	13
1.7 Objectives.....	15
1.8 Study areas.....	16
1.9 Structure of thesis.....	18
1.10References.....	19
Chapter 2.....	22
2 Seasonal changes in leaf chlorophyll a content and morphology in a sub-tropical mangrove of the Mexican Pacific.....	22
2.1 Introduction.....	22
2.2 Materials and Procedures.....	24
2.3 Results.....	29
2.4 Discussion and conclusions.....	35

2.5	References.....	39
Chapter 3.....		42
3	Assessing the utility of a portable pocket instrument for estimating seasonal mangrove leaf chlorophyll content.....	42
3.1	Introduction.....	42
3.2	Materials and Methods.....	44
3.3	Results.....	46
3.4	Discussion.....	54
3.5	References.....	57
Chapter 4.....		60
4	The influence of seasonality in estimating mangrove leaf chlorophyll a content from hyperspectral data.....	60
4.1	Introduction.....	60
4.2	Materials and Methods.....	62
4.3	Results.....	70
4.4	Discussion.....	74
4.5	References.....	79
Chapter 5.....		84
5	An object-oriented classification method for mapping mangroves in Guinea, West Africa, using multipolarized ALOS PALSAR L-band data.	84
5.1	Introduction.....	84
5.2	Methods.....	86
5.3	Results and discussion	95
5.4	Conclusions.....	111
5.5	References.....	111
Chapter 6.....		115
6	Discussion and Conclusions.....	115

6.1 Summary and general discussion.....	115
6.2 Conclusion	118
6.3 Future directions	119
6.4 References.....	120
Appendices.....	121
Curriculum Vitae	127

List of Tables

Table 2.1: *Laguncularia racemosa*, *Rhizophora mangle*, and *Avicennia germinans* Mann-Whitney U-test median values for chlorophyll a (Chla), leaf area, and leaf length between seasons (n=30). LR: *L. racemosa*, RM: *R. mangle*, AG: *A. germinans*. *Significant U values P=0.05 29

Table 2.2: *Laguncularia racemosa*, *Rhizophora mangle*, and *Avicennia germinans*. Mann-Whitney U-test for the leaf area index (LAI) between seasons (n = 15). *Significant U values P=0.05 30

Table 2.3: *Laguncularia racemosa*, *Rhizophora mangle*, and *Avicennia germinans*. Mann-Whitney U-test for chlorophyll-a (Chla), leaf area, and leaf length between the upper and lower canopy in both seasons (n=30). LR: *L. racemosa*, RM: *R. mangle*, AG: *A. germinans* *Significant U P=0.05..... 35

Table 3.1: Analysis of covariance F-test (ANCOVA) of Chlorophyll-a (Chla) and CCM-200 readings between the regression lines from the dry and rainy season. LR: *L. racemosa*, RM: *R. mangle*, AG: *A. germinans*. * Significant F-observed values at p=0.05 47

Table 3.2: Analysis of covariance F-test (ANCOVA) of Chlorophyll Content Index (CCI) and corresponding Chlorophyll-a (Chla) between the regression lines from the poor/dwarf and healthy conditions. LR: *L. racemosa*, RM: *R. mangle*, AG: *A. germinans*. * Significant F-observed values at p=0.05 48

Table 3.3: Analysis of covariance F-test (ANCOVA) of Chlorophyll-b (Chlb) and CCM-200 readings between the regression lines from the dry and rainy season. LR: *L. racemosa*, RM: *R. mangle*, AG: *A. germinans*. * Significant F-observed values at p=0.05 52

Table 3.4: Analysis of covariance F-test (ANCOVA) of Chlorophyll Content Index (CCI) and corresponding Chlorophyll-b (Chlb) between the regression lines from the poor/dwarf and healthy conditions. LR: *L. racemosa*, RM: *R. mangle*, AG: *A. germinans*. * Significant F-observed values at p=0.05 52

Table 3.5: Analysis of covariance F-test (ANCOVA) of total chlorophyll (TChl) and CCM-200 readings between the regression lines from the dry and rainy season. LR: <i>L. racemosa</i> , RM: <i>R. mangle</i> , AG: <i>A. germinans</i> . * Significant F-observed values at p=0.05	53
Table 3.6: Analysis of covariance F-test (ANCOVA) of Chlorophyll Content Index (CCI) and corresponding total chlorophyll (TChl) between the regression lines from the poor/dwarf and healthy conditions. LR: <i>L. racemosa</i> , RM: <i>R. mangle</i> , AG: <i>A. germinans</i> . * Significant F-observed values at p=0.05	53
Table 4.1: Vegetation indices selected for this study	64
Table 4.2: Pearson correlation matrix of Chla and VI versus significant components and its eigenanalysis during the dry season.....	68
Table 4.3: Pearson correlation matrix of Chla and VI versus significant components and its eigenanalysis during the rainy season.....	69
4.4: Regression analysis of leaf Chla content and hyperspectral VI.....	71
Table 5.1: SAR data collected from the ALOS-PALSAR space-borne sensor	88
Table 5.2: Single (HH), and dual (HH+HV) polarization modes accuracy assessment at level 1 (saltpan, mangrove, water), using a combination of shape/color and compactness/smoothness multiresolution segmentation approach.....	96
Table 5.3: The error matrix for the single pol (HH) data at level-1 using a multiresolution segmentation scale of 40.....	97
Table 5.4 The error matrix for the dual pol (HH + HV) data at level-1 using a multiresolution segmentation scale of 20.....	101
Table 5.5: The error matrix for the single pol (HH) data at level-2 using a multiresolution segmentation scale of 10 within the mangrove area	102
Table 5.6: The error matrix for the dual pol (HH+HV) data at level-2 using a multiresolution segmentation scale of 5 within the mangrove area	104

Table 5.7: The error matrix for the dual pol (HH+HV) data at level-1 using a Lee 3x3 filter with a multiresolution segmentation scale of 20..... 106

Table 5.8: The error matrix for the dual pol (HH+HV) data at level-2 using a Lee 3x3 filter with a multiresolution segmentation scale of 5..... 106

List of Figures

Figure 1.1: Mangrove zones loss examples due to expansion of urban areas in Conakry, Guinea (a), transformation through aquaculture in southern Thailand (b), hydrological obstructions such as “tapos” in Agua Brava, Mexico (c), and soil hypersalinity in Teacapan, Mexico (d). Source: GoogleEarth images (a, b)	2
Figure 1.2: White mangrove <i>Laguncularia</i> sp (a, b), red mangrove <i>Rhizophora</i> sp (c, d), and black mangrove <i>Avicennia</i> sp (e, f).....	3
Figure 1.3: Black mangrove pneumatophores and salt glands within the leaves (a, b respectively). White mangrove salt glands (c) and root systems allowing growing after physical damage (d). Red mangrove aerial roots (e) and a viviparous seed (f).....	4
Figure 1.4: Typical mangrove zonation in a costal lagoon. Red mangrove (<i>Rhizophora</i> sp), white mangrove (<i>Laguncularia</i> sp), and black mangrove (<i>Avicennia</i> sp). (Source: photo taken by Francisco Flores Verdugo, 2009).....	6
Figure 1.5: Fringe white mangrove class (a), fringe red mangrove (c), and fringe black mangrove (e). White mangrove basin class (b), red basin mangrove (d), and black basin mangrove (f).....	7
Figure 1.6: Typical tropical mangrove zonation.....	9
Figure 1.7: Typical sub-tropical mangrove zonation.....	9
Figure 1.8: Optical CCM-200 (a), optical assessment samples of mangrove leaves (b), ASD FieldSpec HandHeld device with plantprobe (c)	11
Figure 1.9: Typical hyperspectral vegetation reflectance curve (450-1000 nm).....	12
Figure 1.10: Examples of IKONOS visible (a), false color IKONOS 4, 3, 2 (b), ALOS L-band HH (c), and ALOS L-band HH+HV (d) over mangrove areas in Guinea, West Africa using data from the fifth chapter of this thesis.....	15

Figure 1.11: Sub-tropical mangrove system within the Urias channel, Mexico (a), and tropical mangrove system within the Yelitono and Mabala Islands, Guinea (b).....	17
Figure 2.1: Data collection sites at the south end of the Urias mangrove system	26
Figure 2.2: <i>Laguncularia racemosa</i> , <i>Rhizophora mangle</i> , and <i>Avicennia germinans</i> . Upper and lower canopy leaf chlorophyll-a (Chla) content by season. Each box plot depicts the mean (small square), the minimum and maximum sample, the lower quartile (25%), the median (50%), the upper quartile (75%), and the lowest and highest sample with 1.5 interquartile ranges of the lower and upper quartile (*). Also, mean is shown at the top of each box plot.....	31
Figure 2.3: <i>Laguncularia racemosa</i> , <i>Rhizophora mangle</i> , and <i>Avicennia germinans</i> . Upper and lower canopy leaf area (cm ²) by season. Each box plot depicts the mean (small square), the minimum and maximum sample, the lower quartile (25%), the median (50%), the upper quartile (75%), and the lowest and highest sample with 1.5 interquartile ranges of the lower and upper quartile (*). Also, mean is shown at the top of each box plot.....	32
Figure 2.4: <i>Laguncularia racemosa</i> , <i>Rhizophora mangle</i> , and <i>Avicennia germinans</i> . Upper and lower canopy leaf length (cm) by season. Each box plot depicts the mean (small square), the minimum and maximum sample, the lower quartile (25%), the median (50%), the upper quartile (75%), and the lowest and highest sample with 1.5 interquartile ranges of the lower and upper quartile (*). Also, mean is shown at the top of each box plot.....	33
Figure 2.5: <i>Laguncularia racemosa</i> , <i>Rhizophora mangle</i> , and <i>Avicennia germinans</i> . Upper and lower Leaf Area Index (LAI) by season. Each box plot depicts the mean (small square), the minimum and maximum sample, the lower quartile (25%), the median (50%), the upper quartile (75%), and the lowest and highest sample with 1.5 interquartile ranges of the lower and upper quartile (*). Also, mean is shown at the top of each box plot.....	34
Figure 3.1: Seasonal scatter plots and fitted linear regression lines of Chlorophyll Content Index (CCI) using a CCM-200 instrument against the chlorophyll-a (Chla) derived from chemical analysis (n=30). Each graph depicts the linear equation with 95% confidence	49

Figure 3.2: Seasonal scatter plots and fitted linear regression lines of Chlorophyll Content Index (CCI) using a CCM-200 instrument against the chlorophyll-b (Chlb) derived from chemical analysis (n=30). Each graph depicts the linear equation with 95% confidence	50
Figure 3.3: Seasonal scatter plots and fitted linear regression lines of Chlorophyll Content Index (CCI) using a CCM-200 instrument against the total chlorophyll (TChl) derived from chemical analysis (n=30). Each graph depicts the linear equation with 95% confidence	51
Figure 4.1: Predicted Chla content during the dry season (May), based on the regression equations from Table 4.4. T-observed values (T), standard error of estimate (SE). Data plotted along a 1:1 line.....	72
Figure 4.2: Predicted Chla content during the rainy season (October), based on teh regression equations from Table 4.4. T-observed value (T), standard error of estimate (SE). Data plotted along a 1:1 line.....	73
Figure 5.1: Location of the mangrove islands of Guinea, Western Africa	87
Figure 5.2:Characterized representation of the land cover classes examined for the classification: (a) Saltpan, (b) Tall Red Mangrove, (c) Dwarf Red Mangrove, (d) Black Mangrove).....	89
Figure 5.3: Flowchart for the HH L=band ALOS PALSAR data.....	92
Figure 5.4: Flowchart for the HH+HV L-band ALOS PALSAR data	93
Figure 5.5: Multiresolution segmentation objects. HH L-band ALOS PALSAR data (a). Objects for: (b) shape=0.9, compactness=0.5; (c) shape=0.5, compactness=0.5; (d) shape=0.1, compactness=0.5; (e) shape=0.1, compactness=0.1; (f) shape=0.1, compactness=0.9	98
Figure 5.6: Multiresolution segmentation objects. HH+HV L-band ALOS PALSAR data (a). Objects for: (b) shape=0.9, compactness=0.5; (c) shape=0.5, compactness=0.5; (d) shape=0.1, compactness=0.5; (e) shape=0.1, compactness=0.1; (f) shape=0.1, compactness=0.9	99

Figure 5.7: Accuracy assessment for the HH and HH+HV L-band using different scales at level 1	100
Figure 5.8: Accuracy assessment for the HH and HH+HV L-band using different scales at level 2.....	103
Figure 5.9: Accuracy assessment using different SAR filters from the optimal HH and HH+HV multiresolution scale at levels 1-2. a = HH level 1; b = HH+HV level 1; c = HH level 2; d = HH+HV level 2.....	105
Figure 5.10: Object-based classification of L-band ALOS PALSAR. HH level 1 segmentation scale of 40 (a); HH level 2 segmentation scale of 10 (b); HH+HV level 1 segmentation scale of 20 using a 3x3 Lee filter (c); HH+HV level 2 segmentation scale of 5 using a 3x3 Lee filter. Black rectangles represent locations for figure 5.11	109
Figure 5.11: Examples of mangrove species mapping using a HH+HV ALOS PALSAR data object-based classification with a 3x3 Lee filter. From left to right: enhanced false color IKONOS composite (NIR, R, G); original ALOS HH+HV data; Object-oriented classification; Field photograph.....	110

List of Appendices

Appendix A: List of abbreviations.....	121
Appendix B: Permission letter from Marine Ecology Progress Series.....	122
Appendix C: Permission letter from Bulletin of Marine Sciences	123
Appendix D: Permission letter from Wetlands, Ecology and Management.....	124
Appendix E: Permission letter from International Journal of Remote Sensing.....	126

Chapter 1

1 Mangroves

Mangroves are wetland plants represented by a variety of tree species that grow along protected intertidal coastlines where deposition and transport of sediment are common. The principal adaptations of mangroves, which make these plants unique among tree species, consist of a well-developed tolerance to both salt water and low oxygen levels in sediments (Saenger, 2002). These adaptations make mangrove trees capable of survival and growth along tropical and sub-tropical coasts where environmental conditions limit the distribution of other terrestrial plants.

Mangrove forests are considered among the most important coastal habitats maintaining an ecological balance between the terrestrial and oceanic fluxes (Blasco et al. 1996), as well as providing local economic support for coastal communities (Walters et al. 2008). Important characteristics of mangroves include high forest productivity (Raven et al. 1992), organic carbon dynamics (Komiyama et al. 2008), nutrient cycling (Feller et al. 1999), coastal protection (Saenger 2002), , macro-faunal interactions (Cannicci et al. 2008), litter fall decomposition (Kristensen et al. 2008), and providing habitat for a variety of terrestrial and marine fauna (Nagelkerken et al. 2008) including endangered and migratory bird species (Lacerda 2002).

Despite its ecological importance, there has been a considerable loss of mangrove areas in recent years due to urbanization (Polidoro et al. 2010) (Fig. 1.1 a), transformations through aquaculture ponds (Seto and Fragkias 2007) (Fig. 1.1 b), hydrological obstructions (Kamali and Hashim 2011) (Fig. 1.1c), soil hypersalinity (Fig. 1.1 d), deforestation (Walters et al. 2008), and climate change (Gilman et al. 2008).

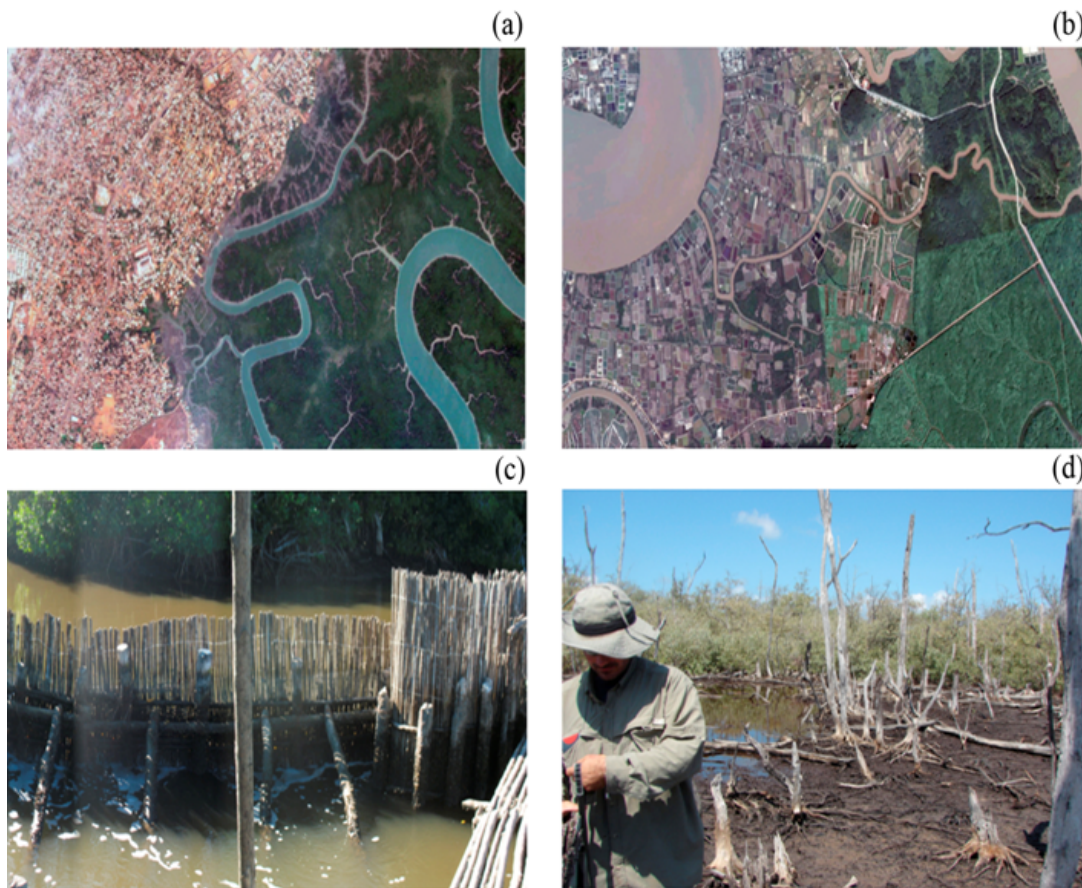


Figure 1.1: Mangrove zones loss examples due to expansion of urban areas in Conakry, Guinea (a), transformation through aquaculture in southern Thailand (b), hydrological obstructions such as “tapos” in Agua Brava, Mexico (c), and soil hypersalinity in Teacapan, Mexico (d). Source: GoogleEarth images (a, b)

1.1 Mangrove species classification

Mangroves describe an ecological group of 36 species of halophytic trees belonging to eight different families distributed worldwide (Tomlinson 1986). However, the most common species belong to just three families including the Combretaceae (white mangrove *Laguncularia* sp) (Fig. 1.2 a), the Rhizophoraceae (red mangrove *Rhizophora* sp) (Fig. 1.2 c), and the Avicenniaceae (black mangrove *Avicennia* sp) (Fig. 1.2 e) (Spalding et al. 2010). It is important to note that the common names for these three

families are recognized worldwide and are represented by the color of the trunk or the color beneath the tree bark (Fig. 1.2 b, 1.2 d, 1.2 f).

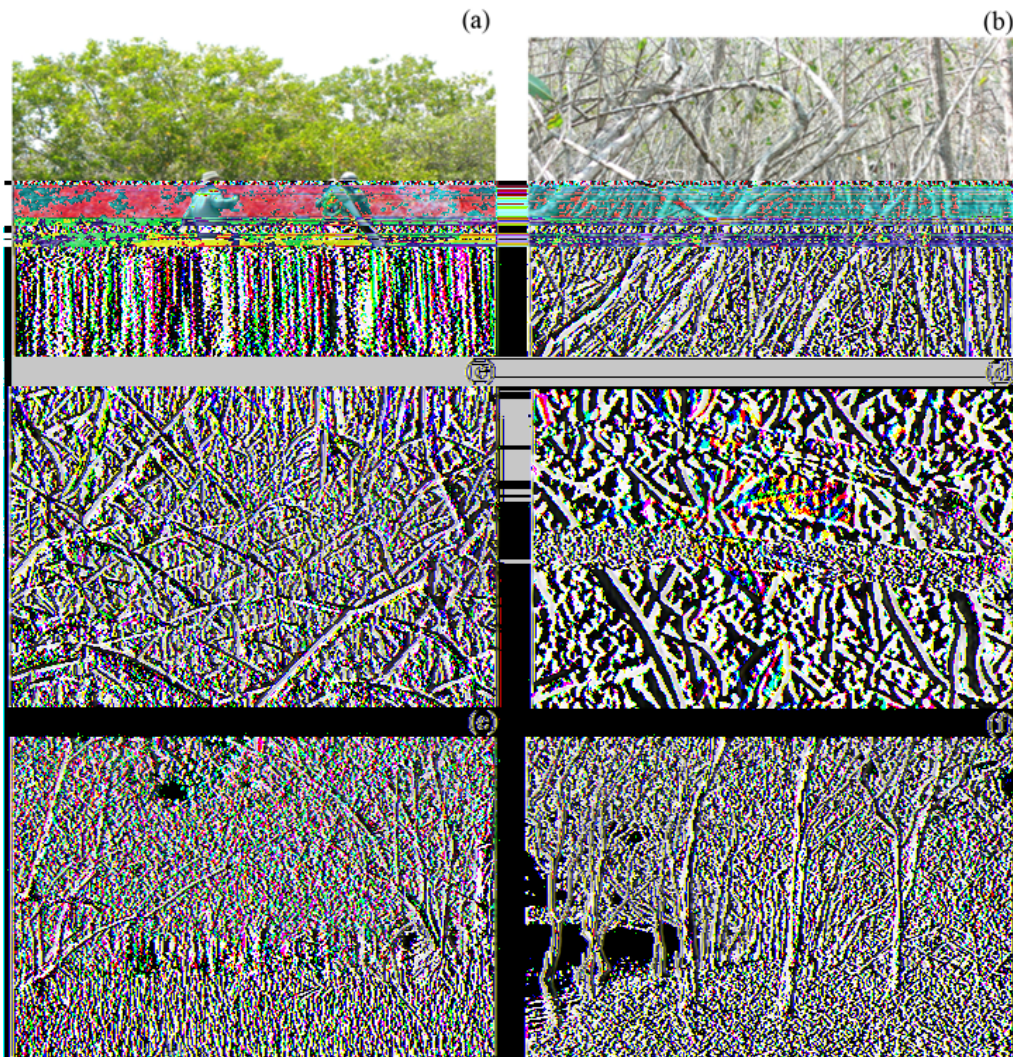


Figure 1.2: White mangrove *Laguncularia* sp (a, b), red mangrove *Rhizophora* sp (c, d), and black mangrove *Avicennia* sp (e, f)

Each mangrove family has developed several morphological adaptations for tropical and sub-tropical environments in order to grow where soil salinity and evaporation rates are high. The black mangroves possess pneumatophores in the base of the tree, which allow the acquisition of oxygen by the roots in anoxic soil (Fig. 1.3 a). Moreover, black mangrove leaves contain several secretion glands, which helps in the expulsion of salt (Fig. 1.3 b). The white mangrove possesses two small glands near the

base of each leaf that exclude salt (Fig. 1.3 c). White mangroves are also known for presenting an advanced vegetative reproduction process, allowing the generation of new plants when the main tree is physically disturbed (Fig. 1.3 d). The red mangroves are easily distinguishable through their unique aerial roots (Fig. 1.3 e), which allow the plant to be suspended over the water. The red mangroves also possess viviparous seeds (Fig. 1.3 f), which are able to float and produce a new plant relatively faster than the germination process of other species of trees.

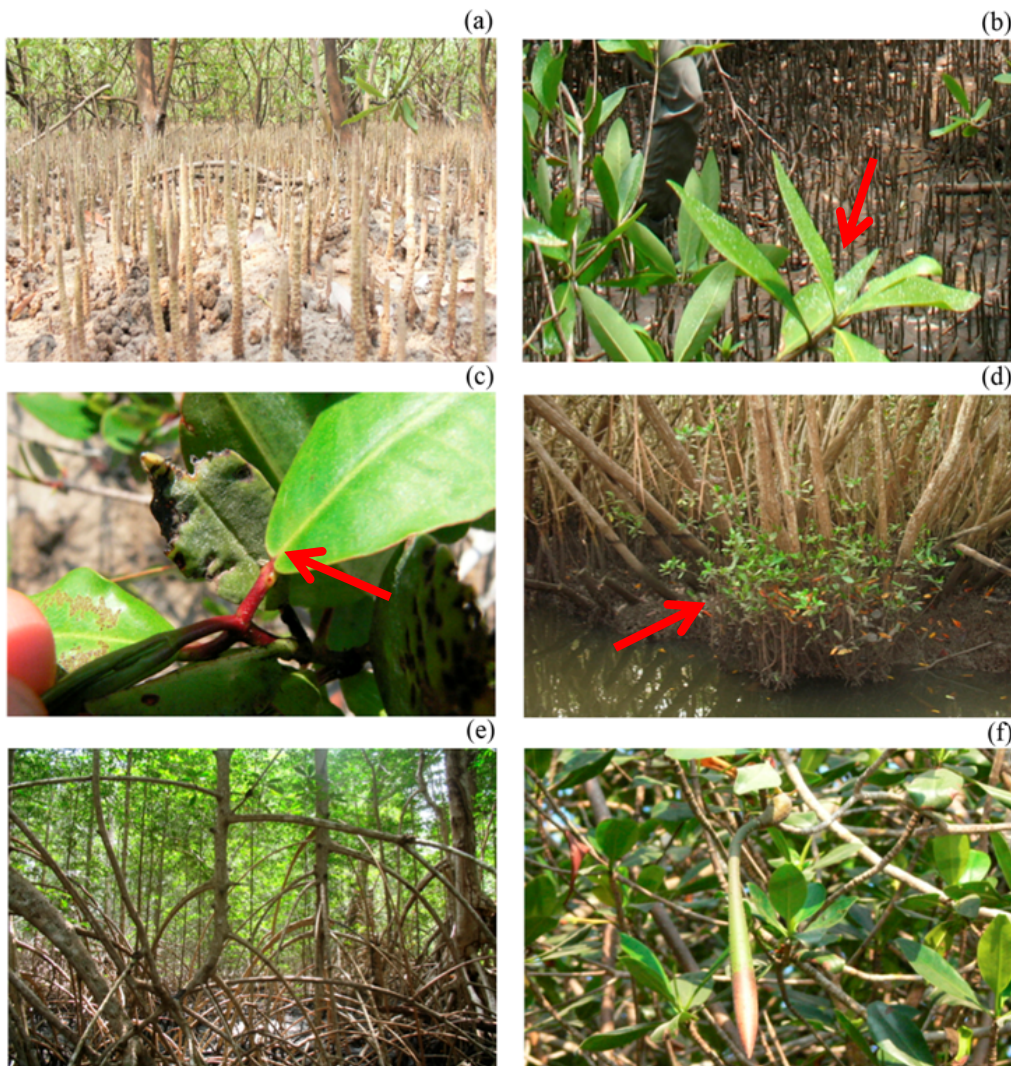


Figure 1.3: Black mangrove pneumatophores and salt glands within the leaves (a, b respectively). White mangrove salt glands (c) and root systems allowing growing after physical damage (d). Red mangrove aerial roots (e) and a viviparous seed (f)

1.2 Physiognomic classification and mangrove zonation

In relatively undisturbed mangrove forest areas where suitable substrate is available, single-species zonation is common parallel to the coastline. The causes of species zonation depend on many aspects. However, the frequency of tidal inundation, soil salinity, and the topographic slope are the three major physical factors controlling mangrove species zonation in tropical and sub-tropical latitudes.

Each mangrove species has a particular salt tolerance range depending on morphological adaptations. For example, some species are quite intolerant to hypersaline conditions (e.g. *Rhizophora* sp and *Laguncularia* sp) whereas others persist through long drought periods and constant levels of high soil salt (*Avicennia* sp). Consequently, red mangrove is usually located along the main channels where tidal mixing is strong, while the black mangrove more inland, where hypersaline conditions are the norm (Fig. 1.4).

It is important to note that when a mangrove species is out of its normal zone, its primary production is low in comparison with that of the species characteristic of the zone (Saenger 2002). As a consequence, environmental stress is a key indicator of the ecological response of each mangrove family. However, in large environments where flat topographic slopes are present (e.g. 1 cm/km); the separation among mangrove species is not evident. Consequently, Lugo and Snedaker (1974) included a physiognomic classification into five major mangrove communities (fringe, riverine, overwash, basin, and dwarf forest) according to total biomass, tree height, and fresh water availability.

Fringe mangrove forests occur on protected shorelines along the main inundation channels where elevation is higher than mean high tide (white mangrove Fig. 1.5 a; red mangrove Fig. 1.5 c; and black mangrove Fig. 1.5 e). Riverine mangrove forest consists of floodplain areas along river and creek drainages. Overwash forest is located on low islands in shallow coastal lagoons where incoming tidal velocities are high enough to wash over the trees. Basin forest is located in inland areas along drainage depressions with minimum tidal influence (white mangrove Fig. 1.5 b; red mangrove Fig. 1.5 d; and black mangrove Fig. 1.5 f). Dwarf mangroves consist of dense trees with no more than 2 m in height.

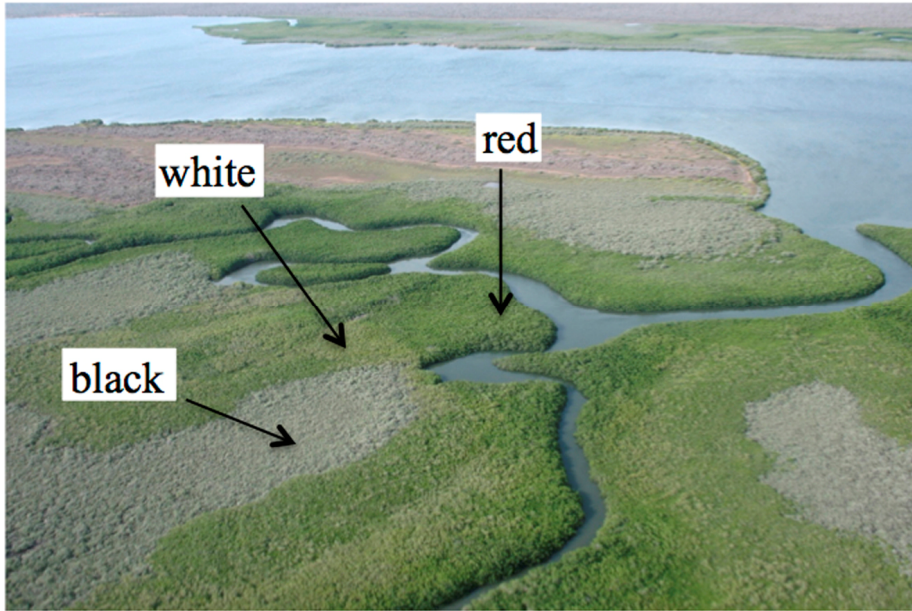


Figure 1.4: Typical mangrove zonation in a costal lagoon. Red mangrove (*Rhizophora* sp), white mangrove (*Laguncularia* sp), and black mangrove (*Avicennia* sp). (Source: photo taken by Francisco Flores Verdugo, 2009)

1.3 Mangrove worldwide distribution

Tropical mangrove forests are best developed around the Equator where annual rainfall is more than 200 cm. Tropical rainfall patterns along with strong tidal mixing generate maximum soil salinity concentration of 15 ‰ within tropical mangrove forests (Spalding et al. 2010 Fig. 1.6). Tropical mangrove physical characteristics include a considerable higher trunk height within the riverine and fringe classes in all three species compared to the basin classes (Fig. 1.6). Freshwater wetlands are located more inland as well as the presence of saltpan areas especially during the short dry season, followed by rainforest vegetation even further inland.



Figure 1.5: Fringe white mangrove class (a), fringe red mangrove (c), and fringe black mangrove (e). White mangrove basin class (b), red basin mangrove (d), and black basin mangrove (f)

Sub-tropical mangrove forests are located at arid areas along the Tropic of Cancer in the northern hemisphere and the Tropic of Capricorn in the southern hemisphere. Annual precipitation rates in sub-tropical coasts are less than 50 cm and environmental conditions present more stressful situations due to an increase in solar radiation and soil salinity in these regions (Fig. 1.7). Mangrove distribution in the sub-tropics is under environmental conditions where freshwater availability is seasonal, affecting the

physiological development of trees through an increase or decrease of ground salinity (Field 1995). As a consequence, there could be a seasonal decrease in mangrove net primary productivity (Saenger 2002) and growth (Raven et al. 1992). The sub-tropical mangrove fringe class is lower in height (3-10 m) compared to the same tropical mangrove species in a fringe community (>25 m). Sub-tropical basin classes are characterized by extensive dense bushes with a height less than 2 m, particularly within the black mangrove species. Moreover, saltpans are located inland where soil salinity is high and only small halophytes can survive.

Worldwide, the highest global diversity of mangroves is in Africa and Asia where the taxon attains their maximum development. However, just three true major species and one mangrove associate species are present in the Pacific and Atlantic coast of the Americas (Spalding et al. 2010). These species are: red mangrove *Rhizophora mangle*, white mangrove *Laguncularia racemosa*, black mangrove *Avicennia germinans*, and the mangrove associate, bottom wood *Conocarpus erectus*. However, there are reports of minor populations of *Rhizophora harrisonii*, *Rhizophora racemosa*, *Avicennia bicolor*, and *Avicennia schaueriana* in the eastern coast of Brazil (Spalding et al. 2010).

1.4 Mangrove pigments

Environmental stressors are common in mangrove forest areas where increased solar radiation and ground salinity concentrations affect the metabolism and growth of the plants. As a consequence, the link between mangrove biophysical responses to environmental stressors has been a major topic for many ecologists in recent decades. In fact, many works in mangrove ecology have concluded that the concentration of pigment content in mangrove leaves can be associated with environmental stressors such as water availability (Lacerda 2002), soil salinity (Steinke et al. 1993), temperature, and sunlight (Saenger 2002).

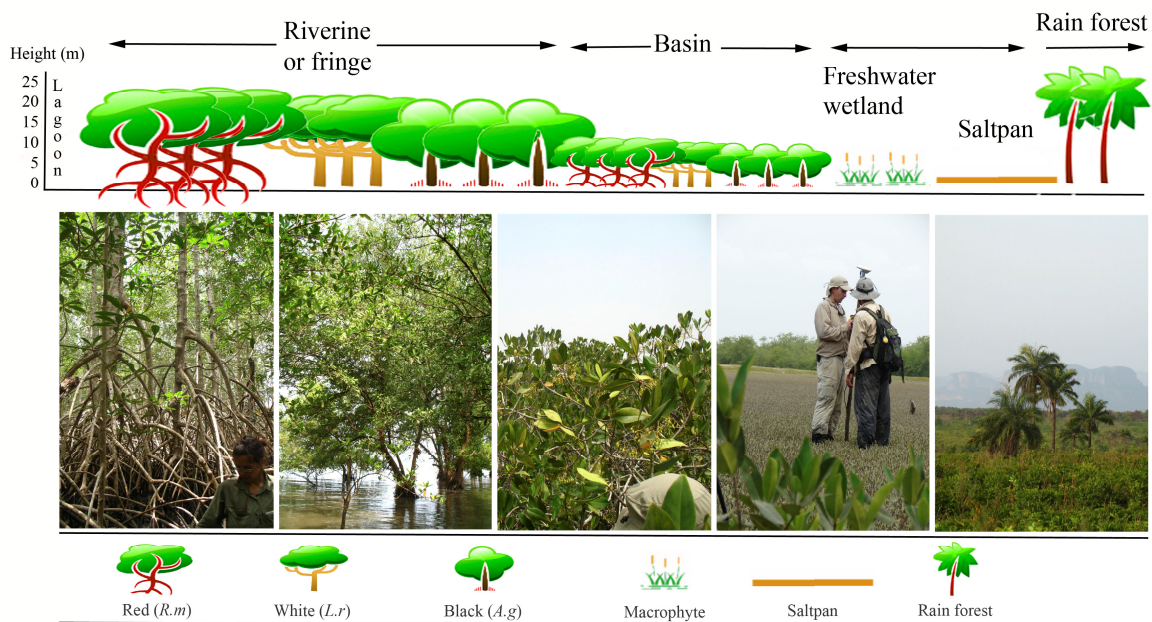


Figure 1.6: Typical tropical mangrove zonation

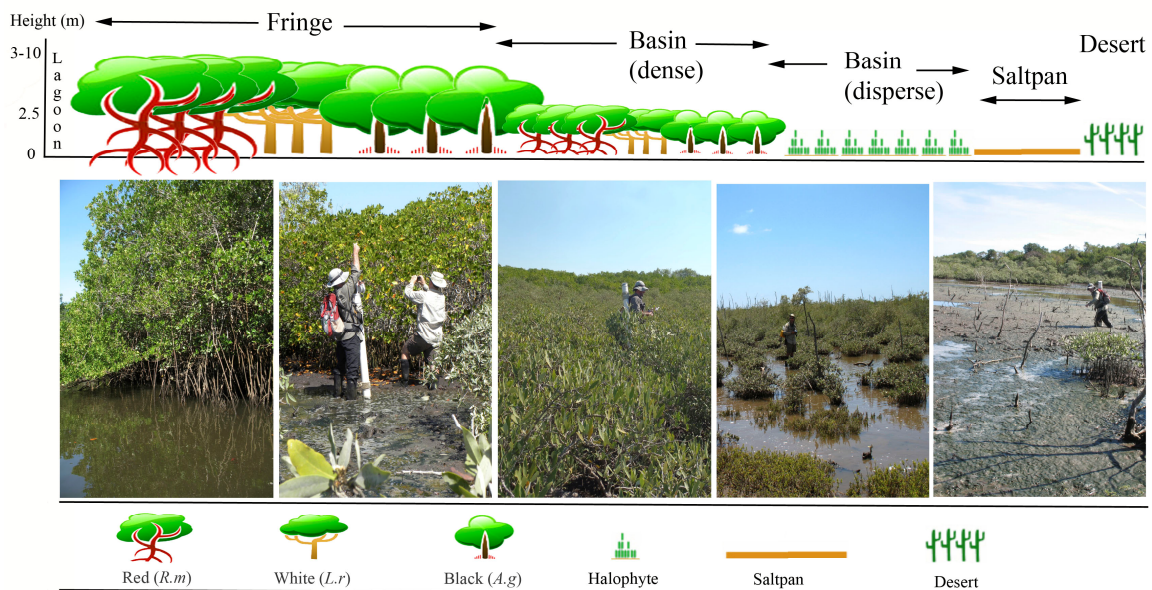


Figure 1.7: Typical sub-tropical mangrove zonation

Chlorophyll-a (Chla) and chlorophyll-b (Chlb) are the two most important pigments used in the photosynthesis process during the conversion of light energy into chemical energy (Blackburn 2007). Chla absorbs most of the energy from wavelengths of blue and red light while Chlb captures light at a slightly different wavelength (Eichhorn et al 2005). Moreover, the total chlorophyll (i.e., Chla+Chlb) extends the absorption spectrum range and can be related to physiological stress since there is an inverse relationship between the concentration of chlorophylls and plant health (Peñuelas and Fillela 1998). As a consequence, mangrove growth and health status can be indicative of pigment level changes (Raven et al. 1992) and can provide reliable information regarding the relationships between plants and their environment.

Traditional leaf pigment content determination uses organic solvents extraction coupled by spectrophotometric absorbance quantification (Wellburn 1994). Such absorbance is transformed to leaf pigment content by using published algorithms (Hendry and Price 1993; Andrew et al. 2002; Richardson et al. 2002). Unfortunately, the traditional method is relatively expensive, time consuming, and most importantly, a destructive process. Consequently, many non-destructive optical alternatives have been developed as new approaches for leaf pigment content estimation using the absorbance of the intact leaf in the field and in the laboratory (Gamon and Surfus 1999). Such optical methods include the Chlorophyll Content Meter (CCM-200) (Fig. 1.8 a) and hyperspectral sensing devices (Fig. 1.8 c) that could assess the potential chlorophyll pigment content from different species of mangrove leaves (Fig. 1.8 b) by using specific wavelengths with maximum sensitivity to leaf pigments (Goncalves et al. 2008).



Figure 1.8: Optical CCM-200 (a), optical assessment samples of mangrove leaves (b), ASD FieldSpec HandHeld device with plantprobe (c)

1.5 Mangrove hyperspectral data assessment

Portable hyperspectral spectrometers (e.g. ASD FieldSpec HandHeld device) essentially allow the application of remote sensing technology at leaf level, by continuously recording reflectance at many closely-spaced wavelengths (every 1 nm) across the visible and near infrared spectrum (e.g. 450-1000). Figure 1.9 depicts a typical vegetation reflectance curve showing a minimum reflectance in the blue and red bands, with relatively higher reflectance in the green band, and maximum reflectance in the

near-infrared region. The abrupt change in slope at the transition between green and near-infrared bands is known as the “red-edge”, and is of key importance for accurate pigment content determination (Horler et al. 1983; Vogelman et al. 1993; Filella and Peñuelas 1994). Hyperspectral remote sensing data at leaf level have indicated that there are specific combinations of wavebands (i.e. Vegetation Indices) from the electromagnetic spectrum that can be used to non-destructively quantify leaf pigments, and consequently, primary productivity models at leaf and canopy level. There are many vegetation indices (VI) in the literature that employ hyperspectral data for the accurate quantification of pigment content, moisture, and stress. Most of the traditional VI use only reflectance data from the red and the near-infrared portions of the electromagnetic spectrum, whereas only a few VI utilize information from the red-edge and the green channels.

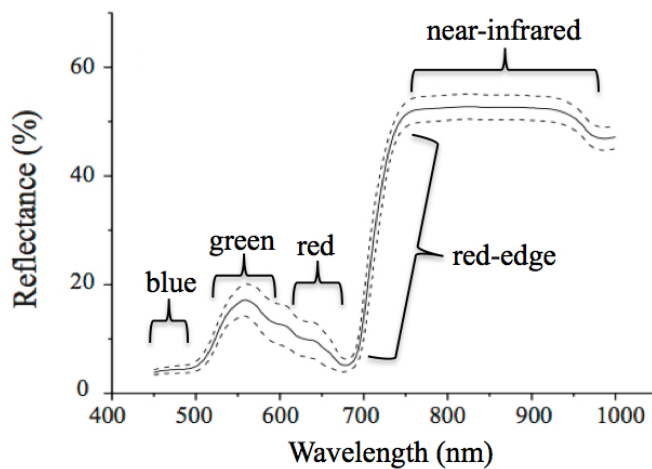


Figure 1.9: Typical hyperspectral vegetation reflectance curve (450-1000 nm)

Currently, hyperspectral data at leaf level is one of the most important tools used for the accurate classification of mangrove species under environmental conditions in terms of tree health and stress. Moreover, *in situ* hyperspectral assessment at leaf level is the first step for the spaceborne or airborne multispectral or hyperspectral imagery for canopy assessment especially at pixel-level.

1.6 Remote Sensing of mangrove areas

Given the alarming loss of mangrove areas and the logistical difficulties of working in mangrove forests, there has been a substantial research-based application of remote sensing methodologies in monitoring mangrove conditions using biophysical variables (e.g. Green et al. 1997; Kovacs et al. 2005; Kovacs et al. 2009; Kovacs et al. 2010; Heumann 2011). There are several available optical spaceborne sensors for mangrove ecology assessments (e.g., Landsat TM, Quickbird, Spot, IKONOS, Worldview). However, most of the traditional sensors present very broad spatial resolution (≈ 30 m per pixel) such as Landsat TM, which makes it difficult to assess mangrove forests especially in non-healthy environments where sparsely vegetated areas are common. Another problem with these sensors is the very broad spectral resolution (i.e. multispectral imagery), which allows the reflected information of just 3 to 8 different bands including the blue, green, red, and near-infrared wavelengths.

Regarding mangrove forests mapping, Kovacs et al (2005) using information from IKONOS sensors and *in situ* LAI, were able to accurately create a classification image of a degraded mangrove forests of the Mexican Pacific. The high spatial resolution of multispectral IKONOS (4 m per pixel) and the link between IKONOS multispectral imagery with *in situ* LAI were key in the classification of mangrove areas at species level. However, as remote sensing technology advanced, new generations of hyperspectral spaceborne sensors (e.g. Hyperion) have become available, that measure energy in narrower and more numerous bands than multispectral sensors. These hyperspectral sensors have more continuous spectral bands and are more sensitive to subtle variations in reflected energy. As a consequence, hyperspectral sensors could improve the ecological assessment of mangrove biophysical variables over large areas of forests using more information compared to traditional multispectral data.

There are many advantages of using hyperspectral optical imagery for mangrove forest assessments. However, persistent cloud cover areas in the tropics are a major problem limiting optimal optical remotely sensed data. Consequently, the use of Synthetic Aperture Radar (SAR) could be an alternative to traditional optical imagery on tropical mangrove forests. Unaltered by cloud-cover, SAR imagery has become a useful

tool for the analysis of large areas of mangrove cover using single polarization (e.g. HH, HV, VV) and dual polarization modes (e.g. HH+HV, HH+VV). Although SAR data is extremely important for tropical latitudes, the coarse spatial resolution limits to some extent the usage of this imagery data for mangrove forest assessment. For example, IKONOS multispectral imagery visible (Fig. 1.10 a) and false color near-infrared, red, green (Fig. 1.10 b) present higher spatial resolution compared to ALOS L-band HH (Fig. 1.10 c), and the HH+HV (Fig. 1.10 d). As such, the lower spatial resolution limits the effectiveness by which this type of SAR data can be used to assess mangroves. Consequently, works on mangrove canopy using spaceborne SAR data are of key importance to investigate the degree to which the SAR data can assess mangrove biophysical responses per species and overall mangrove forest health conditions.

Traditional pixel-based classification has been used for monitoring mangrove zones (Green et al. 1998; Manson et al. 2001; Kovacs et al. 2005; 2009, 2010). However, the development of new techniques such as object-based image analysis (OBIA) needs to be demonstrated for detailed characterization of mangrove forests using SAR data (Heumann 2011). OBIA is a relatively recent technology where textural information is used in addition to spectral information for classifying data (Blaschke and Hay 2001). It is particularly useful for the identification of homogeneous groups of pixels, which have similar spectral characteristics. As a result, OBIA could include a variety of conditions such as spectral/spatial information, texture, context, and shape for each object (Herold and Scepan 2002), and could increase the accuracy of SAR data classification of mangrove areas.

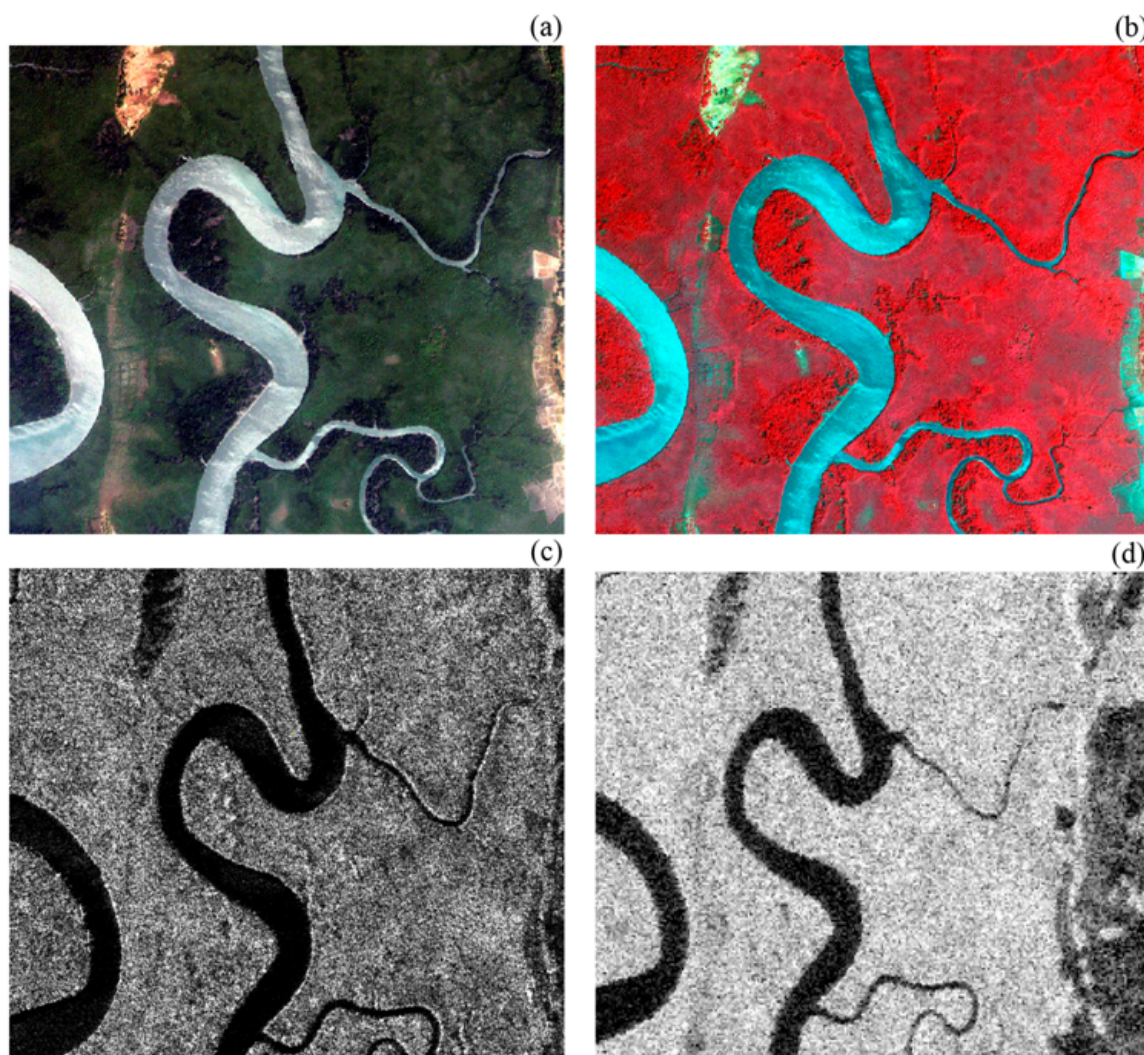


Figure 1.10: Examples of IKONOS visible (a), false color IKONOS 4, 3, 2 (b), ALOS L-band HH (c), and ALOS L-band HH+HV (d) over mangrove areas in Guinea, West Africa using data from the fifth chapter of this thesis

1.7 Objectives

In this thesis, **multiple and new approaches are developed to assess mangrove biophysical variables using *in situ* and remote sensing techniques**. Results from my investigation will provide reliable information regarding mangrove biophysical approaches for optimal ecological assessments, as well as basis for future research

including active and passive remote sensing assessments. It is important to note that previous studies have focused only on very broad biophysical relationships excluding details within each of the mangrove species and conditions of health.

This thesis presents four objectives related to ecological assessments of mangrove forests using *in situ* and remote sensing data. The first objective consists of a seasonal assessment of leaf Chla content in three species of mangrove from the sub-tropics using chemical analysis for the pigment extraction. The second and third objectives assess the feasibility of using a pocket portable instrument (CCM-200) and hyperspectral data for the accurate estimation of seasonal leaf pigments using data from objective 1. The fourth objective evaluates the viability of using OBIA for classification of mangrove species at canopy level using radar data.

1.8 Study areas

The second to the fourth chapters of this thesis were developed using data from a sub-tropical mangrove forest of the Mexican Pacific, while the fifth chapter used data from the tropical western coast of Guinea (Fig. 1.11). The aforementioned two separate study sites were selected based on the premise that the first three objectives required a sub-tropical mangrove system with a prominent dry season, whereas the last objective required an area of full-developed mangrove forest with no other type of terrestrial vegetation. Moreover, there were no available spaceborne SAR data for the study area in Mexico during the field work campaigns. However, the methodology developed for the OBIA classification of the available SAR data in Guinea could be used for future applications of biophysical links between seasonality and OBIA classification.

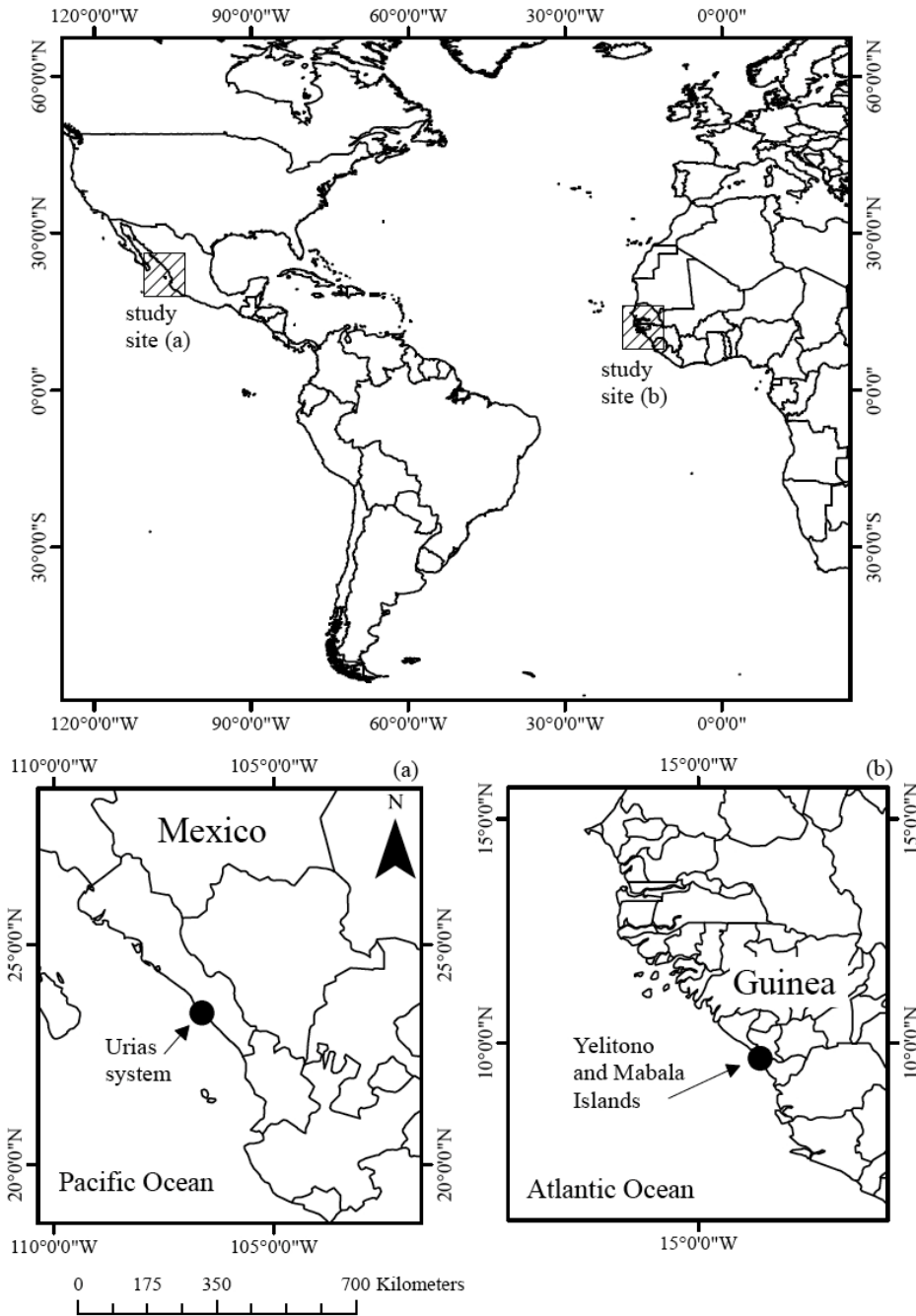


Figure 1.11: Sub-tropical mangrove system within the Urias channel, Mexico (a), and tropical mangrove system within the Yelitono and Mabala Islands, Guinea (b)

1.9 Structure of thesis

After this introductory chapter, Chapters 2 to 5 in this thesis are written in a manuscript format for journal publications. Finally, a discussion and suggestions for future research are provided in the concluding Chapter 6.

Chapter 2 investigates the seasonal variability of leaf biophysical variables such as Chla, leaf length, and Leaf Area Index within the three common species of mangrove in the sub-tropics of Mexico.

Chapter 3 assesses the utility of a portable CCM-200 absorbance unit for optimal estimation of mangrove leaf pigments (Chla, Chlb, and total Chl). The seasonal variability is also evaluated to determine in which period the estimation of leaf pigments is most favorable for all the three major mangrove species under conditions of stress and non-stress. The linear equations between the pigments and the Chlorophyll Content Index (CCI) from the CCM-200 are tested to determine if there are significant differences between the seasons within the same mangrove classes.

Chapter 4 explores the seasonal influence in leaf Chla estimation using *in-situ* hyperspectral sensing data. A series of vegetation indices were used from the hyperspectral electromagnetic spectrum regarding Chla estimation during the dry and rainy seasons.

Chapter 5 analyzes the SAR satellite imagery for optimal assessment of mangrove forests using an object-based classification technique. The single (HH) and dual (HH + HV) polarized scenes from the ALOS PALSAR L-band were selected for this Chapter. The use of SAR filters and a rule-based decision tree process were employed to analyze both sets of data.

1.10 References

- Alongi, D. M. (1998). *Coastal Ecosystem Processes*. CRC Press. 419.
- Andrew, D. R., Shane, P. D., and Graeme, P. B. (2002). An evaluation of noninvasive methods to estimate foliar Chlorophyll content. *New Phytologist*, 153, 185-194.
- Blackburn, G. A. (2007). Hyperspectral remote sensing of plant pigments. *Journal of Experimental Botany*, 58, 855-867.
- Cate, T. M., and Perkins, T. D. (2003). Chlorophyll content monitoring in sugar maple (*Acer saccharum*). *Tree Physiology*, 23, 1077-1079.
- Blasco, F., Saenger, P., and Janodet, E. (1996). Mangroves as indicators of coastal change. *Catena*, 27, 167-178.
- Cannicci, S., Burrows, D., Fratini, S., Smith, III. T. J., Offenberg, J., and Dahdouh-Guebas, F. (2008). Faunal impact on vegetation structure and ecosystem function in mangrove forests: a review. *Aquatic Botany*, 89, 186-20.
- Carter, G. A. (1998). Reflectance wavebands and indices for remote estimation of photosynthesis and stomatal conductance in pine canopies. *Remote Sensing of Environment*, 63(1), 61-72.
- Duke, N. C., Ball, M.C., and Ellison, J. C. (1998). Factors influencing biodiversity and distributional gradients in mangroves. *Global Ecological Biogeography*, 7, 27-47.
- Eichhorn, S., Everett, R., and Raven, P. (2005). *Biology of plants*. New York: W.H. Freeman and company Publishers.
- Feller, I. C., Whigham, D. F., O'Neill, J. P., and McKee, K. L. (1990). Effects of nutrient enrichment on within-stand cycling in a mangrove forest. *Ecology*, 80, 2193-2205.
- Field, C. (1995). Impact of expected climate change on mangroves. *Hydrobiologia*, 295, 75-81.
- Filella, I., and Peñuelas, J. (1994). The red-edge position and shape as indicators of plant chlorophyll content, biomass and hydric status. *International Journal of Remote Sensing*, 15, 1459-1470.
- Fillela, I., Serrano, L., Serra, J. (1995). Evaluating wheat nitrogen status with canopy reflectance indices and discriminant analysis. *Crop Sciences*, 35, 1400-1405.
- Flores-Verdugo, F., Day, J. W., and Briseño-Dueñas, R. (1987). Structure, litter fall, decomposition, and detritus dynamics of mangroves in a Mexican coastal lagoon with an ephemeral inlet. *Marine Ecology Progress Series*, 35, 83-90.
- Flores-Verdugo, F., Gonzalez-Farias, F., Zamorano, F., and Ramirez-Garcia, D. S. (1992). Mangrove ecosystem of the Pacific coast of Mexico: distribution, structure, litterfall, and detritus dynamics. In: Seeliger, U. (1992) *Coastal plant Communities of Latin America*. New York: Academic Press.
- Gamon, J. A., and Surfus, J. S. (1999). Assessing leaf pigment content and activity with a reflectometers. *New Phytology*, 143, 105-117.
- Goncalves, J. F., Moreira, dos Santos, J. U., and Alves, da Silva, E. (2008). Evaluation of a portable Chlorophyll meter to estimate Chlorophyll concentrations in leaves of tropical wood species from Amazonian forest. *Hoehnea*, 35, 185-188.
- Green, E. P., Mumby, P. J., Alaisdair, E. J., Clark, C. D., and Ellis, A. C. (1997). Estimating leaf area index of mangroves from satellite data. *Aquatic Botany*, 58, 11-19.

- Hendry, G. F., and Price, A. H. (1993). *Stress indicators: Chlorophylls and carotenoids*. London: Chapman & Hall.
- Hess, L. L., Melack, J. M., and Simonett, D. S. (1990). Radar detection of flooding beneath the forest canopy: a review. *International Journal of Remote Sensing*, 11, 1313-1325.
- Heumann, B. W. (2011). Satellite remote sensing of mangrove forests: recent advances and future opportunities. *Progress Physical Geography*, 35(1), 87-108.
- Horler, D. N. H., Dockray, M., and Barber, J. (1983). The red-edge of plant leaf reflectance. *International Journal of Remote Sensing*, 4(2), 273-288.
- Kamali, B., and Hashim, R. (2011). Mangrove restoration without planting. *Ecological Engineering*, 37, 387-391.
- Komiyama, A., Ong, J. E., Pongpan, S. (2008). Allometry, biomass, and productivity of mangrove forest: a review. *Aquatic Botany*, 89, 128-137.
- Kovacs, J. M., Flores-Verdugo, F., Wang, J., and Aspen, L. P. (2004). Estimating leaf area index of a degraded mangrove forest using high spatial resolution satellite data. *Aquatic Botany*, 80, 13-22.
- Kovacs, J. M., Wang, J., and Flores-Verdugo, F. (2005). Mapping mangrove leaf area index at the species level using IKONOS and LAI-2000 sensors for the Agua Brava Lagoon, Mexican Pacific. *Estuarine Coastal and Shelf Science*, 62, 377-384.
- Kovacs, J. M., Vandenberg, C. V., and Flores-Verdugo, F. (2006). Assessing fine beam RADARSAT-1 backscatter from a white mangrove (*Laguncularia racemosa* (Gaertner)) canopy. *Wetlands Ecology and Management*, 14, 401-408.
- Kristensen, E., Bouillon, S., Dittmar, T., and Marchand, C. (2008). Organic carbon dynamics in mangrove ecosystems: a review. *Aquatic Botany*, 89, 201-219.
- Lacerda, L. D. (2002). *Mangrove ecosystems: function and management*. Berlin.:Springer.
- Lugo, A. E., and Snedaker, S. C. (1974). The ecology of mangroves. *Annual Review of Ecology and Systematics*, 5, 39-64.
- Nagelkerken, I., Blaber, S. J. M., Bouillon, S., Green, P., Haywood, M., Kirton, L. G., Meynecke, J. O., Pawlik, J., Penrose, H. M., Sasekumar, A., and Somerfield, P. J. (2008). The habitat function of mangroves for terrestrial and marine fauna: a review. *Aquatic Botany*, 89, 155-185.
- Penuelas, J., and Fillela, I. (1998). Visible and near-infrared reflectance techniques for diagnosing plant physiological status. *Trends in Plant Science*, 3, 151-156.
- Polidoro, B.A., Carpenter, K. E., Collis, L., Duke, N.C., et al. (2010). The loss of species: Mangrove extinction risk and Geographic areas of global concern. *PLoS ONE*, 5(4), e10095.
- Raven, P.H., Evert, R.F., and Eichhorn, S.E. (1992). *Biology of plants*. New York: W.H. Freeman.
- Richardson, A. D., Duigan, S. P., and Berlyn, G. P. (2002). An evaluation of noninvasive methods to estimate foliar chlorophyll content. *New Phytology*, 153, 185-194.
- Robertson, A.I., Daniel, P. A., and Dixon, P. (1991). Mangrove forest structure and productivity in the fly river estuary, Papua New Guinea. *Marine Biology*, 111, 147-155.

- Rogers, K., Saintilan, N., and Heijnis, H. (2005). Mangrove encroachment of salt marsh in Western Port Bay, Victoria: the role of sedimentation, subsidence, and sea level rise. *Estuaries*, 28, 551–55.
- Saenger, P. (2002). *Mangrove ecology, silviculture and conservation*. Kluwer Academic Publishers, Dordrecht: Kluwer Academic Publishers.
- Saintilan, N., and Wilton, K. (2001). Change in the distribution of mangroves and saltmarshes in Jervis Bay, Australia. *Wetlands Ecology Management*, 9, 409–420.
- Seto, K. C., and Fragkias, M. (2007). Mangrove conversion and aquaculture development in Vietnam: A remote sensing-based approach for evaluating the Ramsar Convention on Wetlands. *Global Environmental Change*, 17, 486-500.
- Spalding, M., Kainuma, M., and Collins, L. (2010). *World atlas of mangroves*. Washington: Earthscan.
- Steinke, T. D., Holland, A. J., and Singh, Y. (1993). Leaching losses during decomposition of mangrove leaf litter. *South African Journal Botany*, 59, 21–25.
- Tomlinson, P. B. (1986). *The botany of mangroves*. Cambridge: Cambridge University Press.
- Ulaby, F. T., Moore, R. K., and Fung, A. K. (1986). *Volume scattering and emission theory, advanced systems and applications*. In *Microwave remote sensing: active and passive*. Dedham: Artech House, Inc).
- Valiela, I., Boen, J. L., and York, J. K. (2001). Mangrove forest: One of the worlds threatened major tropical environments. *Bioscience*, 51, 807-815.
- Vogelman, J. E., Rock, B. N., and Moss, D. M. (1993). Red-edge spectral measurements from sugar maple leaves. *International Journal of Remote Sensing*, 14(8), 1563-1575.
- Walters, B. B., Ronnback, P., Kovacs, J.M., Crona, B., Hussain, A., Badola, R., Dahdouh-Guebas, F., and Barbier, E. (2008). Ethnobiology, socio-economics and management of mangrove forests: a review. *Aquatic Botany*, 89, 220-236.
- Wellburn, A. R. (1994). The spectral determination of chlorophylls a and b, as well as total carotenoids, using various solvents with spectrophotometers of different resolution. *Journal of Plant Physiology*, 144, 307-313.

Chapter 2

2 Seasonal changes in leaf chlorophyll a content and morphology in a sub-tropical mangrove of the Mexican Pacific.¹

2.1 Introduction

Leaf chemical properties are the principal determinants of plant physiology and of highly active biochemical processes such as photosynthesis (Evain et al. 2004). Among the most common variations that interact with plant photosynthesis are diurnal changes of incident irradiance, ambient temperature, and humidity (Schulze & Caldwell 1994). Additionally, seasonal changes in the availability of water and nutrients (Gilman et al. 2008) affect the effectiveness of pigments in light capture and utilization (Evain et al. 2004). Amongst the various leaf pigments, chlorophyll-a (Chla) is a key compound responsible for photosynthesis, physiology, and other biological functions in plants. Consequently, changes in Chla can indicate plant growth (Raven et al. 1992) or disturbances from stressors (Blackburn 2007).

The aforementioned disturbances are commonplace in high, locally stressed canopies such as mangrove forests. These forested wetlands are predominantly intertidal and occur worldwide in the sub-tropics and tropics (Nagelkerken et al. 2008) along sheltered and shallow water coastlines (Hogarth 1999) where high irradiation is the norm (Evain et al. 2004) and natural and anthropogenic disturbances are common. The importance of ecological field surveys of these systems may have implications in developing fast and accurate assessments regarding the state of these highly productive forested habitats for future conservation measures. Mangroves are an essential resource for a variety of local activities (Walters et al. 2008), provide for a variety of macrofaunal

¹ A version of this chapter has been published: **Flores-de-Santiago F.**, Kovacs JM., Flores-Verdugo F. (2012). Seasonal changes in leaf chlorophyll a content and morphology in a sub-tropical mangrove forest of the Mexican Pacific. **Marine Ecology Progress Series**. 444, 57-68. (<http://dx.doi.org/10.3354/meps09474>).

interactions (Cannicci et al. 2008), are highly productive (Komiya et al. 2008), and provide habitat for a variety of terrestrial and marine fauna (Nagelkerken et al. 2008).

For mangroves, the concentrations of leaf pigments can be associated with environmental factors such as ambient temperature/sunlight (Saenger 2002), water availability (Lacerda 2002), and salinity (Steinke et al. 1993). Thus, in a sub-tropical mangrove forest where fresh water availability is seasonal, precipitation patterns could affect the physiological development of the mangrove trees, resulting in an increase or decrease of ground salinity (Field 1995). As a consequence, in sub-tropical regions there could be a seasonal decrease in net primary productivity (Saenger 2002) and growth (Raven et al. 1992). As well, a seasonal increase in the availability of sulfate in water may occur, which could increase anaerobic decomposition (Saintilan & Wilton 2001, Rogers et al. 2005) and thus potentially alter the competition between mangrove species (Lacerda 2002) resulting in decreasing diversity within mangrove areas (Duke et al. 1998). In anthropogenically stressed mangroves, these conditions (e.g. hypersalinity) may be exasperated, resulting in large-scale mangrove loss or degradation as shown in a mangrove forest just south of the Urias system (Kovacs et al. 2005).

Each species of mangrove has a particular range of tolerance to environmental factors such as water salinity. For example, some species are relatively intolerant to hypersaline conditions (e.g. *Rhizophora mangle*), whereas others are quite capable of tolerating high salinities of over 60 ‰ (e.g. *Avicennia germinans*) (Moroyoqui-Rojo & Flores-Verdugo 2005). These differences among the species could be assessed using leaf biophysical variables such as leaf area index (LAI), leaf area, leaf length, and Chl_a content. LAI is defined as the one-sided green leaf area per unit ground surface area (m²/m²) using the differences between direct PAR from the top of the canopy and PAR from below the canopy (Decagon Devices Inc, 2013). Specifically, seasonal differences in LAI and Chl_a content could be related to organic carbon dynamics such as litter fall decomposition rates (Flores-Verdugo et al. 1987, Kristensen et al. 2008), nutrient cycling characteristics (Feller et al. 1999), and mangrove paleoecological reconstructions (Ellison 2008). The variability of inter-species leaf morphology (e.g. leaf area, leaf length) could be associated with faunal retention rates (Cannicci et al. 2008), mangrove ecosystem

seasonal dynamics (Berger et al. 2008), and differences in canopy ecological habitat for faunal species (Nagelkerken et al. 2008). Moreover, all of these data could be valuable in describing and predicting seasonal patterns of forest productivity (Raven et al. 1992).

Yet another potentially important characteristic to consider is seasonal change in the vertical distribution of pigments within the mangrove canopy. Such potential variability could depend on many factors, including acclimation to light penetration (Saenger 2002), characteristics of each species (Raven et al. 1992), and the environment itself (Ciganda et al. 2009). Moreover, it could provide key information regarding our understanding of the role that mangrove species play in response to a variety of factors, including climate change. The main objective of this investigation was to compare the leaf biophysical parameters (Chla content, leaf area, and leaf length) between the rainy and dry seasons in a degraded mangrove forest of the Mexican Pacific. This would also include assessing whether any seasonal differences can occur in the upper and lower canopies. These data can be of utmost importance when trying to establish effective monitoring programs of mangrove forest productivity. In particular, these data can be used to determine the optimal times to map estimated mangrove biomass from remotely sensed data. This is extremely important given that the spectral vegetation indices used in such operations are directly dependent on the leaf canopy structure and leaf Chla content.

2.2 Materials and Procedures

Data were collected along the south end of the Urias mangrove system (Fig. 2.1) during 2 seasons, the dry season of May 2010 (mean precipitation of 0.1 mm) and at the end of the rainy season in October 2010 (mean precipitation of 190 mm; INEGI 2010). According to the federal government (INEGI 2010), the historical meteorological data (1986 to 2010) indicates that the 2010 dry and rainy seasons were normal in regards to precipitation and ambient temperature. The driest and rainiest years were 1994 and 2000, respectively.

The Urias system is a shallow, saline; vertically mixed body of water of approximately 18 km² which is located in the coastal plain of the southeastern Gulf of California (23° 10' N, 106° 20' W). Previous authors have indicated that during the dry

season, this estuary becomes fully inversed (Alvarez 1977, Agraz-Hernández 1999, Moroyoqui-Rojo 2005). In other words, the salinity increases monotonically from the mouth to the head. It has also been suggested that the removal of water by the mangrove trees (Hogarth 1999) and the high estuarine evaporation rates (Ridd & Stieglitz 2002) may combine to raise the soil salinity during the dry season, resulting in areas characterized by a hypersaline state which are common in this system. The fringe mangroves, which consist of healthy trees, receive ample water from the adjacent river at high tide during the rainy season. The basin mangrove communities, consisting primarily of dwarf trees and/or trees in poor condition, receive runoff water from the mainland, decreasing soil salinity during this season. Healthy mangrove trees located along the fringe are exposed to frequent full strength tidal influence (up to 1.5 m; Hogarth 1999), while the basin mangrove trees are located more inland exposed to infrequent tidal inundation (Saenger 2002).

The surface of the substrate in the mangrove is generally smooth with a few small channels and depressions, with a relatively gentle overall slope extending towards the open water of the main tidal channel (Moroyoqui-Rojo 2005). The lagoon is partly bordered by a mangrove forest ecosystem, which is best developed along the edge and supports 3 dominant species: red mangrove *Rhizophora mangle*, black mangrove *Avicennia germinans*, and white mangrove *Laguncularia racemosa*.

Based on height and distance to water, the mangroves in this arid sub-tropical region differ considerably from their wet tropical counterparts in 2 major ways. First, river discharge into the wetlands is highly seasonal, with very large flows in the wet season followed by several months of negligible discharge. Second, large areas of mangrove and saltpan often infringe on this coastal type lagoon. As a result, many of these arid coastal lagoons become hypersaline for much of the year. Similar to the mangrove system just south of this region, anthropogenic changes, particularly related to hydrological modifications (e.g. roads, aquaculture diversion) have resulted in a degraded system with prominent areas now consisting of dwarf and poor condition stands of each species (Kovacs et al. 2008, 2009). Consequently, 6 classes of mangrove have been identified for this system: dwarf and poor condition red, black, and white mangrove and

healthy red, black, and white mangrove. Although the descriptions of these classes are qualitative, their classification has been done quantitatively utilizing standard image-processing methods based on their unique spectral properties as identified from remotely sensed digital data (Kovacs et al. 2008, Zhang et al. 2012).

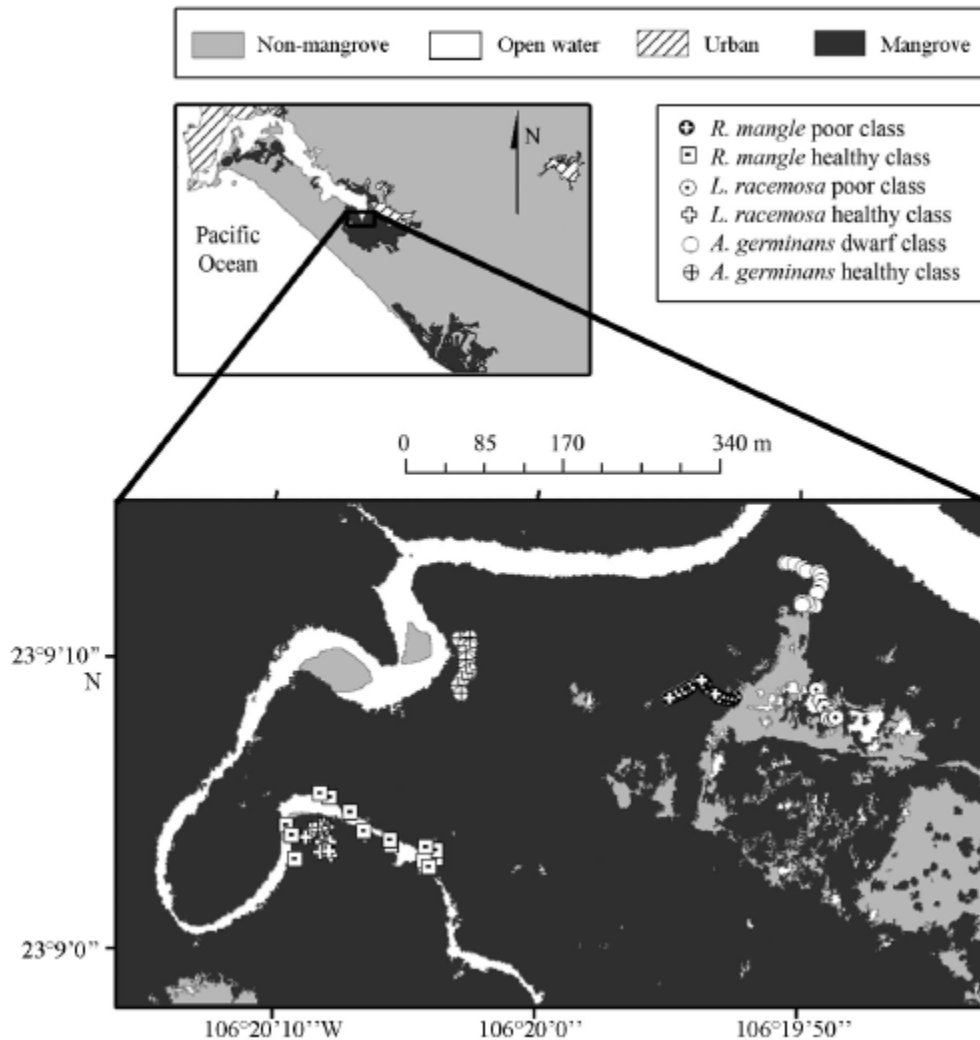


Figure 2.1: Data collection sites at the south end of the Urias mangrove system

LAI is defined as the 1-sided leaf area per ground surface area (Wilhelm et al. 2000) found in the near infrared spectrum of the canopy reflectance properties. With regards to the LAI measurements, an AccuPAR LP-80 (Decagon Devices) ceptometer was used to quantify *in situ* LAI for every species of mangrove in this system. The device measures the incoming photosynthetically active radiation (PAR) through 80 sensors

incorporated along the linear probe. I quantified LAI based on 1 above and the average of 8 readings below canopy using the following equation from the AccuPAR LP-80 manual (Decagon Devices Inc. 2013):

$$LAI = \frac{\left[\left(1 - \frac{1}{2K} \right) fb - 1 \right] \ln \tau}{A(1 - 0.47fb)} \quad (1)$$

Where fb is beam fraction. (A) is determined by the instrument based upon the leaf distribution and the canopy leaf absorption qualities. For this sampling it was assumed to be 0.9. Tau (τ) is the ratio of PAR measured below the canopy to PAR above the canopy, and the extinction coefficient (K) is determined automatically by the LP-80 using the latitude, longitude, and the minutes of the day to calculate the zenith angle (θ):

$$K = \frac{1}{2 \cos \theta} \quad (2)$$

The beam fraction (fb) depends on the high and low limits of the potential PAR and the zenith angle with the following set of equations:

$$r = \frac{PAR}{2550(\cos \theta)} \quad (3)$$

$$fb1 = 48.57 + r(-59.024 + r(24.835)) \quad (4)$$

$$fb = 1.395 + r(-14.47 + r(fb1))$$

A stratified random sampling method was employed to make sure each mangrove class within the system was analyzed. For each class, I sampled 15 sites in a longitudinal pattern taking approximately 8 LAI readings per site. A post-processing GPS was used to ensure that seasonal readings could be collected for each site. As with the LAI sites, I selected 3 mangrove trees from each class for the pigment analysis. For each tree, 10 leaves were taken from the top of the canopy (i.e. upper canopy) and 10 leaves from the lower canopy using an extendable pole with a cutter. In order to select just the mature leaves, each of the samples was chosen between the third and fifth leaves from the tip. A

sub-meter GPS location was recorded so that the same leaf collection site could be used for both seasons.

Once cut, each leaf was stored in a plastic bag within a small cooler at 4°C for transportation to the laboratory. The leaf area and length were analyzed using an LI-3000C Portable Area Meter device. Due to the difference in leaf morphology between the mangrove species, I normalized Chla per unit area (mg m^{-2}) using the dimensions of the diameter of a copper cylinder. Specifically, one leaf circle (1.25 cm in diameter) from each leaf of each sample was cut out with the cylinder. Care was taken to avoid the circles that included main leaf veins. Plant material for each sample was then dissolved with 100 ml of 80% acetone. A spectrophotometric assay was then conducted to extract information of peak absorption at 646 and 663 nm (Lichtenthaler & Wellburn 1983).

I used a Q-Q plot to test the normality of error of estimates for all data (i.e. LAI, Chla, leaf area, leaf length). This test is based on an ordered plot of residual errors of an equation against normal quantile $sq(j)$. In this test, if the data lie in proximity to a straight line, then I cannot reject the null hypothesis of normality. To measure the straightness of the Q-Q plot, I used the correlation coefficient of the Q-Q plot, which is defined as follows:

$$r_Q = \frac{\sum_{j=1}^n (x_j - \bar{x})(q_j - \bar{q})}{\sqrt{\sum_{j=1}^n (x_j - \bar{x})^2} \sqrt{\sum_{j=1}^n (q_j - \bar{q})^2}} \quad (5)$$

Where (x) is the theoretical quantile, (q) is the sample quantile, (j) are the points of paired quantiles, and (n) is the total observation number. Consequently, at the 5% significance level ($\alpha = 0.05$) and $n = 60$, I used the critical value of 0.98 (Johnson & Wichern 1992).

Differences in Chla content, leaf area, leaf length, and LAI were tested using Minitab® and Origin® software. When the data were not normally distributed, each of the 3 parameters was tested using non-parametrical statistics (Mann-Whitney *U*-test). However, averages and standard deviations are provided though not analyzed for comparison between the mangrove classes. The tests were used to examine for differences between the upper and lower canopies for both seasons.

2.3 Results

Of all comparisons for normality, most r_Q values were below the critical value; therefore, I used non-parametric tests. Significant differences in Chla content ($p < 0.05$, $n = 30$) were found between seasons for the upper and lower canopies of the white poor, red poor, and black dwarf classes (Table 2.1). Among these differences, it is clear that all 3 species experienced an increase in leaf Chla content during the rainy season (Fig. 2.2). By contrast, for healthy mangroves of all 3 species, no significant differences in Chla content were observed between seasons ($p = 0.05$, $n = 30$) in the upper leaves (Table 2.1). With the exception of the ‘white healthy’ class, which had higher Chla content during the dry season (Fig. 2.2), a lack of seasonal differences was also observed for the lower canopy leaves of the healthy mangroves.

Table 2.1: *Laguncularia racemosa*, *Rhizophora mangle*, and *Avicennia germinans* Mann-Whitney U-test median values for chlorophyll a (Chla), leaf area, and leaf length between seasons ($n = 30$). LR: *L. racemosa*, RM: *R. mangle*, AG: *A. germinans*.

***Significant U values $P = 0.05$**

Species and class	Chla (mg m^{-2})			Leaf area (cm^2)			Leaf length (cm)		
	May	Oct	<i>U</i>	May	Oct	<i>U</i>	May	Oct	<i>U</i>
Upper									
LR poor	20.9	26.6	15*	No data			No data		
LR healthy	31.6	30.9	536	14.7	18.2	301*	6	10	48*
RM poor	24.9	33.3	117*	34.7	29.0	541	9.6	12.3	94
RM healthy	43.2	42.6	418	48.1	50.6	420	11.3	14.6	90*
AG dwarf	24.7	36.2	15*	10.9	10.4	503	99.5	9.7	430
AG healthy	32.0	36.7	341	20.2	24.0	306*	13.0	13	479
Lower									
LR poor	23.5	26.5	160*	19.1	19.2	424	6.7	9.2	65*
LR healthy	33.4	27.0	809*	14.3	15.5	371	6.2	9.6	41*
RM poor	31.3	39.9	194*	27.9	25.8	406	8.4	12.5	42*
RM healthy	36.7	37.8	376	49.1	46.9	529	15.5	15.4	500
AG dwarf	32.1	36.7	225*	13.1	10.2	583*	8.8	9.1	454
AG healthy	32.2	33.2	354	29.6	29.0	514	13.5	12.3	543

With regards to the leaf area and leaf length, no data were recorded for the white poor upper leaves during October due to data loss (corrupt file). Most of the classes showed no significant seasonal differences ($p = 0.05$, $n = 30$) in leaf area. In the case of white and black healthy upper leaves (Table 2.1), a significant increase in leaf area was

recorded during the rainy season (Fig. 2.3). Moreover, the length of the leaves in the upper canopy increased significantly ($p=0.05$, $n=30$) for white healthy, red poor, and red healthy mangroves during the rainy season (Table 2.1, Fig. 2.4). No significant differences ($p=0.05$, $n=30$) were found in the lower canopies of black healthy, black dwarf, and red healthy (Table 2.1). With regards to LAI, no significant difference ($p=0.05$, $n=15$) was observed between the seasons for the white poor, red poor, red healthy, black dwarf, and black healthy mangrove classes (Table 2.2). However, a significant difference ($p=0.05$, $n=15$) was found in the white healthy mangrove with an increase in LAI occurring during the rainy season (Fig. 2.5).

Table 2.2: *Laguncularia racemosa*, *Rhizophora mangle*, and *Avicennia germinans*.

Mann-Whitney U-test for the leaf area index (LAI) between seasons (n = 15).

***Significant U values P=0.05**

Class	Median LAI		U
	May	October	
<i>L. racemosa</i>			
Poor	1.4	1.2	106
Healthy	2.5	3.6	28*
<i>R. mangle</i>			
Poor	2.1	2.4	68
Healthy	5.7	5.1	151
<i>A. germinans</i>			
Dwarf	1.5	1.5	95
Healthy	3.6	2.9	137

During the dry season, Chla content showed no significant difference ($p=0.05$, $n=30$) between upper and lower canopy leaves for the white healthy and the black healthy mangroves (Table 2.3). The white poor, red poor, and black dwarf classes showed a higher Chla content within the lower leaves when compared to the red healthy, which presented higher Chla content in the upper leaves (Table 2.3). With regards to leaf area, the white healthy, red healthy, and black dwarf mangroves did not show any significant differences ($p=0.05$, $n=30$). The red poor mangroves did have significantly higher leaf area in the upper leaves. In contrast, the white poor and black healthy showed an increase in leaf area in the lower leaves. The length of leaves showed no significant difference ($p=0.05$, $n=30$) in the white healthy, black dwarf, and black healthy classes. The white

poor and the red healthy did have significantly higher leaf lengths in the lower leaves, whereas the red poor had significantly higher leaf lengths in the upper canopy.

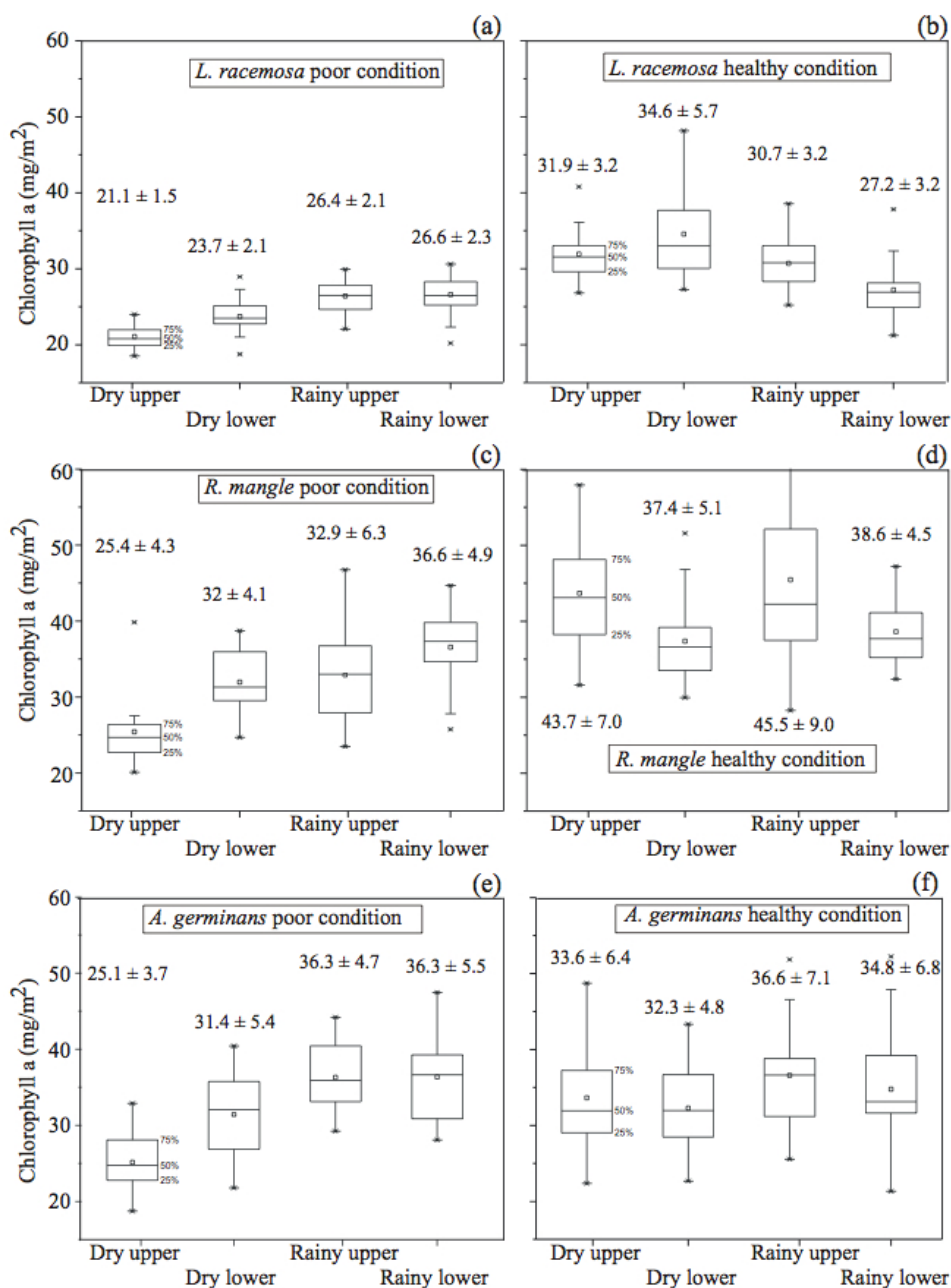


Figure 2.2: *Laguncularia racemosa*, *Rhizophora mangle*, and *Avicennia germinans*. Upper and lower canopy leaf chlorophyll-a (Chla) content by season. Each box plot depicts the mean (small square), the minimum and maximum sample, the lower quartile (25%), the median (50%), the upper quartile (75%), and the lowest and

highest sample with 1.5 interquartile ranges of the lower and upper quartile (*). Also, mean is shown at the top of each box plot

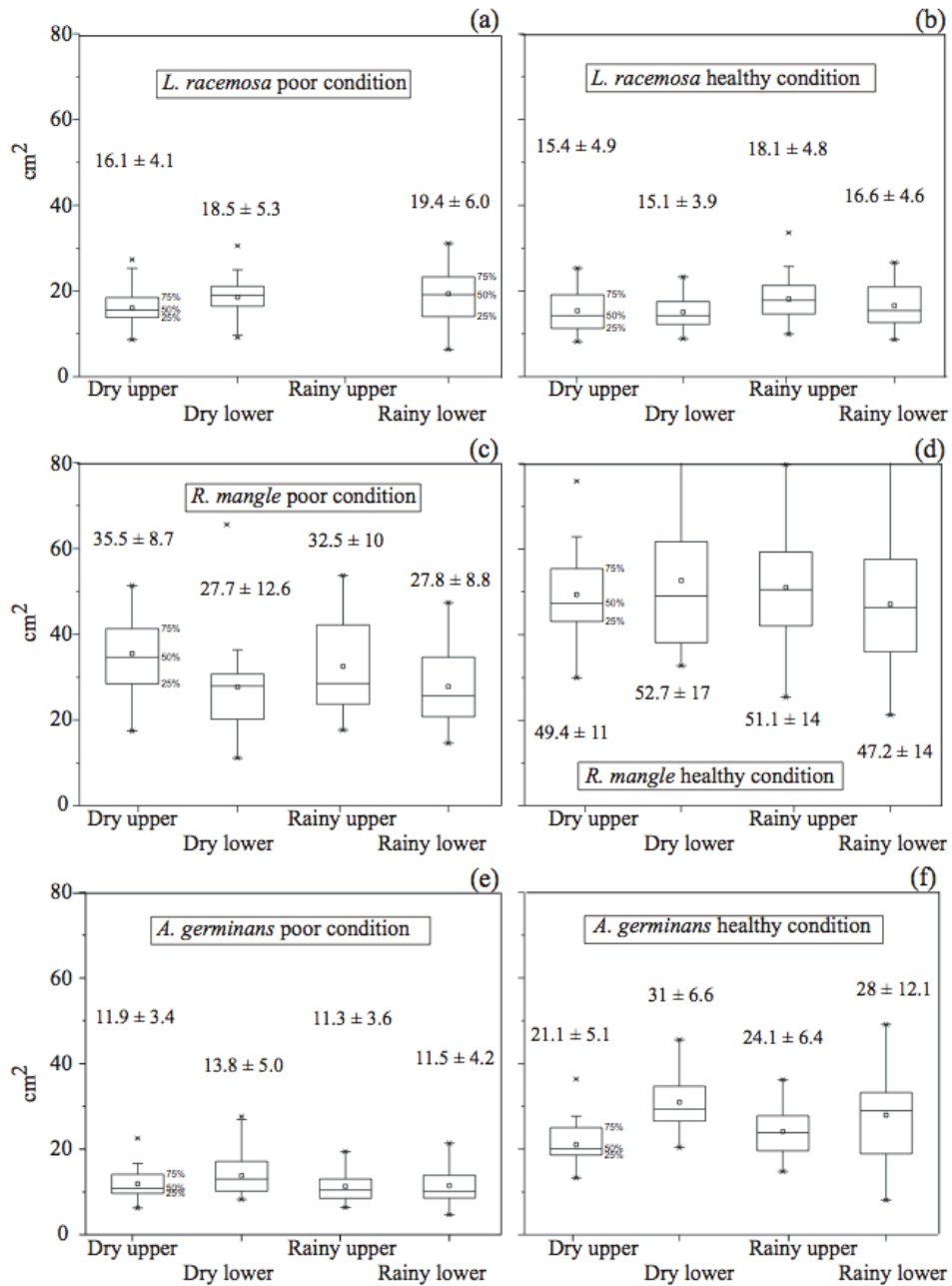


Figure 2.3: *Laguncularia racemosa*, *Rhizophora mangle*, and *Avicennia germinans*. Upper and lower canopy leaf area (cm²) by season. Each box plot depicts the mean (small square), the minimum and maximum sample, the lower quartile (25%), the median (50%), the upper quartile (75%), and the lowest and highest sample with 1.5

interquartile ranges of the lower and upper quartile (*). Also, mean is shown at the top of each box plot

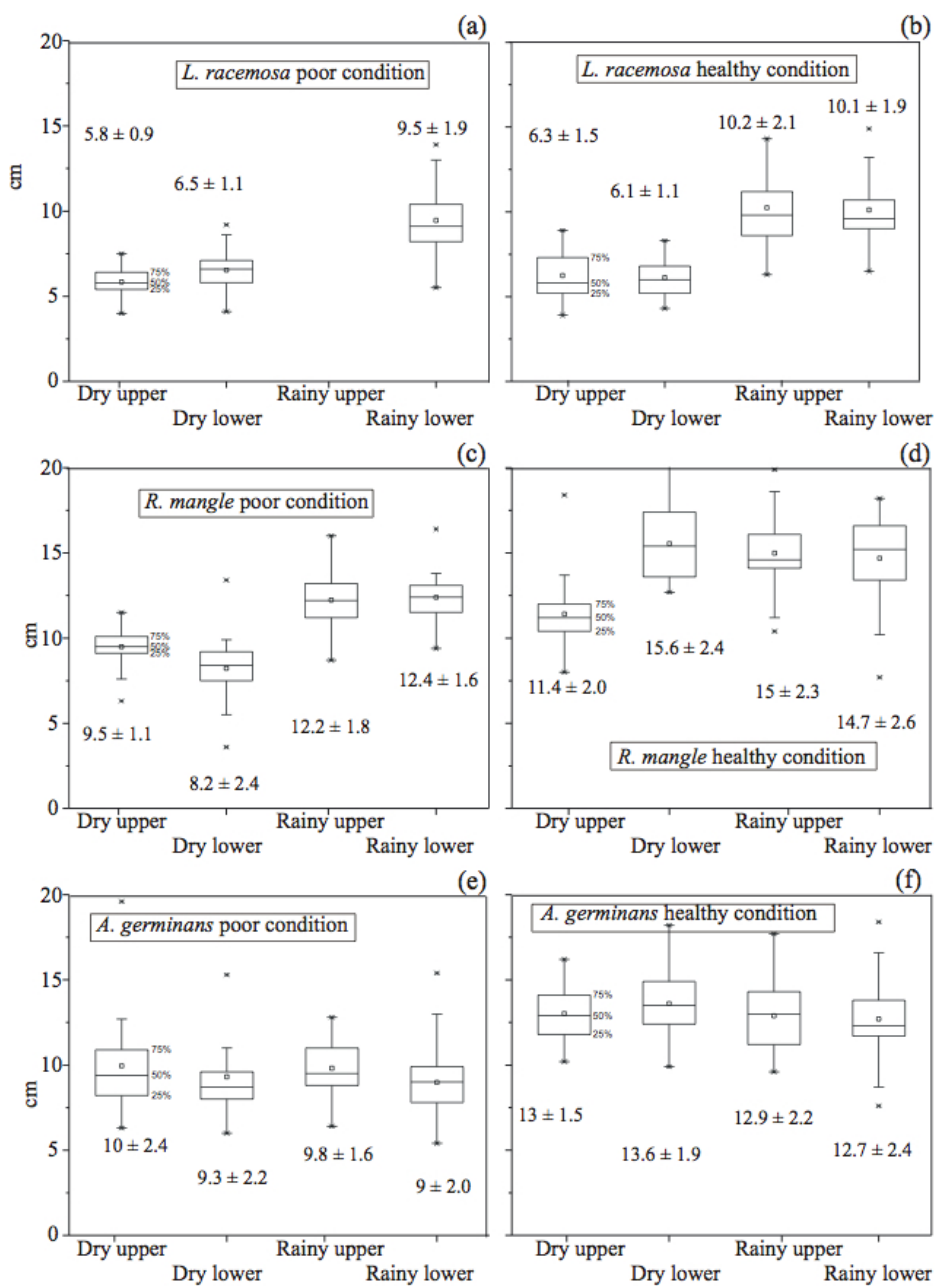


Figure 2.4: *Laguncularia racemosa*, *Rhizophora mangle*, and *Avicennia germinans*. Upper and lower canopy leaf length (cm) by season. Each box plot depicts the mean (small square), the minimum and maximum sample, the lower quartile (25%), the median (50%), the upper quartile (75%), and the lowest and highest sample with 1.5

interquartile ranges of the lower and upper quartile (*). Also, mean is shown at the top of each box plot

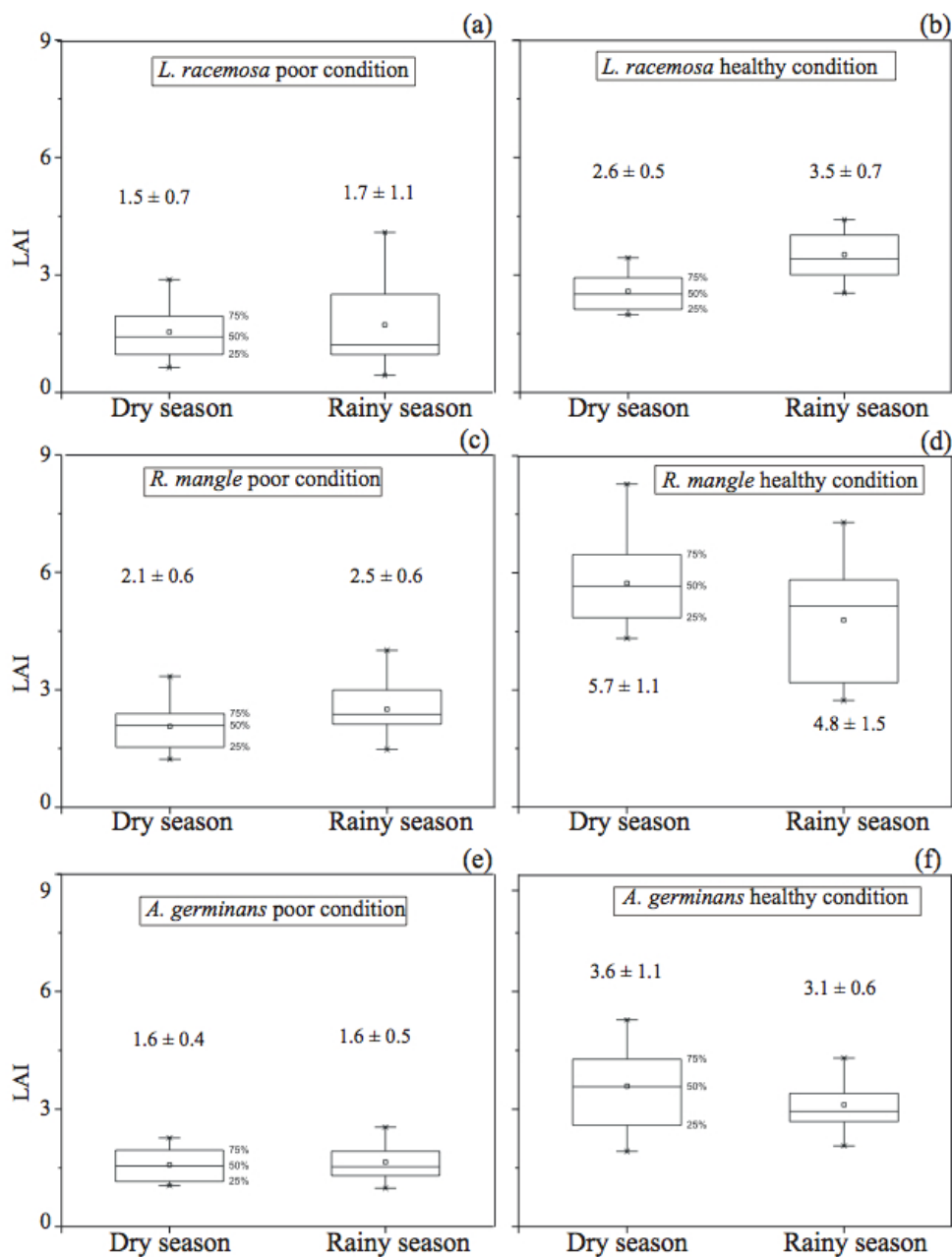


Figure 2.5: *Laguncularia racemosa*, *Rhizophora mangle*, and *Avicennia germinans*. Upper and lower Leaf Area Index (LAI) by season. Each box plot depicts the mean (small square), the minimum and maximum sample, the lower quartile (25%), the median (50%), the upper quartile (75%), and the lowest and highest sample with 1.5

interquartile ranges of the lower and upper quartile (*). Also, mean is shown at the top of each box plot

Table 2.3: *Laguncularia racemosa*, *Rhizophora mangle*, and *Avicennia germinans*. Mann-Whitney U-test for chlorophyll-a (Chla), leaf area, and leaf length between the upper and lower canopy in both seasons (n=30). LR: *L. racemosa*, RM: *R. mangle*, AG: *A. germinans* *Significant U P=0.05

Species and class	Chla (mg m ⁻²)			Leaf area (cm ²)			Leaf length (cm)		
	Upper	Lower	U	Upper	Lower	U	Upper	Lower	U
May									
LR poor	20.9	23.5	142*	15.6	19.1	291*	5.9	6.7	269*
LR healthy	31.6	33.4	338	14.7	14.3	449	6	6.2	463
RM poor	24.9	31.3	110*	34.7	27.9	658*	9.6	8.4	661*
RM healthy	43.2	36.7	697*	48.1	49.1	425	11.3	15.5	68*
AG dwarf	24.7	32.1	154*	10.9	13.1	357	9.5	8.8	551
AG healthy	32.0	32.2	485	20.2	29.6	91*	13.0	13.5	368
October									
LR poor	26.6	26.5	419		No data			No data	
LR healthy	30.9	27.0	723*	18.2	15.5	536	10	9.6	482
RM poor	33.3	37.5	266*	29.0	25.8	581	12.3	12.5	440
RM healthy	52.3	41.6	676*	50.6	46.9	523	14.6	15.4	451
AG dwarf	36.2	36.7	453	10.4	10.2	454	9.7	9.1	594*
AG healthy	36.7	33.2	518	24.0	29.0	346	13	12.3	455

With regards to the rainy season (Table 2.3), the Chla content showed no significant difference ($p=0.05$, $n=30$) between the lower and upper leaves in the white poor, black dwarf, and black healthy mangroves. The white healthy and the red healthy classes presented higher Chla content in the upper leaves, and the red poor showed higher content in the lower leaves. No significant differences in leaf area were found among all 6 classes. Regarding leaf length, no significant differences were found with the exception of the black dwarf, which had significantly larger leaves in the upper canopy during this season.

2.4 Discussion and conclusions

Where seasonal gradients are involved, the pattern of Chla content and leaf morphology can be used to express the ecological changes of species as key indicators of the physiological stage, productivity, and stress of a mangrove forest. In this

investigation, I determined that variability in Chla can occur amongst various mangrove classes found within a degraded forest of the sub-tropics. Specifically, in this study area, the Chla content of all three mangrove species in poor condition showed seasonal dependence, unlike those that were healthy. As previously described by Kovacs et al. (2011), the fringe mangrove of this region of Mexico is typically healthy, whereas basin mangrove is more often found in a poor/dwarf condition. The leaf morphology patterns observed in this study agree with Tomlinson (1986), in that I found bigger leaves in the healthy classes, in particular red and black mangrove, while black dwarf and white poor showed the lowest leaf area and length (Figs. 3 and 4). This is suggestive of a direct relationship between the leaf morphology and the physical state of the trees.

It has been noted that different light and shade requirements in adults of *Laguncularia racemosa* are indicative of a shade-intolerant response (Smith 1992, McKee 1995), suggesting a pattern in which leaves from the lower canopy and under thicker cover receive less light during the rainy season. As seen with the increase in LAI during the rainy season in healthy stands, this could decrease Chla content in the lower leaves and therefore result in more stress because of the low irradiances as depicted in Fig. 2.2. By contrast, the apparent lack of change in the Chla content in healthy leaves from the upper canopy suggests that the aforementioned shade-intolerant pattern from the lower canopy is present in this type of healthy forest. However, the higher leaf area and leaf length during the rainy season may indicate that at the top of the canopy, the Chla content has no apparent dependence on the morphology of the leaves.

Regarding the white mangrove in poor condition, the shade-intolerant pattern (Smith 1992, McKee 1995) was not observed, as there was no change in LAI. Moreover, the higher Chla content and leaf length during the rainy season indicate that this poor-condition forest is distinctly seasonal in its development. Tomlinson (1986) indicated that for this species, branching occurs during the rainy season, with an extended period of inactivity during the dry season, suggesting that at high irradiances and lack of fresh water, the vegetative survival and competitiveness of *Laguncularia racemosa* could depend on an efficient display of foliage and the ability to respond to environmental changes and stress.

Regarding the red poor condition, the increases in Chla content and leaf length during the rainy season in both upper and lower canopies suggest that this type of forest greatly depends on fresh water availability and shade as previously reported by Farnsworth & Ellison (1996). In contrast, the lack of seasonal change within the healthy forest in LAI and leaf morphology suggests moderate sun-shade flexibility. Ellison & Farnsworth (1993) reported that *Rhizophora mangle* is capable of adapting to different light levels, including gaps within the canopy. It was noted in the field that the majority of healthy *R. mangle* were found in a continuous stand along the main channel where no other species of mangrove could constrain the availability of light. The lack of observed seasonal change in LAI, Chla, and leaf area in this study would suggest an adaptation of fringe *R. mangle* to constant tidal flushing.

In this study, a high Chla content was found in the upper leaves of healthy red mangrove during the rainy season. Lugo et al. (1975) indicated that the non-shaded leaves (i.e. upper canopy) of this species might show a net photosynthetic rate twice as high as that of the shaded leaves (lower canopy). Regardless of canopy composition, it has been reported that *Rhizophora mangle* trees can assume a shade-tolerant (Farnsworth & Ellison 1996) and shade-intolerant (Snedaker 1995) pattern. In this study, the red mangrove in poor condition could be indicative of a shade-tolerant pattern, with higher content of Chla in the lower canopy. By contrast, the healthy red mangrove in this study would indicate a more shade-intolerant trend, with higher Chla content in the upper canopy where the availability of light is higher as compared to the shaded leaves in the lower canopy.

The patterns of the black dwarf mangrove suggest a distinctive seasonal pattern similar to the red mangrove in poor condition, with the only difference being no significant seasonal change in LAI. The low Chla content during the dry season could be the result of increasing soil temperature and decreasing humidity (Sherman et al. 2000), as these trees are typically close or adjacent to drier uplands (i.e. saltpan). Ball & Critchley (1982) reported that shaded leaves of *Avicennia germinans* can have a higher Chla content during the dry season, suggesting a more intolerant pattern to light

availability (Feller et al. 2007), and thus revealing a high vulnerability to photoinhibition (Cheeseman 1994).

Within healthy black mangrove forest, Gratani (1997) suggested that the major acclimation of leaves in a lower canopy with low irradiance is the development of thinner leaves. In my study, I did not measure leaf thickness. However, the apparent lack of change in leaf morphology may suggest that healthy *Avicennia germinans* is well adapted to shaded conditions as mentioned by Attiwill & Clough (1980). In the present study, the lack of change in LAI and Chla for the shaded leaves may suggest that this forest does not present significant seasonal changes.

Monitoring the seasonal development of mangrove species and conditions along a mixed environment is important for future research, particularly when dealing with studies that examine remotely sensed data, carbon allocation, or biomass. The observed differences between seasons for some of the species and conditions examined would indicate a clear pattern that this study site is dependent primarily on fresh water availability. Given the large geographic extent and inaccessibility of this type of subtropical canopy, remote-sensing image acquisitions are commonly used to monitor and map mangroves. In particular, for degraded systems, remotely sensed imagery is often used to monitor parameters directly related to the LAI and/or chlorophyll content. For example, many estimates of biomass or LAI from remote sensing platforms are dependent on standard vegetation indices (e.g. the normalized difference vegetation index), which are calculated from spectral reflectance directly related to the canopy thickness and leaf Chla content (Jensen 2005). Consequently, knowing the seasonal changes in these parameters would allow remote sensing specialists to identify the optimal time to acquire imagery for accurate biomass or LAI mapping and monitoring. Moreover, collecting these data on an annual basis could be beneficial for monitoring potential impacts on these particular ecosystems resulting from abnormal years of precipitation and/or temperature.

2.5 References

- Agraz-Hernández, C. M. (1999). Reforestación experimental de manglares en ecosistemas lagunares estuarinos de la costa noroccidental de México. PhD dissertation, Universidad Autónoma de Nuevo León, Monterrey.
- Alvarez, L. R. (1977). Estudio hidrobiológico de los esteros del Astillero Urias y la Sirena, adyacentes a Mazatlán, Sinaloa, México. MSc dissertation, Universidad Nacional Autónoma de México, Mazatlán.
- Attiwill, P. M., and Clough, B. F. (1980). Carbon dioxide and water vapor exchange in the white mangrove. *Photosynthetica*, 14, 40–47.
- Ball, M. C., and Critchley, C. (1982). Photosynthetic response to irradiance by the grey mangrove, *Avicennia marina*, grown under different light regimes. *Plant Physiology*, 70, 1101–1106.
- Berger, U., Rivera-Monroy, V. H., Doyle, T. W., Dahdouh-Guebas, F., and others. (2008). Advances and limitations of individual-based models to analyze and predict dynamics of mangrove forest: a review. *Aquatic Botany*, 89, 260–274
- Blackburn, G. A. (2007). Hyperspectral remote sensing of plant pigments. *Journal of Experimental Botany*, 58, 855–867.
- Cannicci, S., Burrows, D., Fratini, S., Smith, T. J. III., Offenberg, J., and Dahdouh-Guebas, F. (2008). Faunal impact on vegetation structure and ecosystem function in mangrove forests: a review. *Aquatic Botany*, 89, 186–200.
- Cheeseman, J. M. (1994). Depressions of photosynthesis in mangrove canopies. In: Baker, N. R., and Bowyer, J. R. (1994). *Photoinhibition of photosynthesis—from molecular mechanisms to the field*. Oxford: Bios Scientific Publishers.
- Ciganda, V., Gitelson, A., and Schepers, J. (2009). Non-destructive determination of maize leaf and canopy chlorophyll content. *Journal of Plant Physiology*, 166, 57–167.
- Decagon Devices Inc. (2013). LAI LP-80 manual. Available online at: <http://www.decagon.com/> accessed June 26, 2013.
- Duke, N. C., Ball, M. C., and Ellison, J. C. (1998). Factors influencing biodiversity and distributional gradients in mangroves. *Global Ecological Biogeography*, 7, 27–47.
- Ellison, J. C. (2008). Long-term retrospection on mangrove development using sediment cores and pollen analysis: a review. *Aquatic Botany*, 89, 93–104.
- Ellison, A. M., and Farnsworth, E. J. (1993). Seedling survivorship, growth and response to disturbance in Belizean mangal. *American Journal of Botany*, 80, 1137–1145.
- Evain, S., Flexas, J., and Moya, I. (2004). A new instrument for passive remote sensing: 2. Measurement of leaf and canopy reflectance changes at 531 nm and their relationship with photosynthesis and chlorophyll fluorescence. *Remote Sensing of Environment*, 91, 175–185.
- Farnsworth, E. J., and Ellison, A. M. (1996). Sun-shade adaptability of the red mangrove, *Rhizophora mangle* (Rhizophoraceae): changes through ontogeny at several levels of biological organization. *American Journal of Botany*, 83, 1131–1143.
- Feller, I. C., Whigham, D. F., O'Neill, J. P., and McKee, K. L. (1999). Effects of nutrient enrichment on within-stand cycling in a mangrove forest. *Ecology*, 80, 2193–2205.

- Feller, I. C., Lovelock, C. E., and McKee, K. L. (2007). Nutrient addition differentially affects ecological processes of *Avicennia germinans* in nitrogen versus phosphorus limited mangrove ecosystems. *Ecosystems*, 10, 347–359.
- Field, C. (1995). Impact of expected climate change on mangroves. *Hydrobiologia*, 295, 75–81.
- Flores-Verdugo, F., Day, J. W., and Briseño-Dueñas, R. (1987). Structure, litter fall, decomposition, and detritus dynamics of mangroves in a Mexican coastal lagoon with an ephemeral inlet. *Marine Ecology Progress Series*, 35, 83–90.
- Gilman, E. L., Ellison, J., Duke, N. C., and Field, C. (2008). Threats to mangrove from climate change and adaptation options: a review. *Aquatic Botany*, 89, 237–250.
- Gratani, L. (1997). Canopy structure, vertical radiation profile and photosynthetic function in a *Quercus ilex* evergreen forest. *Photosynthetica*, 33, 139–149.
- Hogarth, P. J. (1999). *The biology of mangroves*. New York: Oxford University Press.
- INEGI (Instituto Nacional de Estadística y Geografía). (2010). Anuario estadístico del estado de Sinaloa. Mexico city: INEGI.
- Jensen, J. R. (2005). *Introductory digital image processing: a remote sensing perspective*. London: Pearson Education.
- Johnson, R. A., and Wichern, D. W. (1992). *Applied multivariate statistical analysis*. Englewood Cliffs: Prentice-Hall.
- Komiyama, A., Eong, O. J., and Pongpan, S. (2008). Allometry, biomass, and productivity of mangrove forest: a review. *Aquatic Botany*, 89, 128–137.
- Kovacs, J. M., Wang, J., and Flores-Verdugo, F. (2005). Mapping mangrove leaf area index at the species level using IKONOS and LAI-2000 sensors for the Agua Brava Lagoon, Mexican Pacific. *Estuaries Coastal and Shelf Science*, 62, 377–384.
- Kovacs, J. M., Zhang, C., and Flores-Verdugo, F. (2008). Mapping the condition of mangroves of the Mexican Pacific using C-band ENVISAT ASAR and Landsat optical data. *Ciencias Marinas*, 34, 407–418.
- Kovacs, J. M., King, J. M. L., Flores-de-Santiago, F., and Flores-Verdugo, F. (2009). Evaluating the condition of a mangrove forest of the Mexican Pacific based on an estimated leaf area index mapping approach. *Environmental Monitoring and Assessment*, 157, 137–149.
- Kovacs, J. M., Liu, Y., Zhang, C., Flores-Verdugo, F., and Flores-de-Santiago, F. (2011). A field based statistical approach for validating a remotely sensed mangrove forest classification scheme. *Wetlands Ecology and Management*, 19, 409–421.
- Kristensen, E., Bouillon, S., Dittmar, T., and Marchand, C. (2008). Organic carbon dynamics in mangrove ecosystems: a review. *Aquatic Botany*, 89, 201–219.
- Lacerda, L. D. (2002). *Mangrove ecosystems: function and management*. Berlin: Springer.
- Lichtenthaler, H. K., and Wellburn, A. R. (1983). Determinations of total carotenoids and chlorophylls a and b in leaf extracts in different solvents. *Biochemical Society Transactions*, 11, 591–592.
- Lugo, A. E., Evink, G., Brinson, M. M., Broce, A., and Snedaker, S. C. (1975). Diurnal rates of photosynthesis, respiration and transpiration in mangrove forests in south Florida. In: Golley, F. B., and Medina, E. (1975). *Tropical ecological systems: trends in terrestrial and aquatic research*. Berlin: Springer.

- McKee, K. L. (1995). Interspecific variation in growth, biomass partitioning, and defensive characteristics of neotropical mangrove seedlings: response to light and nutrient availability. *American Journal of Botany*, 82, 299–307.
- Moroyoqui-Rojo, L. (2005). Análisis de la eficiencia en la remoción de nutrientes en un sistema experimental silvo pesquero (manglar-ictiopfauna) con recirculación de agua. MSc dissertation, CIDIR Instituto Politécnico Nacional de México, Guasave.
- Nagelkerken, I., Blaber, S. J. M., Bouillon, S., Green, P., and others. (2008). The habitat function of mangrove for terrestrial and marine fauna: a review. *Aquatic Botany*, 89, 155–185
- Raven, P. H., Evert, R. F., and Eichhorn, S. E. (1992). *Biology of plants*. New York: W. H. Freeman & Company Press.
- Ridd, P. V., and Stieglitz, T. (2002). Dry season salinity changes in arid estuaries fringed by mangroves and saltflats. *Estuaries, Coastal and Shelf Science*, 54, 1039–1049.
- Rogers, K., Saintilan, N., and Heijnis, H. (2005). Mangrove encroachment of salt marsh in Western Port Bay, Victoria: the role of sedimentation, subsidence, and sea level rise. *Estuaries*, 28, 551–559.
- Saenger, P. (2002). *Mangrove ecology, silviculture and conservation*. Dordrecht: Kluwer Academic Publishers.
- Saintilan, N., and Wilton, K. (2001). Change in the distribution of mangroves and saltmarshes in Jervis Bay, Australia. *Wetlands Ecology and Management*, 9, 409–420.
- Schulze, E. D., and Caldwell, M. M. (1994). *Ecophysiology of photosynthesis*. Berlin: Springer-Verlag.
- Sherman, R. E., Fahey, T. J., and Battles, J. J. (2000). Small-scale disturbance and regeneration dynamics in a neotropical mangrove forest. *Journal of Ecology*, 88, 165–178.
- Smith, T. J. (1992). *Forest structure*. In: Robertson, A. I., and Alongi, D. M. (1992). *Tropical mangrove ecosystems*. Coastal and Estuarine Studies No. 41. Washington D.C.: American Geophysical Union.
- Snedaker, S. C. (1995). Mangroves and climate change in the Florida and Caribbean region: scenarios and hypotheses. *Hydrobiologia*, 295, 43–49.
- Steinke, T. D., Holland, A. J., and Singh, Y. (1993). Leaching losses during decomposition of mangrove leaf litter. *South African Journal of Botany*, 59, 21–25.
- Tomlinson, P. B. (1986). *The botany of mangroves*. Cambridge: Cambridge University Press.
- Walters, B. B., Rönnbäck, P., Kovacs, J. M., Crona, B., and others. (2008). Ethnobiology, socio-economics and management of mangrove forests: a review. *Aquatic Botany*, 89, 220–236.
- Wilhelm, W. W., Ruwe, K., and Schlemmer, M. R. (2000). Comparison of three leaf area index meters in a corn canopy. *Crop Sciences*, 40, 1179–1183.
- Zhang, C., Liu, Y., Kovacs, J. M., Flores-Verdugo, F., Flores-de-Santiago, F., and Chen, K. (2012). The hyperspectral response to varying levels of leaf pigments collected from a degraded mangrove forest. *Journal of Applied Remote Sensing*, 6, 063501.

Chapter 3

3 Assessing the utility of a portable pocket instrument for estimating seasonal mangrove leaf chlorophyll content.²

3.1 Introduction

Both chlorophyll-a (Chla) and chlorophyll-b (Chlb) are considered two of the most important leaf pigments, as they are accountable for the majority of the conversion of light energy into stored chemical energy within plants (Blackburn 2007). Chla is essential in the energy phase of photosynthesis whereas Chlb captures light at a slightly different wavelength (Eichhorn et al. 2005). Moreover, the pigment content variation in total chlorophyll (i.e., Chla+Chlb) between and within species is important for several reasons. First, the amount of solar radiation absorbed by a leaf depends on the foliar concentrations of photosynthetic pigments, and therefore low concentrations of chlorophylls can directly limit photosynthetic activity and hence primary production (Fillela et al. 1995). Second, pigmentation can be directly related to physiological stress because concentrations of chlorophylls tend to decrease under stress and during senescence (Peñuelas and Fillela 1998). Consequently, quantifying these proportions can provide important information regarding the relationships between plants and their environment.

Traditionally, chemical methodologies for pigment contents are determined using extraction in an organic solvent, which is followed by the spectrophotometric determination of absorbance by the extracted pigment solution (Wellburn 1994). The actual conversion of the absorbance values to concentration of pigments are then determined using empirical model equations (Hendry and Price 1993, Richardson et al. 2002). Unfortunately, the chemical method of pigment extraction is a destructive process

² A version of this chapter has been published: **Flores-de-Santiago F.**, Kovacs JM., Flores-Verdugo F. (2013). Assessing the utility of a portable pocket instrument for estimating seasonal mangrove leaf chlorophyll content. **Bulletin of Marine Science**. 89(2), 621-633. (<http://dx.doi.org/10.5343/bms.2012.1032>).

that can be relatively expensive and, most importantly, time consuming. A recent alternative to this strategy is the use of non-destructive optical methods for measurement and estimation of leaf pigment contents (Meroni et al. 2009). Optical methods generally yield a chlorophyll index value that expresses, or can potentially be converted to, relative chlorophyll pigment concentration (Goncalves et al. 2008).

The Opti-Sciences CCM-200 Chlorophyll Content Meter is marketed as an instrument that is pocket portable, inexpensive, rapid and easy to use, and provides fast, accurate chlorophyll index readings on the intact leaves of plants, particularly for crops. The CCM-200 avoids the need for grinding or destructive chlorophyll assays (Opti-Sciences 2002), does not require hazardous compounds or specially trained personnel, and the data acquired can be rapidly downloaded for *a posteriori* computer-based analysis (Cate and Perkins 2003). Moreover, the CCM-200 could be useful for improving health assessments such as plant stress and leaf senescence (Biber 2007). The CCM-200 operates by differential absorption of light at two wavelengths, one in the near infrared (931 nm), and one through the peak absorbance of chlorophyll (653 nm). Using calibrated light emitting diodes and receptors, this unit calculates the Chlorophyll Content Index (CCI), which is defined as the ratio of transmission at 931 nm to 653 nm through a leaf sample (Opti-Sciences 2002).

Under conditions of stress (e.g., salinity, drought, high irradiance, and high temperature) plants are often exposed to more radiant energy than is needed for photosynthesis and this places severe limits on plant growth (Ehrenfeld 1990). The mechanisms for disposing of excess energy are limited, manifesting changes within the photosystem as a function of pigments and heat dissipation (Neumann et al. 2008). Mangrove ecosystems are particularly sensitive to periodic, short-term flooding due to coastal tide dynamics (Young et al. 1995) which makes them particularly sensitive to slight modifications in the environment, whether anthropogenic or naturally induced, which can result in considerable stress. For example, Flores-de-Santiago et al. (2012) reported that in a sub-tropical mangrove forest where fresh water availability is extremely seasonal, precipitation patterns affect the leaf Chl_a content variation resulting in an increase in leaf Chl_a content during the rainy season in poor/dwarf stands of

Laguncularia racemosa, *Rhizophora mangle*, and *Avicennia germinans*. Consequently, monitoring such stress using a rapid and relatively inexpensive instrument for estimating pigment variation could be extremely useful when trying to assess ecological impacts.

Given the alarming reports of recent mangrove loss (Valiela et al. 2001, Duke et al. 2007, Polidoro et al. 2010) and the importance of these forests for local communities (Walters et al. 2008), organic carbon dynamics (Kristensen et al. 2008), climate change (Gilman et al. 2008), fauna interactions (Nagelkerken et al. 2008), and primary productivity (Komiyama et al. 2008), a cost-efficient, user friendly, and rapid technique for monitoring pigments could be extremely useful for resource management and scientists studying and/or monitoring mangroves. Consequently, the purpose of this investigation is to determine the feasibility of using CCI, the unit of measure of the CCM-200 portable Chlorophyll Content Meter, as an accurate estimator of the seasonal variation of leaf chlorophyll contents, Chla, Chlb, and total chlorophyll (TChl) for a wide range of species under various conditions in a mangrove forest representing a degraded state.

3.2 Materials and Methods

The study was conducted within the Urias estuary, which is positioned on an alluvial plain that extends along the Pacific coast within the Mexican state of Sinaloa (23° 10' N and 106° 20' W). Located in a tropical sub-humid zone, this system comprises of 800 ha that includes tidal channels, seasonal flood plains and a substantial mangrove community (Flores-Verdugo et al. 1987). The mean annual air temperature ranges from 24 to 26 °C and the annual total precipitation, which occurs primarily in the summer, ranges between 800 to 1000 mm (INEGI 2010). The system supports three dominant species of mangrove: red mangrove (*R. mangle*), black mangrove (*A. germinans*), and white mangrove (*L. racemosa*) (Flores-de-Santiago et al. 2012). Moreover, based on biophysical characteristics and species (Kovacs et al. 2011), this mangrove community can be classified according to three classes: healthy and dwarf black mangrove, healthy and poor condition red mangrove, and healthy and poor condition white mangrove. The poor condition and dwarf mangroves (i.e. stressed) are located mostly inland and in small channels with little tidal influence whereas most of the healthy mangroves are located

along the main channels where daily tidal flushing is common. Recent hydrological modifications, including diversions for aquaculture ponds and new road constructions, may have resulted in this degraded state. This situation is similar to what is occurring in another mangrove system just south of this area (Kovacs et al. 2005, Kovacs et al. 2008, Kovacs et al. 2009).

In this study the fieldwork was conducted along the south end of the Urías channel at the end of the dry (May) and the end of the rainy (October) seasons in 2010. I selected three representative trees for each mangrove species along the system. From each tree, 10 random leaves were selected for the CCM-200 readings and pigment chemical analysis assessment. Following Biber (2007), I clipped one leaf between the 3rd to 5th leaves from the tip of each apical branch so that only mature leaves were collected. A total of 30 samples from each class of mangrove were collected. For each sample four measurements were taken from the central portion of the leaf with a hand held Chlorophyll Content Meter CCM-200 (Opti-Sciences, Tyngsboro, Massachusetts, USA) while avoiding the midrib. This instrument has a 0.71 cm² measurement area, and calculates a Chlorophyll Content Index (CCI) based on transmittance measurements at 653 and 931 nm. The claimed accuracy of the CCM-200 is ± 1.0 CCI units and this instrument has the advantage of being able to measure CCI directly from the leaves in the field (Opti-Sciences 2002). Following the CCM-200 measurements, all leaves were immediately placed in plastic bags and stored in a cooler at around 4 °C prior to transportation to the laboratory for chemical pigment content assessment.

With regards to the actual chlorophyll composition, one 1.25 cm² leaf circle sample was cut out of each leaf using a circular metal pipe, again taking care to avoid the midrib. This leaf material was then crushed and dissolved in 100 ml of acetone at 80%. Each sample for the pigment assessment was filtered through a GF/C Whatman of 47mm pore size. The absorbance was measured at the Chla and Chlb peaks (around 646 and 663 nm) using a JascoV-530UV-VIS spectrophotometer (Jasco Inc., Great Dunmow, UK). Chla and Chlb were then calculated according to the Lichtenthaler and Wellburn (1983) equations. TChl was calculated from the sum of Chla and Chlb. The six classes of mangrove were separated according to the two distinct seasons (dry and rainy). For each

season, I used the coefficient of determination (R^2) and analysis of variance F -test (ANOVA) as a first approach in order to examine the linear association between pigment chemical analysis (Chla, Chlb, and TChl) and the corresponding CCI readings.

Differences in the regression lines by class between the dry and rainy seasons were tested using an analysis of covariance F -test (ANCOVA). The ANCOVA tests were also used to examine differences between the regression lines from the poor/dwarf and healthy classes for all species.

3.3 Results

Figure 3.1 depicts the R^2 and F -test ANOVA observed values for each of the linear regressions ($n=30$ /class). The Chla regression models presented significant F and higher R^2 values (Fig. 3.1) when plotted with poor/dwarf stands during the dry season (Fig. 3.1 a, c, e). In contrast, healthy stands recorded higher R^2 and F -observed values during the rainy season even though for both seasons the slopes were lower than for the stressed plants (Fig. 3.1 b, d, f). However, all three stressed classes (poor/dwarf) presented higher overall R^2 when compared to the healthy trees (Fig. 3.1). Although the Chla regression models showed no apparent differences in the slopes between the dry and rainy seasons for some classes, there were significant differences calculated ($p=0.05$) between the slopes according to the ANCOVA F -test results for all classes except the *A. germinans* healthy condition (Table 3.1). *L. racemosa* healthy condition recorded the lowest R^2 of 0.36 during the dry season (Fig. 3.1 f). In addition, no significant difference ($p<0.05$) was only found in *R. mangle* between the poor and healthy stands during the dry season (Table 3.2).

Although the Chla regression models showed strong linear associations with the CCI, the Chlb were found to be less well correlated, having both lower R^2 and F -observed values (Fig. 3.2). Chlb samples did not fit well to the linear models with the exception of the *A. germinans* dwarf class during the dry season with a R^2 of 0.80 (Fig. 3.2 a). Interestingly, *R. mangle* and *L. racemosa* healthy classes (Fig. 3.2 7d and f) had the lowest R^2 and F -observed values for both seasons. *A. germinans* dwarf and healthy, as well as *R. mangle* poor conditions were the only classes that did not record differences between the regression lines of Chlb during both seasons (Table 3.3). Moreover, *R.*

mangle rainy was the only class that did not present significant differences between the regression lines of the poor and healthy stands (Table 3.4).

With regards to TChl, the linear models showed a similar pattern to those of the Chla with slightly lower R^2 values for all six classes during both seasons (Fig. 3.3). The ANCOVA analysis between the dry and rainy season linear equations showed significant differences for all six mangrove classes (Table 3.5). Moreover, the ANCOVA analysis between the poor/dwarf and healthy classes showed no differences in the linear regressions in the *R. mangle* during both the dry and rainy seasons (Table 3.6).

Table 3.1: Analysis of covariance F-test (ANCOVA) of Chlorophyll-a (Chla) and CCM-200 readings between the regression lines from the dry and rainy season. LR: *L. racemosa*, RM: *R. mangle*, AG: *A. germinans*. * Significant F-observed values at $p=0.05$

Species and class	Source of variation	df	MS	F
LR poor	Adjusted means	1	261.7	40.9*
	Error	57	6.4	
LR healthy	Adjusted means	1	1161.6	118.5*
	Error	57	9.8	
RM poor	Adjusted means	1	296	18.3*
	Error	57	16.2	
RM healthy	Adjusted means	1	397.1	28.4*
	Error	57	14	
AG dwarf	Adjusted means	1	424.7	82*
	Error	57	5.2	
AG healthy	Adjusted means	1	52.6	3.7
	Error	57	14.3	

Table 3.2: Analysis of covariance F-test (ANCOVA) of Chlorophyll Content Index (CCI) and corresponding Chlorophyll-a (Chla) between the regression lines from the poor/dwarf and healthy conditions. LR: *L. racemosa*, RM: *R. mangle*, AG: *A. germinans*. * Significant F-observed values at p=0.05

Species and class	Source of variation	df	MS	F
LR dry	Adjusted means	1	566.7	23.9*
	Error	57	23.7	
RM dry	Adjusted means	1	9.6	0.4
	Error	57	22.6	
AG dry	Adjusted means	1	1307	137.6*
	Error	57	9.5	
LR rainy	Adjusted means	1	53.7	21.5*
	Error	57	2.5	
RM rainy	Adjusted means	1	96.7	9.9*
	Error	57	9.8	
AG rainy	Adjusted means	1	428.7	43.3*
	Error	57	9.9	

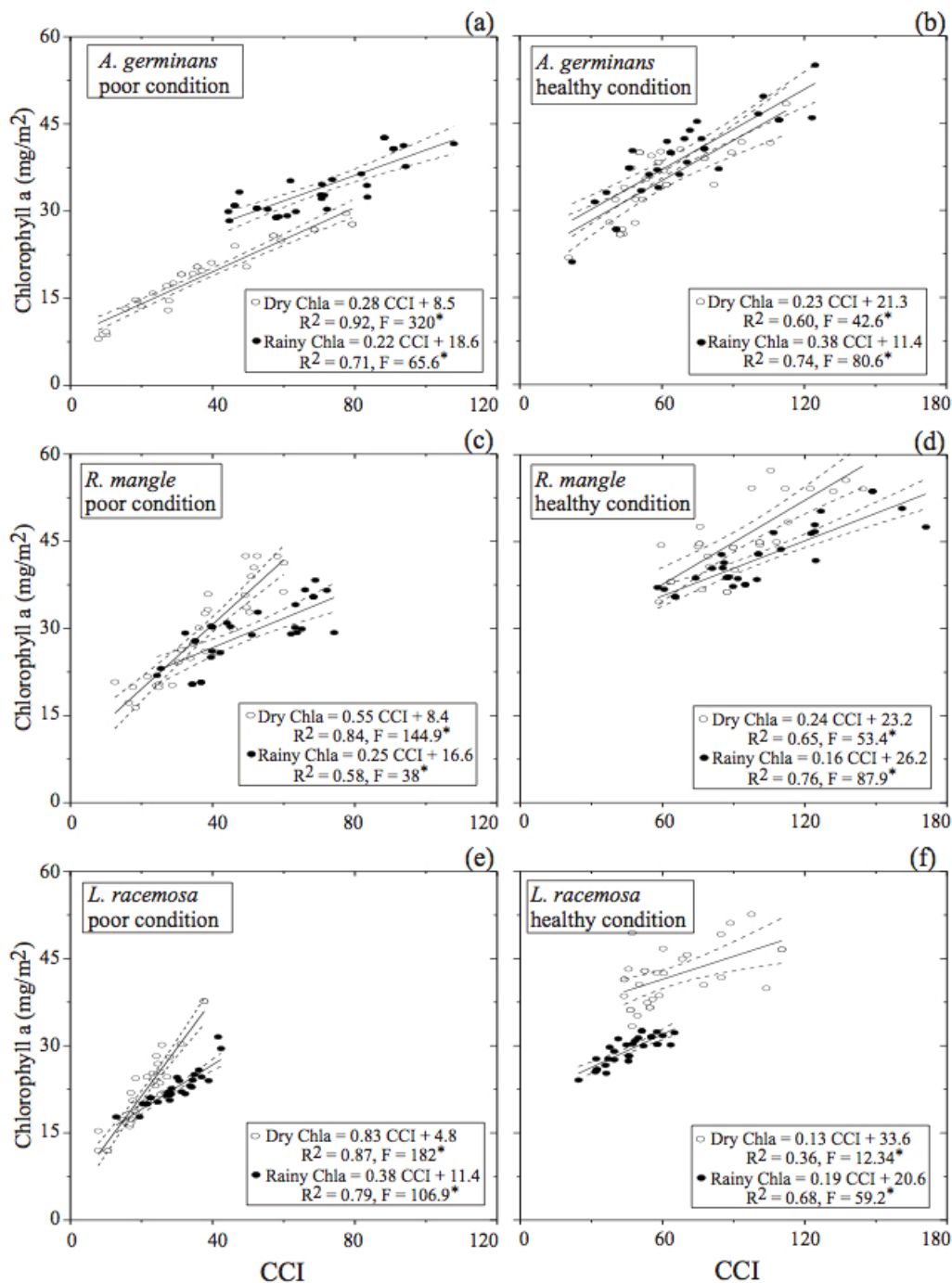


Figure 3.1: Seasonal scatter plots and fitted linear regression lines of Chlorophyll Content Index (CCI) using a CCM-200 instrument against the chlorophyll-a (Chla) derived from chemical analysis (n=30). Each graph depicts the linear equation with 95% confidence

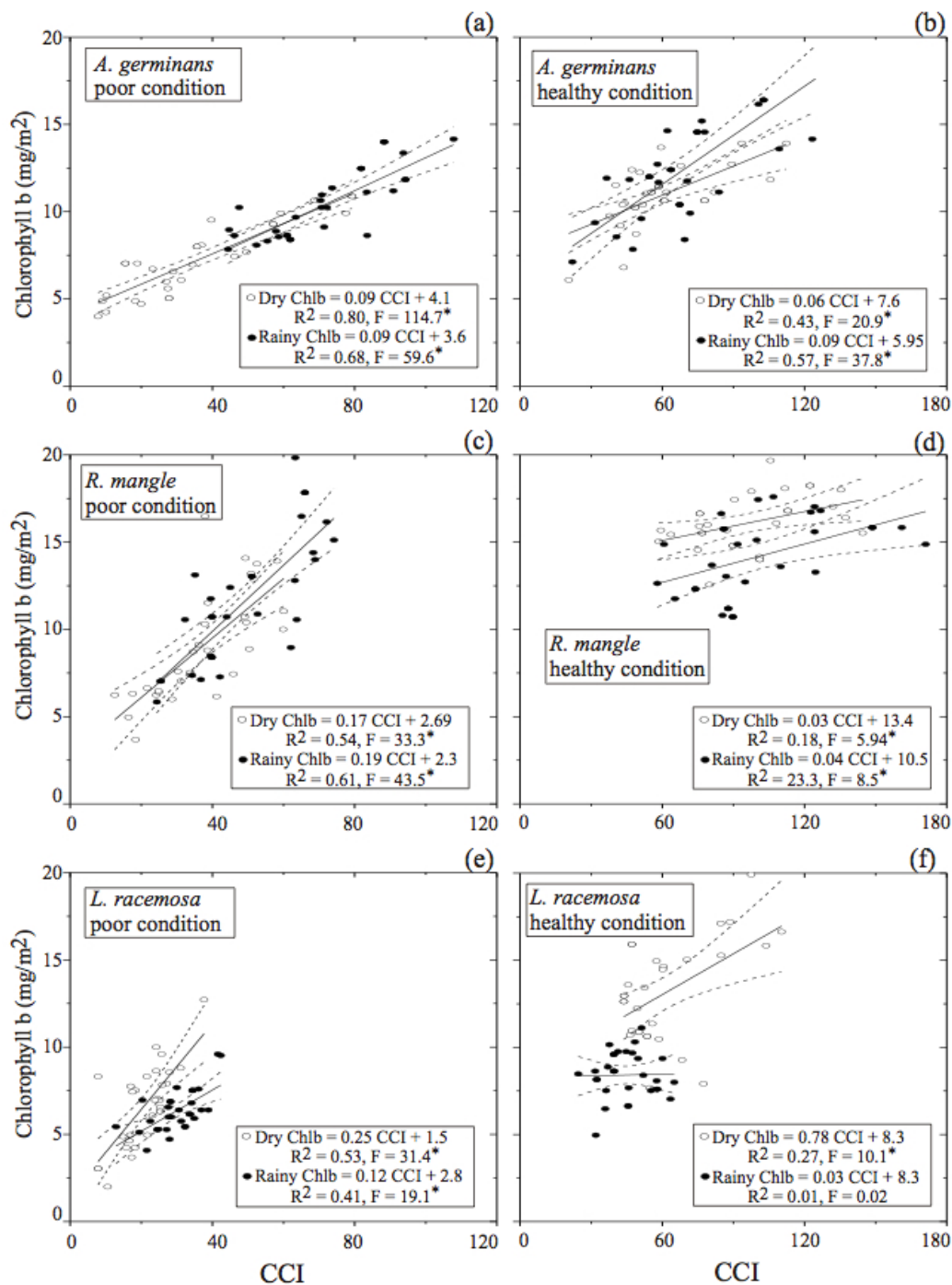


Figure 3.2: Seasonal scatter plots and fitted linear regression lines of Chlorophyll Content Index (CCI) using a CCM-200 instrument against the chlorophyll-b (Chlb) derived from chemical analysis (n=30). Each graph depicts the linear equation with 95% confidence

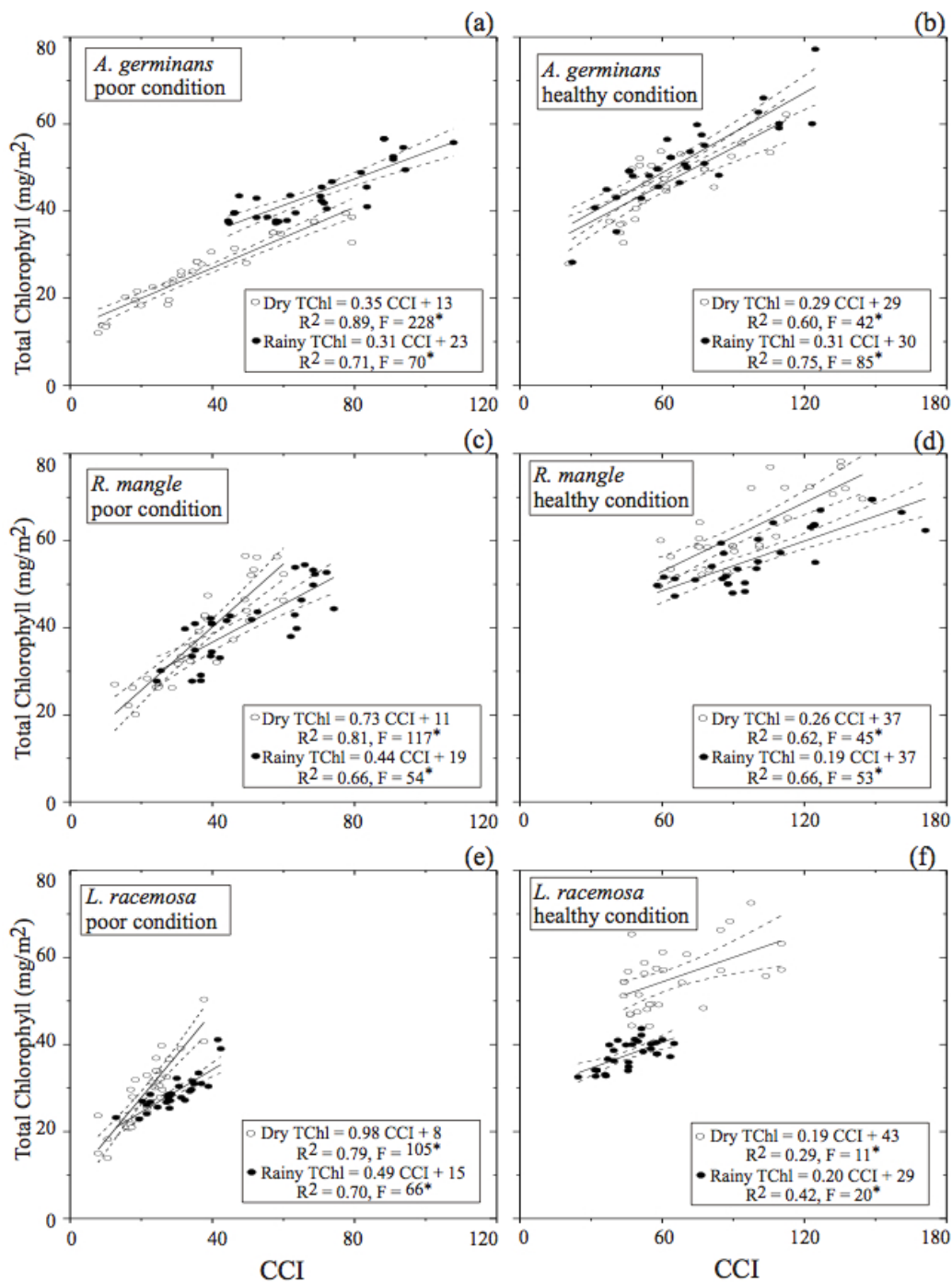


Figure 3.3: Seasonal scatter plots and fitted linear regression lines of Chlorophyll Content Index (CCI) using a CCM-200 instrument against the total chlorophyll (TChl) derived from chemical analysis (n=30). Each graph depicts the linear equation with 95% confidence

Table 3.3: Analysis of covariance F-test (ANCOVA) of Chlorophyll-b (Chlb) and CCM-200 readings between the regression lines from the dry and rainy season. LR: *L. racemosa*, RM: *R. mangle*, AG: *A. germinans*. * Significant F-observed values at $p=0.05$

Species and class	Source of variation	df	MS	F
LR poor	Adjusted means	1	40	20*
	Error	57	2	
LR healthy	Adjusted means	1	159.3	37*
	Error	57	4.3	
RM poor	Adjusted means	1	2.4	0.5
	Error	57	5.1	
RM healthy	Adjusted means	1	62.7	21.6*
	Error	57	2.9	
AG dwarf	Adjusted means	1	0.01	0.009
	Error	57	1.1	
AG healthy	Adjusted means	1	8.4	2.6
	Error	57	3.2	

Table 3.4: Analysis of covariance F-test (ANCOVA) of Chlorophyll Content Index (CCI) and corresponding Chlorophyll-b (Chlb) between the regression lines from the poor/dwarf and healthy conditions. LR: *L. racemosa*, RM: *R. mangle*, AG: *A. germinans*. * Significant F-observed values at $p=0.05$

Species and class	Source of variation	df	MS	F
LR dry	Adjusted means	1	31.4	6.2*
	Error	57	5.1	
RM dry	Adjusted means	1	47.3	9.9*
	Error	57	4.8	
AG dry	Adjusted means	1	44.4	31.7*
	Error	57	1.4	
LR rainy	Adjusted means	1	19.8	12.4*
	Error	57	1.6	
RM rainy	Adjusted means	1	7.1	1
	Error	57	6.8	
AG rainy	Adjusted means	1	75.3	26.9*
	Error	57	2.8	

Table 3.5: Analysis of covariance F-test (ANCOVA) of total chlorophyll (TChl) and CCM-200 readings between the regression lines from the dry and rainy season. LR: *L. racemosa*, RM: *R. mangle*, AG: *A. germinans*. * Significant F-observed values at $p=0.05$

Species and class	Source of variation	df	MS	F
LR poor	Adjusted means	1	424.6	33.4*
	Error	57	12.7	
LR healthy	Adjusted means	1	2232	101.5*
	Error	57	22	
RM poor	Adjusted means	1	235	8.3*
	Error	57	28.3	
RM healthy	Adjusted means	1	776.1	34.3*
	Error	57	22.6	
AG dwarf	Adjusted means	1	515.7	53.2*
	Error	57	9.7	
AG healthy	Adjusted means	1	113.8	4.9*
	Error	57	23.1	

Table 3.6: Analysis of covariance F-test (ANCOVA) of Chlorophyll Content Index (CCI) and corresponding total chlorophyll (TChl) between the regression lines from the poor/dwarf and healthy conditions. LR: *L. racemosa*, RM: *R. mangle*, AG: *A. germinans*. * Significant F-observed values at $p=0.05$

Species and class	Source of variation	df	MS	F
LR dry	Adjusted means	1	1026.7	24.4*
	Error	57	42	
RM dry	Adjusted means	1	24.3	0.6
	Error	57	41.2	
AG dry	Adjusted means	1	1950	121.9*
	Error	57	16	
LR rainy	Adjusted means	1	129.7	19.1*
	Error	57	6.8	
RM rainy	Adjusted means	1	60.1	2.4
	Error	57	25.5	
AG rainy	Adjusted means	1	842.9	49.5*
	Error	57	17	

3.4 Discussion

Portable CCM-200 instruments have been used in the estimation of leaf chlorophyll concentrations in tropical forests (e.g., Goncalves et al. 2008), but not many other types of environments (Cate and Perkins 2003, Biber 2007) including subtropical mangrove forests. For this investigation, it is evident that there was a moderate to strong linear relationship between the CCI and the pigments especially with Chla and TChl. Such strong linear co-variability has been previously reported by Andrew et al (2002) and Ghasemi et al (2011). In my study, the coefficient of determination between the CCI and the pigments present different amounts of variability between the two seasons and within the six classes. It had been noted previously that there is a seasonal variation in leaf Chla content in this particular subtropical mangrove forest (Flores-de-Santiago et al. 2012), as a consequence there should be differences between the seasons in the estimation of pigments using the CCM-200.

The results from this investigation provide strong evidence that the CCI, recorded by the CCM-200 device, can be used for pigment content estimation of Chla and TChl. In particular, CCI values were most strongly correlated with Chla as determined by the absorbance of extracted pigments. With regards to Chla contents, my values were much lower (0.001-0.005 mg/cm²), compared to those reported by Andrew et al. (2002) (0.000-0.040 mg/cm²). The strong linear association between the CCI and the Chla was previously reported by Andrew et al. (2002), especially in the lower Chla values. Andrew et al. (2002) showed that Chla contents higher than 0.020 mg/cm² starting to present heteroskedasticity (i.e. and increase in the variability along the fitted regression line), increasing the error in predicting Chla from the regression equation. Therefore, the low Chla content presented in this sub-tropical mangrove leaves make the CCM-200 an ideal instrument for Chla estimation.

Several factors may have influenced the cases where low relationships were observed in this study (e.g., Chlb). Among them, an important source of error with the CCM-200 may be the wavelengths used. The simple ratio calculation used to derive the CCI (% transmittance at 931 nm divided by the % transmittance at 653 nm) can be influenced by leaf optical properties. For example, the attenuation of light in the 931 nm

infrared wavelength is assumed to correct for the leaf structural characteristics that may cause variability in the 653 nm region (Markwell et al. 1995). However, the wavelength used in the CCI ratio at 653 nm is located between the two maximum absorbance peaks of both Chla (662 nm) and Chlb (642 nm). Typically in this specific region of the spectrum (653 nm) the Chla absorbance curve for vegetation starts to increase, while the Chlb curve decrease. Therefore, the wavelength used in the CCI ratio at 653 nm may result in a higher variability for estimation of either chlorophyll molecule, compared to more targeted wavelength used to determine either Chla or Chlb alone.

Another problem could be attributed to leaf thickness and/or leaf dryness as a result of excessive environmental salinity levels. Moreover, the seasonal pigment variation, especially in the poor classes, could possibly influence the variability of the samples and thus the optical properties of the leaves (Flores-de-Santiago et al. 2012). Previous studies have shown (Sobrado 1999, Macfarlane and Burchett 2001, Naidoo 2006) that forests of *Avicennia species* are known to be very sensitive to stress factors such as excess salinity and high heavy metal content. For this lagoon, a previous study did show high heavy metal content (Cd, Co, Cr, Cu, Fe, Mn, Ni, Pb, and Zn) in the substrate (Marmolejo et al. 1990). Moreover, given that the majority of the *A. germinans* leaves, particularly the dwarf ones, are quite narrow and small and that the CCM-200 window is quite large (0.90 cm diameter), higher variability in measurements may be expected for this species compared to the other two mangroves (Biber 2007). Yet another potential factor influencing variability and thus the relationships between pigments and CCI is shaded leaves (Richardson et al. 2002). In particular, *R. mangle* contains a dense canopy which often contains thick leaves with a dense package of chlorophyll. This thickness in all the healthy mangrove classes may prevent enough of the LED light at 653 nm to be properly transmitted through the leaf (Biber 2007). Specifically, *R. mangle* have a thick non-assimilatory cell layer over the photosynthetic cell (Koizumi et al. 1998). This layer may reflect more of the light than what would be absorbed by Chlb in the red mangrove, which could have resulted in the observed weaker estimation.

In this study, the weakest predictors were observed when examining Chlb content. Fortunately, the quantification of Chla and TChl is more useful when trying to examine

photosynthetic performance and why previous investigators (e.g., Biber 2007) have focused on these pigments for crops and terrestrial forests. The R^2 values are higher for Chla than for Chlb, which could be explained by the fact that Chla concentrations per unit mass are typically double those of Chlb, and that the absorption feature in the red wavelengths of the former tends to obscure that of the latter (Blackburn 1998). The lower R^2 and F -observed values for the TChl compared to Chla are attributed to the poor estimation of Chlb in all six classes.

Although the coefficients of determination for the estimation of Chlb in some classes were highly variable, the relative high R^2 between the CCI and Chla contents suggests that the handheld CCM-200 can be used to predict Chla and TChl for a subtropical mangrove forest with an R^2 as high as 0.92 depending on the species and the season. Despite the aforementioned limitations, the CCM-200 has the potential to enable a fast, convenient, and non-destructive way of determining pigment content, making it a useful instrument when evaluating biophysical parameters for mangrove inventories. Moreover, the relative cheap cost of this device and ease of use makes it an ideal tool in countries where other traditional techniques are economically prohibitive. However, it is recommended that local regression equations must be developed especially in the tropics where the same mangrove species are under different environmental conditions. Given that this investigation examined the feasibility of the CCM-200 for chlorophyll estimation based on the most common species of mangrove found in the Americas, future considerations could include developing similar models for other mangrove species that dominate in other regions of the tropics and sub-tropics. Finally, it must be noted that a previous study has shown (Andrew, 2002) that measurements from the CCM-200 are similar to those collected using a rival commercially available instrument the SPAD-502. The CCM-200 differs most from the SPAD-502 in regards to the leaf area sampling size and cost of the instrument. The sampling area of the CCM-200 is ten times larger and the cost of the instrument approximately a third of that of the SPAD-502.

3.5 References

- Andrew, D., Richardson, S. P., and Graeme, P. B. (2002). An evaluation of noninvasive methods to estimate foliar chlorophyll content. *New Phytology*, 153, 185-194.
- Biber, P. D. (2007). Evaluating a chlorophyll content meter on three coastal wetland plant species. *Agriculture Food Environmental Science*, 1(2), 1-11.
- Blackburn, G. A. (1998). Quantifying chlorophylls and carotenoids at leaf and canopy scales: an evaluation of some hyperspectral approaches. *Remote Sensing Environmental*, 66, 273-285.
- Blackburn, G. A. (2007). Hyperspectral remote sensing of plant pigments. *Journal of Experimental Botany*, 58, 855-867.
- Cate, T. M., and Perkins, T. D. (2003). Chlorophyll content monitoring in sugar maple (*Acer saccharum*). *Tree Physiology*, 23, 1077-1079.
- Duke, N. C., Meynecke, J. O., Dittman, S., Ellison, A. M., Anger, K., Berger, U., Cannicci, S., Diele, K., Ewel, K. C., Field, C. D., Koedam, N., Lee, S. Y., Marchand, C., Nordhaus, I., and Dahdouh-Guebas, F. (2007). A world without mangroves?. *Science*, 317, 41-42.
- Ehrenfeld, J. G. (1990). Dynamics and processes of barrier island vegetation. *Aquatic Science*, 2, 437-480.
- Eichhorn, S., Everett, R., and Raven, P. (2005). *Biology of plants*. New York: W.H. Freeman and company Publishers.
- Fillela, I., Serrano, L., and Serra, J. (1995). Evaluating wheat nitrogen status with canopy reflectance indices and discriminant analysis. *Crop Science*, 35, 1400-1405.
- Flores-de-Santiago, F., Kovacs, J. M., and Flores-Verdugo, F. (2012). Seasonal changes in leaf chlorophyll *a* content and morphology in a sub-tropical mangrove forest of the Mexican Pacific. *Marine Ecology Progress Series*, 444, 57-68.
- Flores-Verdugo, F., Day, J. W., and Briseño-Dueñas, R. (1987). Structure, litter fall, decomposition, and detritus dynamics of mangroves in a Mexican coastal lagoon with an ephemeral inlet. *Marine Ecology Progress Series*, 35, 83-90.
- Ghasemi, M., Arzani, K., Yadollahi, A., Ghasemi, S., and Sarikhanikhorrani, S. (2011). Estimate of leaf chlorophyll and nitrogen content in Asian pear (*PyrusserotinaRehd.*) by CCM-200. *Notes Science Biology*, 3(1), 91-94.
- Gilman, E. L., Ellison, J., Duke, N., and Field, C. (2008). Threats to mangrove from climate change and adaptation options: a review. *Aquatic Botany*, 89, 237-250.
- Goncalves, J. F., Moreira dos Santos, J. U., and Alves da Silva, E. (2008). Evaluation of a portable chlorophyll meter to estimate chlorophyll concentrations in leaves of tropical wood species from Amazonian forest. *Hoehnea*, 35, 185-188.
- Hendry, G.F., and Price, A. H. (1993). *Stress indicators: chlorophylls and carotenoids*. London: Chapman & Hall.
- INEGI (Instituto Nacional de Estadística, Geografía e Informática). 2010. Anuario estadístico del estado de Sinaloa. INEGI. Mexico.
- Kovacs, J. M., Wang, J., Flores-Verdugo, F. (2005). Mapping mangrove leaf area index at the species level using IKONOS and LAI-2000 sensors for the Agua Brava Lagoon, Mexican Pacific. *Estuarine Coastal and Shelf Science*, 62, 377-384.
- Kovacs, J.M., Zhang, C., and Flores-Verdugo, F. (2008). Mapping the condition of mangroves of the Mexican Pacific using C-band ENVISAT ASAR and Landsat optical data. *Ciencias Marinas*, 34, 407-418.

- Kovacs, J. M., King, J. M. L., Flores de Santiago, F., and Flores-Verdugo, F. (2009). Evaluating the condition of a mangrove forest of the Mexican Pacific based on an estimated leaf area index mapping approach. *Environmental Monitoring Assessment*, 157, 137-149.
- Kovacs, J. M., Liu, Y., Zhang, C., Flores-Verdugo, F., and Flores de Santiago, F. (2011). A field based statistical approach for validating a remotely sensed mangrove forest classification scheme. *Wetlands Ecology and Management*, 19, 409-421.
- Kristensen, E., Bouillon, S., Dittmar, T., and Marchand, C. (2008). Organic carbon dynamics in mangrove ecosystems: a review. *Aquatic Botany*, 89, 201-219.
- Koizumi, M., Takahashi, K., and Mineuchi, K. (1998). Light gradients and the transverse distribution of chlorophyll fluorescence in mangrove and Camellia leaves. *Annals of Botany*, 81, 527-533.
- Komiyama, A., Ong, J. E., and Pongpan, S. (2008). Allometry, biomass, and productivity of mangrove forest: a review. *Aquatic Botany*, 89, 128-137.
- Lichtenthaler, H. K., and Wellburn, A. R. (1983). Determinations of total carotenoids and chlorophylls a and b in leaf extracts in different solvents. *Biochemical Society Transactions*, 11, 591-592.
- Macfarlane, G. R., and Burchett, M. D. (2001). Photosynthetic pigments and peroxidase activity as indicators of heavy metal stress in the grey mangrove, *Avicennia marina* (Forsk.) Vierh. *Marine Pollution Bulletin*, 42(3), 233-240.
- Markwell, J., Osterman, J. C., and Mitchell, J. L. (1995). Calibration of the Minolta SPAD-502 leaf chlorophyll meter. *Photosynthetica Research*, 46, 467-472.
- Marmolejo, R., Marmolejo, C., and Paez, O. (1990). Trace metals in tropical coastal lagoons bivalves, *Mytellastrigata*. *Bulletin of Environmental Contamination and Toxicology*, 45, 545-551.
- Meroni, M., Rossini, M., and Guanter, L. (2009). Remote sensing of solar induced chlorophyll fluorescence: Review of methods and applications. *Remote Sensing of Environment*, 113, 2037-2051.
- Nagelkerken, I., Blaber, S. J. M., Bouillon, S., Green, P., Haywood, M., Kirton, L. G., Meynecke, J. O., Pawlik, J., Penrose, H. M., Sasekumar, A., and Somerfield, P. J. (2008). The habitat function of mangroves for terrestrial and marine fauna: A review. *Aquatic Botany*, 89, 155-185.
- Naidoo, G. (2006). Factors contributing to dwarfing in the mangrove *Avicennia marina*. *Annals of Botany*, 97, 1095-1101.
- Naumann, J. C., Anderson, J. E., and Young, D. R. (2008). Linking physiological responses, chlorophyll fluorescence and hyperspectral imagery to detect salinity stress using the physiological reflectance index in the coastal shrub, *Myricacerifera*. *Remote Sensing of Environment*, 112, 3865-3875.
- Opti-Sciences. (2002). CCM-200 Chlorophyll Content Meter.
- Peñuelas, J., and Fillela, I. (1998). Visible and near-infrared reflectance techniques for diagnosing plant physiological status. *Trends in Plant Science*, 3, 151-156.
- Polidoro, B. A., Carpenter, K. E., et al. (2010). The loss of species: Mangrove extinction risk and Geographic areas of global concern. *PLoS ONE*, 5(4), e10095.
- Richardson, A. D., Duigan, S. P., and Berlyn, G. P. (2002). An evaluation of noninvasive methods to estimate foliar chlorophyll content. *New Phytology*, 153, 185-194.

- Sobrado, M. A. (1999). Drought effects on photosynthesis of the mangrove *Avicennia germinans* under contrasting salinities. *Trees*, 13, 125-130.
- Valiela, I., Boen, J. L., and York, J. K. (2001). Mangrove forest: One of the worlds threatened major tropical environments. *Biosciences*, 51, 807-815.
- Walters, B. B., Rönnbäck, P., Kovacs, J. M., Crona, B., Hussain, S. A., Badola, R., Primavera, J. H., Barbier, E., and Dahdouh-Guebas, F. (2008). Ethnobiology, socio-economics and management of mangrove forests: a review. *Aquatic Botany*, 89:220-236.
- Wellburn, A. R. (1994). The spectral determination of chlorophylls a and b, as well as total carotenoids, using various solvents with spectrophotometers of different resolution. *Journal of Plant Physiology*, 144, 307-313.
- Young, D. R., Shao, G., and Porter, J. H. (1995). Spatial and temporal growth dynamics of barrier island shrub thickets. *American Journal of Botany*, 82, 628-645.

Chapter 4

4 The influence of seasonality in estimating mangrove leaf chlorophyll a content from hyperspectral data.³

4.1 Introduction

Mangrove forests have a wide geographical distribution in the tropics and subtropics, and have a vital role in maintaining the equilibrium of coastal lagoons and estuaries (Blasco et al. 1996) as well as providing an important renewable resource for local peoples (Walters et al. 2008). The importance of the mangrove ecosystem can be related to a variety of unique factors including litter fall decomposition rates (Flores-Verdugo et al. 1987; Kristensen et al. 2008), nutrient cycling characteristics (Feller et al. 1999), faunal retention rates (Cannicci et al. 2008), faunal interactions (Nagelkerken et al. 2008), climate change (Gilman et al. 2008), and forest productivity (Raven et al. 1992; Komiyama et al. 2008). Despite their ecological importance there has been a significant loss of mangrove forests globally in recent years (Valiela et al. 2001; Duke et al. 2007; Polidoro et al. 2010).

Leaf chlorophyll content is an important bio-indicator of plant physiological state because it plays key roles in photosynthesis (Lichtenthaler 1998). Consequently, the estimation of chlorophyll contents (e.g. chlorophyll-a) could provide critical information in assessing mangrove forest condition (e.g. degraded) at regional and global scales as well as for modeling ecosystem productivity. Given their high spatial coverage and the logistical difficulties of working in mangrove forests, there has been a long history of applying remote sensing in monitoring mangrove condition using biophysical variables such as Leaf Area Index (Blasco et al. 1998; Kovacs et al. 2005, 2009, 2010). In remote sensing the use of high spectral resolution data collected from ground base hyperspectral

³ A version of this chapter has been published: **Flores-de-Santiago F.**, Kovacs JM., Flores-Verdugo F. (2013). The influence of seasonality in estimating mangrove leaf chlorophyll a content from hyperspectral data. **Wetlands, Ecology and Management** 21(3), 193-207 (<http://dx.doi.org/10.1007/s11273-013-9290-x>).

sensors can be useful for determining whether certain coarser spectral resolution data collected from airborne or space-borne remotely sensed devices can be useful for such endeavors including mangroves (Kamaruzaman and Kasawani, 2007).

Despite the increased use of remote sensing vegetation indices (VI) for mangrove forest assessments no research has been done in comparing the use of hyperspectral data collected during contrasting seasons. In a recent study of sub-tropical mangroves in Mexico, Flores-de-Santiago et al. (2012) found significant seasonal changes in mangrove leaf chlorophyll-a (Chla) content. Specifically, they found an increase of leaf Chla content during the rainy season for dwarf and poor stands of *Rhizophora mangle*, *Avicennia germinans*, and *Laguncularia racemosa*. Consequently, such leaf Chla seasonality may play a pivotal role in remote sensing VI assessments and thus impact ecological modeling, primary productivity, and carbon balance studies of mangroves that are based primarily on remote sensing data from one season.

Previous hyperspectral remote sensing studies have indicated that there are specific combinations of wavebands (i.e. VI), collected within the electromagnetic spectrum, that can be used to non-destructively quantify leaf chlorophyll content. According to Carter (1998) and Vogelmann et al. (1993), the most important region of the spectrum is the red-edge position (670–780 nm) where abrupt change in vegetation reflectance between the red and near-infrared regions occurs. This pattern results from the combined effects of strong chlorophyll absorption in the red region and high leaf reflectance in the near-infrared region (Horler et al. 1983). The shape and position of the red-edge are highly influenced by fluctuations of Chla content and leaf biophysical structure (Filella and Peñuelas 1994). As a consequence, an increase in the amount of leaf Chla generally causes a shift in the red-edge position to longer wavelengths due to an expansion in the red zone (Gitelson et al. 1996). Conversely, a decrease in leaf Chla content, most commonly associated with stress periods or senescence, have been linked to a shift towards shorter wavelengths in this red-edge position (Rock et al. 1988).

Some of the most commonly used VI in remote sensing (e.g., NDVI, SR) are based primarily on the contrast between the red and the near-infrared regions of the

electromagnetic spectrum. Such broadband indices (>10 nm) have limitations and are only effective in distinguishing broad differences in vegetation conditions (e.g. greenness, Leaf Area Index, Cho et al. 2006). Alternatively, an increasing number of narrow waveband (<10 nm) hyperspectral sensors have been designed to quantify more specific factors such as chlorophyll cover using more refined red-edge wavebands (Carter and Miller 1994; Gitelson and Merzlyak 1997). VI derived from these narrow bands could provide a more sensitive assessment of mangrove canopy biochemical properties such as Chla estimations.

Zhang et al. (2012) recently conducted a comprehensive study regarding the relationships between pigment contents and hyperspectral responses (350-2500 nm) in a mangrove forest of the sub-tropics for classifying mangrove forest condition. This study was based solely on data collected from the dry season. Therefore, the main focus of my study is to determine whether such relationships, and to what degree, persist during the rainy season when Chla leaf content may increase as the result of more favorable environmental conditions. In addition, I will determine the most appropriate VI to use based on a more limited range of spectral data (450-1000 nm), which is typical of the more affordable commercially available spectroradiometers.

4.2 Materials and Methods

The Urías system is a small coastal lagoon (8 km²) located on an alluvial plain within the state of Sinaloa, Mexico (23° 10' N and 106° 20' W). The system supports three true-mangrove species for the East Pacific region: red mangrove (*Rhizophora mangle*), black mangrove (*Avicennia germinans*), and white mangrove (*Laguncularia racemosa*) (Moroyoqui-Rojo 2005). Due to differences in seasonal leaf Chla content in this mangrove system (Flores-de-Santiago et al. 2012), the hyperspectral fieldwork was conducted along the south end of the Urías system during the dry (May) and rainy (October) seasons of 2010. For each season, I selected 30 random leaves located through the canopy from each of the six classes of mangrove identified for this system: stressed/dwarf black, red, and white mangrove, and healthy red, black, and white mangrove. It is important to note that a minimum leaf sample size of 22 ($\alpha=0.05$) was determined for the hyperspectral analysis of the data collected using traditional stratified

sample size method (Sokal and Rohlf 1994). Regarding leaf mangrove collection during the field campaigns, I followed leaf collection procedures described in detail by Biber (2007), Flores-de-Santiago et al. (2012, 2013), and Zhang et al. (2012). Specifically, the 3rd to the 5th leaves from the tip were clipped in order to maintain a sample of just mature leaves. Once cut, all samples were stored in a plastic bag within a small cooler at 4 °C for transportation to the laboratory. Although the descriptions of these mangrove classes of this region of México are qualitative, their classification scheme has been recently validated qualitatively using statistical methods based on *in situ* biophysical parameter data (Kovacs et al. 2011) and using standard image-processing methods based on spectral properties (Zhang et al. 2012).

For each season, leaf hyperspectral reflectance was measured using a FieldSpec HandHeld device (ASD Inc.). The HandHeld unit has a spectral range of 325-1075 nm with a spectral resolution of 1.0 nm. Additionally, the FieldSpec HandHeld device was equipped with a plant probe unit. Both devices were attached to one another using an optic fiber. Reflectance values below 450 nm and above 1000 nm were deleted due to noise inherent to the device. Based on the literature, I selected 35 VI specifically designed to detect leaf pigments and vegetation stress within my limited spectral range (Table 4.1). Leaf Chla content was measured using the same leaf samples from the hyperspectral analysis. Due to the difference in leaf morphology between the mangrove species (i.e. length, wide), I normalized leaf Chla per unit area (mg/m^2) using the dimensions of the diameter from a copper cylinder. Specifically, a 1.25 cm diameter leaf circle was taken from each sample using the cutting cylinder. Care was taken to avoid collecting the circles from the main leaf veins. The plant material was then dissolved with 100 ml of 80% acetone and a spectrophotometric assay was then conducted to extract information of peak absorption at 646 and 663 nm (Lichtenthaler and Wellburn 1983).

Table 4.1: Vegetation indices selected for this study

Index acronym	Algorithm	References
B_N1	R_{800}/R_{550}	Buschmann and Nagel (1993)
C_1	R_{695}/R_{670}	Carter (1994)
G_M1	R_{750}/R_{550}	Gitelson and Merzlyak(1996)
GNDVI	$(R_{801} - R_{550})/(R_{801} + R_{550})$	Daughtry et al(2000)
LCI	$(R_{850} - R_{710})/(R_{850} - R_{680})$	Datt(1999)
L_G_L1	R_{440}/R_{690}	Lichtenthaler et al(1996)
L_G_L2	R_{750}/R_{700}	Lichtenthaler et al(1996)
MCARI	$[(R_{700} - R_{670}) - 0.2(R_{700} - R_{550})](R_{700}/R_{670})$	Daughtry et al(2000)
MCARI1	$1.2[2.5(R_{800} - R_{670}) - 1.3(R_{800} - R_{550})]$	Haboudane et al(2004)
MCARI2	$1.5[2.5(R_{800} - R_{670}) - 1.3(R_{800} - R_{550})]$ $\sqrt{(2R_{800} + 1)^2 - (6R_{800} - 5\sqrt{R_{670}}) - 0.5}$	Haboudane et al (2004)
MCARI/OSAVI	$\frac{[(R_{750} - R_{705}) - 0.2(R_{750} - R_{550})](R_{750}/R_{705})}{\left[\frac{(1+0.16)(R_{750}-R_{705})}{(R_{750}+R_{705}+0.16)}\right]}$	Wu et al(2008)
MSAVI	$\frac{1}{2} \left[2R_{800} + 1 - \sqrt{(2R_{800} + 1)^2 - 8(R_{800} - R_{670})} \right]$	Qi et al(1994)
mSR ₇₀₅	$(R_{750} - R_{445})/(R_{705} + R_{445})$	Sims and Gamon(2002)
MSR	$\frac{(R_{750}/R_{705}) - 1}{\sqrt{(R_{750}/R_{705}) + 1}}$	Wu et al(2008)
MTVII	$1.2[1.2(R_{800} - R_{550}) - 2.5(R_{670} - R_{550})]$	Haboudane et al(2004)
MTVI2	$1.5[1.2(R_{800} - R_{550}) - 2.5(R_{670} - R_{550})]$ $\sqrt{(2R_{800} + 1)^2 - (6R_{800} - 5\sqrt{R_{670}}) - 0.5}$	Haboudane et al(2004)
ND ₇₀₅	$(R_{750} - R_{705})/(R_{750} + R_{705})$	Sims and Gamon(2002)
NDI	$(R_{800} - R_{740})/(R_{800} + R_{740})$	Müller et al(2008)
NDVI	$(R_{800} - R_{670})/(R_{800} + R_{670})$	Rouse et al(1973) Peñuelas et al(1994)
NPCI	$(R_{680} - R_{430})/(R_{680} + R_{430})$	
OSAVI	$\frac{(1 + 0.16)(R_{800} - R_{670})}{(R_{800} + R_{670} + 0.16)}$	Rondeaux et al(1996)
PRI	$(R_{531} - R_{570})/(R_{531} + R_{570})$	Gamon et al(1992)
PSRI	$(R_{680} - R_{500})/R_{750}$	Merzlyak et al (1999)
PSSR _a	R_{800}/R_{680}	Blackburn(1998)
RARS _a	R_{675}/R_{700}	Chapelle and Kim(1992)
RDVI	$(R_{800} - R_{670})/\sqrt{(R_{800} + R_{670})}$	Rougean and Breon(1995)
REIP	$R_{700} + 40 \left[\frac{0.5(R_{670} + R_{780}) - R_{700}}{R_{740} - R_{700}} \right]$	Horler (1983)
SAVI	$\frac{(R_{780} - R_{670})(1 + L)}{(R_{780} + R_{670} + L)}$	Huete (1988)
SIPI	$(R_{800} - R_{445})/(R_{800} + R_{680})$	Peñuelas and Inque (1999)
SR	R_{800}/R_{670}	Jordan(1969)
TCARI	$3 \left[(R_{700} - R_{670}) - 0.2(R_{700} - R_{550}) \left(\frac{R_{700}}{R_{670}} \right) \right]$	Haboudane et al(2002)

TCARI/OSAVI	$3 \frac{[(R_{750} - R_{705}) - 0.2(R_{750} - R_{550}) \left(\frac{R_{750}}{R_{705}}\right)]}{\left[\frac{(1+0.16)(R_{750}-R_{705})}{(R_{750}+R_{705}+0.16)}\right]}$	Wu et al(2008)
TVI	$0.5[120(R_{750} - R_{550}) - 200(R_{670} - R_{550})]$	Broge and Leblanc (2001)
Vog1	R_{740}/R_{720}	Vogelmann et al(1993)
Z_T1	R_{750}/R_{710}	Zarco-Tejada et al(2001)

R_{xxx} refers to leaf reflectance at wavelength xxx in nanometers.

The hyperspectral data collected from the three species of mangrove was aggregated into one single data set per season, knowing that the red mangrove typically presents the highest leaf Chla content, followed by the black mangrove, and then the white mangrove in this environment (Flores-de-Santiago et al. 2012; Zhang et al. 2012). The 35 VI from Table 4.1 were chosen to represent most of the traditional and recently developed Chla and leaf biophysical estimators derived from hyperspectral reflectance. Using the aforementioned 35 algorithms from the VI and the Chla content from each sample, a matrix was created as follows:

$$M_1 = \begin{bmatrix} Chla_{s_1} & VI_{1s_1} & VI_{2s_1} & \dots & VI_{35s_1} \\ Chla_{s_2} & VI_{1s_2} & VI_{2s_2} & \dots & VI_{35s_2} \\ \vdots & \vdots & \vdots & \ddots & \vdots \\ Chla_{s_{180}} & VI_{1s_{180}} & VI_{2s_{180}} & \dots & VI_{35s_{180}} \end{bmatrix}$$

Where $Chla_{s_i}$ is the Chla content from sample i , and VI_{1-35} are the vegetation indices from each sample created from Table 4.1 algorithms. It is important to note that M_1 is an example using data from the dry season, however I use a similar matrix for the rainy season data.

I applied a Principal Component Analysis (PCA) to define the optimal co-variability between the leaf Chla content and these VI, and treated each season (dry and rainy) as two independent sets for the PCA analysis. Consequently, PCA involves the creation of eigenvectors from M_2 , resulting in a new matrix as follows:

$$M_2 = \begin{bmatrix} b_{01} & b_{181} & b_{362} & \dots & b_{6335} \\ b_{02} & b_{182} & b_{363} & \dots & b_{6336} \\ \vdots & \vdots & \vdots & \ddots & \vdots \\ b_{180} & b_{361} & b_{542} & \dots & b_{6514} \end{bmatrix}$$

where b_i are the eigenvectors for each data from the original matrix. The eigenvector created from the PCA approach involves condensing information contained in the original variables into a smaller set of dimensions (i.e. components). The process is accomplished by creating linear combinations of the original variables, which are oriented in directions that best describe the maximum variation among the individual sampling (McGarigal et al. 2000). In other words, for each season I treated each VI and the Chla content as separate variables in order to find the component into which the variables were grouped. I tested 36 components ($n=36$ variables) using eigenanalysis from the M_1 and M_2 data into 36 sets of new polynomiums:

$$\left\{ \begin{array}{l} pc_1 = \left(\prod_{k=1}^{180} b_{01} Chla_k \right) + \left(\prod_{k=1}^{180} b_{02} VI_{1k} \right) + \dots + \left(\prod_{k=1}^{180} b_{180} VI_{35k} \right) \\ pc_2 = \left(\prod_{k=1}^{180} b_{181} Chla_k \right) + \left(\prod_{k=1}^{180} b_{182} VI_{1k} \right) + \dots + \left(\prod_{k=1}^{180} b_{360} VI_{35k} \right) \\ \vdots \\ pc_{36} = \left(\prod_{k=1}^{180} b_{6335} Chla_k \right) + \left(\prod_{k=1}^{180} b_{6336} VI_{1k} \right) + \dots + \left(\prod_{k=1}^{180} b_{6514} VI_{35k} \right) \end{array} \right.$$

where pc_i represents the eigenvalues, Chla and VI_{1-35} are the original data from M_2 , k represents each sample from 1-360, and b_i are the eigenvectors from M_2 .

Following the Latent Root Criterion, components (pc_i) which recorded an eigenvalue greater than 1.0 were considered significant (Cliff 1988). The 35 VI and the Chla content were then clustered according to the correlation matrix as follows:

$$M_3 = \begin{bmatrix} Chla_{pc_1} & Chla_{pc_2} & \dots & Chla_{pc_{36}} \\ VI_{1pc_1} & VI_{1pc_2} & \dots & VI_{1pc_{36}} \\ VI_{2pc_1} & VI_{2pc_2} & \dots & VI_{2pc_{36}} \\ \vdots & \vdots & \ddots & \vdots \\ VI_{35pc_1} & VI_{35pc_2} & \dots & VI_{35pc_{36}} \end{bmatrix}$$

Where $Chla_{pc_i}$ and VI_{1-35pc_i} are the results from the correlation matrix between the components (pc_i) and the original M_1 data (Tables 4.2 and 4.3). The Chla content and each VI from M_3 were then grouped with the component having the highest correlation

coefficient. Consequently, for each season I identified the component in which select VI and the Chla content had the highest correlation.

Once the two new sets of VI were selected from the PCA for both the dry and rainy seasons, I used regression analysis between the Chla content and those significant VI. Following a bootstrapping technique (Uraibi et al. 2009), I estimated Chla content from the equations. In the bootstrapping technique one-thirds of the random data were used for model calibration (i.e. linear equations between Chla and VIs) and the remaining two-third for validation. For each selected index I used the standard error of estimate (SE) and the T-test statistics for validation.

The T-test statistic in linear regression is equal to the slope divided by its standard error. The null hypothesis for this test states that the slope is equal to zero. If this is true, then there is no linear relationship between the measured and estimated leaf Chla contents. For 180 samples per season at the 5% significant level ($\alpha=0.05$) the critical T-value is 1.97 (two-tailed). If the T-value from the calculated-estimated leaf Chla content is lower than 1.97, then no significant linear association between the variables is recorded. Moreover, the larger the calculated significant T-value, the better the linear association between the measured and the estimated leaf Chla content.

Table 4.2: Pearson correlation matrix of Chla and VI versus significant components and its eigenanalysis during the dry season

Variable	PC ₁	PC ₂	PC ₃	PC ₄
Chla	+0.18*	+0.07	-0.10	-0.03
B_N1	+0.19	+0.09	+0.06	-0.23
C_1	-0.20*	-0.02	+0.07	-0.06
G_M1	+0.19*	+0.09	+0.06	-0.22
GNDVI	+0.20*	+0.04	+0.05	-0.11
LCI	+0.17	+0.00	-0.26	-0.14
L_G_L1	+0.17	+0.07	-0.17	+0.19
L_G_L2	+0.20*	+0.08	+0.01	-0.14
MCARI	-0.17*	-0.14	+0.15	-0.09
MCARI1	-0.06	-0.29	-0.20	-0.09
MCARI2	+0.04	-0.33	-0.02	+0.03
MCARI/OSAVI	-0.18*	-0.12	+0.16	-0.09
MSAVI	+0.17	-0.19	+0.04	-0.03
mSR ₇₀₅	+0.11	-0.16	+0.32	-0.08
MSR	+0.20*	+0.06	+0.00	-0.09
MTVI1	-0.06	-0.29	-0.20	-0.09
MTVI2	+0.04	-0.33	-0.02	+0.03
ND ₇₀₅	+0.21*	+0.01	-0.02	+0.04
NDI	-0.01	-0.14	-0.39	-0.36
NDVI	+0.15	-0.13	+0.18	+0.12
NPCI	-0.17	-0.04	+0.16	-0.22
OSAVI	+0.13	-0.25	-0.11	-0.14
PRI	-0.10	+0.03	-0.35	+0.11
PSRI	-0.11	+0.16	+0.09	-0.53
PSSR _a	+0.20*	+0.04	+0.08	-0.13
RARS _a	+0.11	+0.21	-0.26	-0.08
RDVI	+0.15	-0.24	-0.05	-0.07
REIP	+0.19*	+0.02	-0.15	+0.12
SAVI	+0.15	-0.23	-0.02	-0.05
SIPI	-0.17	+0.12	+0.05	-0.39
SR	+0.18	-0.08	+0.19	-0.04
TCARI	-0.19*	-0.13	+0.05	-0.05
TCARI/OSAVI	-0.20*	-0.10	+0.06	-0.06
TVI	-0.04	-0.31	-0.18	-0.08
Vog1	+0.20*	+0.08	-0.06	-0.10
Z_T1	+0.20*	+0.08	-0.02	-0.14
Eigenvalue	23.01	8.73	4.19	1.36
Proportion	0.59	0.22	0.11	0.4
Cumulative	0.59	0.81	0.92	0.96

Matrix was generated by principal component analysis.

*Significant correlated with PC1

Table 4.3: Pearson correlation matrix of Chla and VI versus significant components and its eigenanalysis during the rainy season

Variable	PC ₁	PC ₂	PC ₃	PC ₄
Chla	+0.25*	+0.01	+0.16	-0.06
B_N1	+0.00	-0.01	+0.00	-0.07
C_1	-0.20*	+0.00	+0.10	+0.03
G_M1	+0.20*	-0.01	+0.01	-0.07
GNDVI	+0.21*	-0.02	-0.03	-0.05
LCI	+0.15	-0.08	-0.30	-0.03
L_G_L1	+0.18	+0.04	-0.07	+0.33
L_G_L2	+0.20*	-0.01	-0.03	-0.05
MCARI	-0.18*	-0.11	+0.16	-0.03
MCARI1	-0.14	-0.23	-0.16	+0.00
MCARI2	-0.12	-0.29	+0.02	+0.01
MCARI/OSAVI	-0.18*	-0.10	+0.17	-0.03
MSAVI	+0.11	-0.29	+0.04	-0.03
mSR ₇₀₅	+0.12	-0.17	+0.28	-0.20
MSR	+0.21*	-0.01	-0.04	-0.04
MTVI1	-0.14	-0.23	-0.16	+0.00
MTVI2	-0.12	-0.29	+0.02	+0.01
ND ₇₀₅	+0.21*	-0.01	-0.05	-0.02
NDI	-0.03	-0.21	-0.36	-0.02
NDVI	+0.14	-0.16	+0.25	-0.03
NPCI	-0.10	-0.01	+0.00	-0.62
OSAVI	+0.03	-0.31	-0.18	-0.03
PRI	-0.07	+0.00	-0.07	-0.09
PSRI	+0.10	+0.12	+0.01	-0.46
PSSR _a	+0.20*	-0.05	+0.12	-0.09
RARS _a	+0.15	+0.14	-0.27	+0.01
RDVI	+0.05	-0.32	-0.13	-0.03
REIP	+0.19*	+0.01	-0.14	+0.07
SAVI	+0.07	-0.32	-0.10	-0.03
SIPI	-0.14	+0.14	-0.12	-0.44
SR	+0.16	-0.13	+0.24	-0.05
TCARI	-0.20*	-0.06	+0.02	+0.02
TCARI/OSAVI	-0.21*	-0.04	+0.04	+0.02
TVI	-0.12	-0.26	-0.15	-0.03
Vog1	+0.20*	+0.00	-0.13	-0.07
Z_T1	+0.20*	-0.01	-0.07	-0.05
Eigenvalue	22.55	8.26	4.51	1.51
Proportion	0.59	0.21	0.12	0.04
Cumulative	0.59	0.79	0.91	0.94

Matrix was generated by principal component analysis.

*Significant correlated with PC1

4.3 Results

The eigenvalues derived from both the Pearson's correlation matrices obtained through PCA showed that only the first four principal components were significant (Tables 4.2 and 4.3). Moreover, leaf Chla content had the highest correlation in the first component for both the dry and rainy seasons. Consequently, only those VI that also show their highest correlation in the first component can be grouped with Chla. From the 35 VI, only 14 were well correlated with PC1 during both seasons. These 14 VI were C_1, G_M1, GNDVI, L_G_L2, MCARI, MCARI/OSAVI, MSR, Nd₇₀₅, PSSR_a, REIP, TCARI, TCARI/OSAVI, Vog1, and Z_T1. The two traditional VIs, NDVI and SR, were weakly correlated with leaf Chla content (NDVI R²=0.59, SR=0.59 dry season, NDVI R²=0.20, SR=0.28 rainy season).

Seasonal differences between the equations, based on leaf Chla content with the VI, were clearly evident. Overall, the coefficients of determinations (R²) were higher during the dry season (Table 4.4). Among the 14 VIs equations, six VIs (Vog1, C_1, MSR, ND705, Z_T1, and L_G_L2) also showed higher R² (> 0.76) values for the dry season. The leaf Chla estimations for the dry season also presented higher T-observed values and lower SEs (Fig. 4.1) when compared to those calculated from the rainy season data (Fig. 4.2). During the dry season some of the VI that include the 550 nm waveband (e.g., MCARI, MCAR/OSAVI, and TCARI) showed T-observed values as high as those VI that used only wavelengths from the red-edge region such as the Vog1 and the MSR. Although the T-observed values were lower, a similar pattern was found for the rainy season.

4.4: Regression analysis of leaf Chla content and hyperspectral VI

Season	Vegetation Indices	F-observed	Regression equation	Coefficient of determination (R ²)
Dry	Vog1	166*	Chla = -34 + 42.7 X	0.80
	C_1	157*	Chla = 61.8 - 72 X	0.79
	MSR	159*	Chla = 6.27 + 28.5 X	0.79
	ND ₇₀₅	154*	Chla = -6.04 + 71.4 X	0.78
	Z_T1	146*	Chla = -1.07 + 12.3 X	0.77
	L_G_L2	138*	Chla = 4.24 + 7.36 X	0.76
	TCARI/OSAVI	119*	Chla = 53.5 - 80.4 X	0.74
	REIP	108*	Chla = -24.5 + 2.89 X	0.72
	GNDVI	106*	Chla = -26.2 + 94.4 X	0.71
	TCARI	99*	Chla = 53.9 - 110 X	0.70
	PSSR _a	87*	Chla = 9.66 + 2.66 X	0.67
	G_M1	75*	Chla = 5.55 + 5.99 X	0.63
	MCARI/OSAVI	74*	Chla = 46.7 - 80.2 X	0.63
	MCARI	65*	Chla = 46.7 - 107 X	0.60
	Rainy	REIP	117*	Chla = -16.8 + 3.05 X
MCARI/OSAVI		98*	Chla = 47.3 - 31.8 X	0.70
Vog1		93*	Chla = -46 + 55.9 X	0.68
MCARI		88*	Chla = 47.1 - 40.6 X	0.67
C_1		83*	Chla = 73.2 - 86.1 X	0.66
Z_T1		54*	Chla = -2.51 + 16.2 X	0.56
ND ₇₀₅		53*	Chla = -4.13 + 78.9 X	0.55
TCARI/OSAVI		47*	Chla = 53.2 - 57.6 X	0.52
MSR		43*	Chla = 10.5 + 32.7 X	0.50
TCARI		41*	Chla = 52.6 - 72.9 X	0.49
GNDVI		40*	Chla = -15.4 + 76.4 X	0.48
L_G_L2		38*	Chla = 6.95 + 8.98 X	0.47
G_M1		24*	Chla = 15.7 + 3.6 X	0.36
PSSR _a		10*	Chla = 21 + 1.09 X	0.18

X denotes the corresponding vegetation index.

*Significant F-observed values at p<0.05.

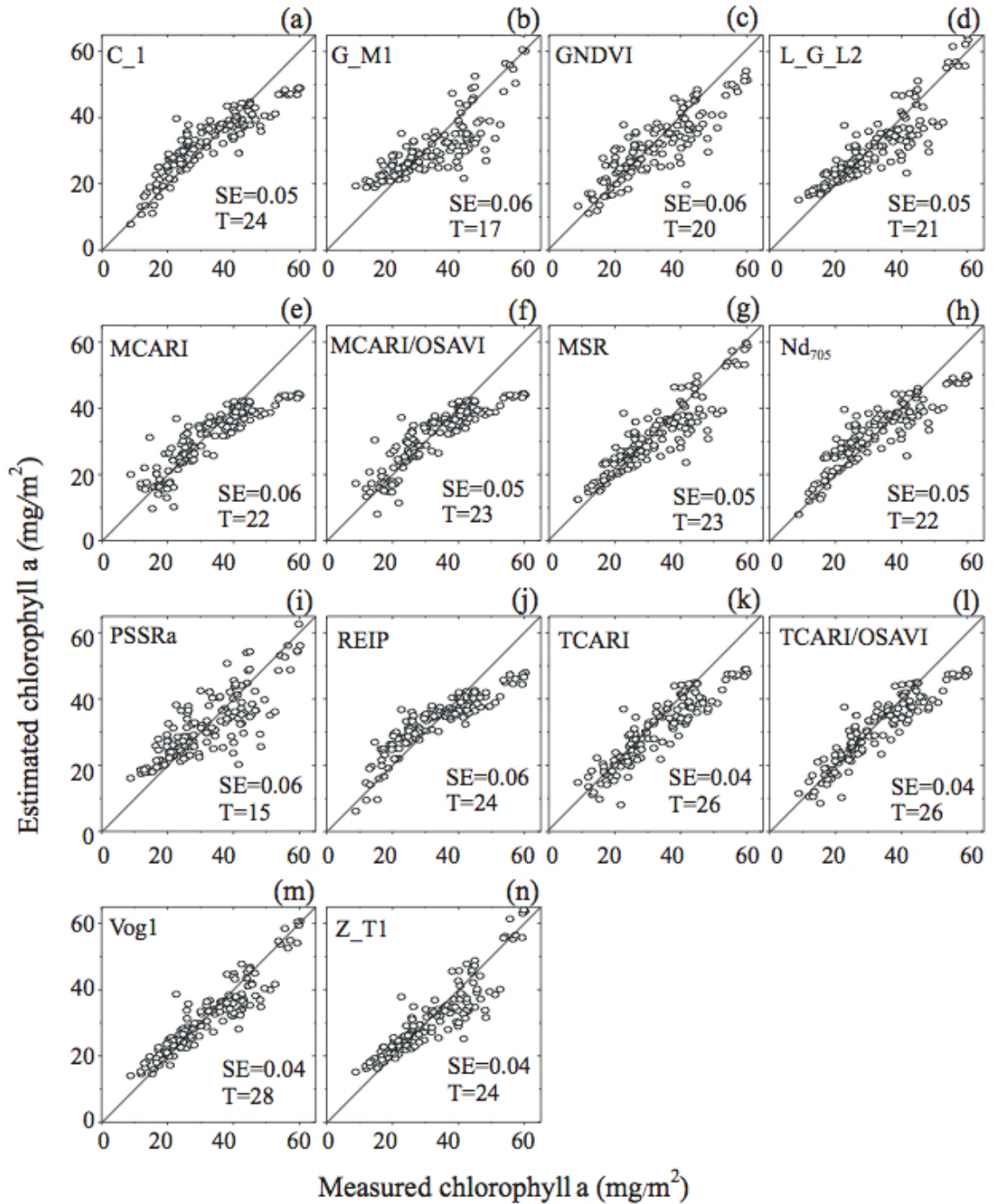


Figure 4.1: Predicted Chla content during the dry season (May), based on the regression equations from Table 4.4. T-observed values (T), standard error of estimate (SE). Data plotted along a 1:1 line

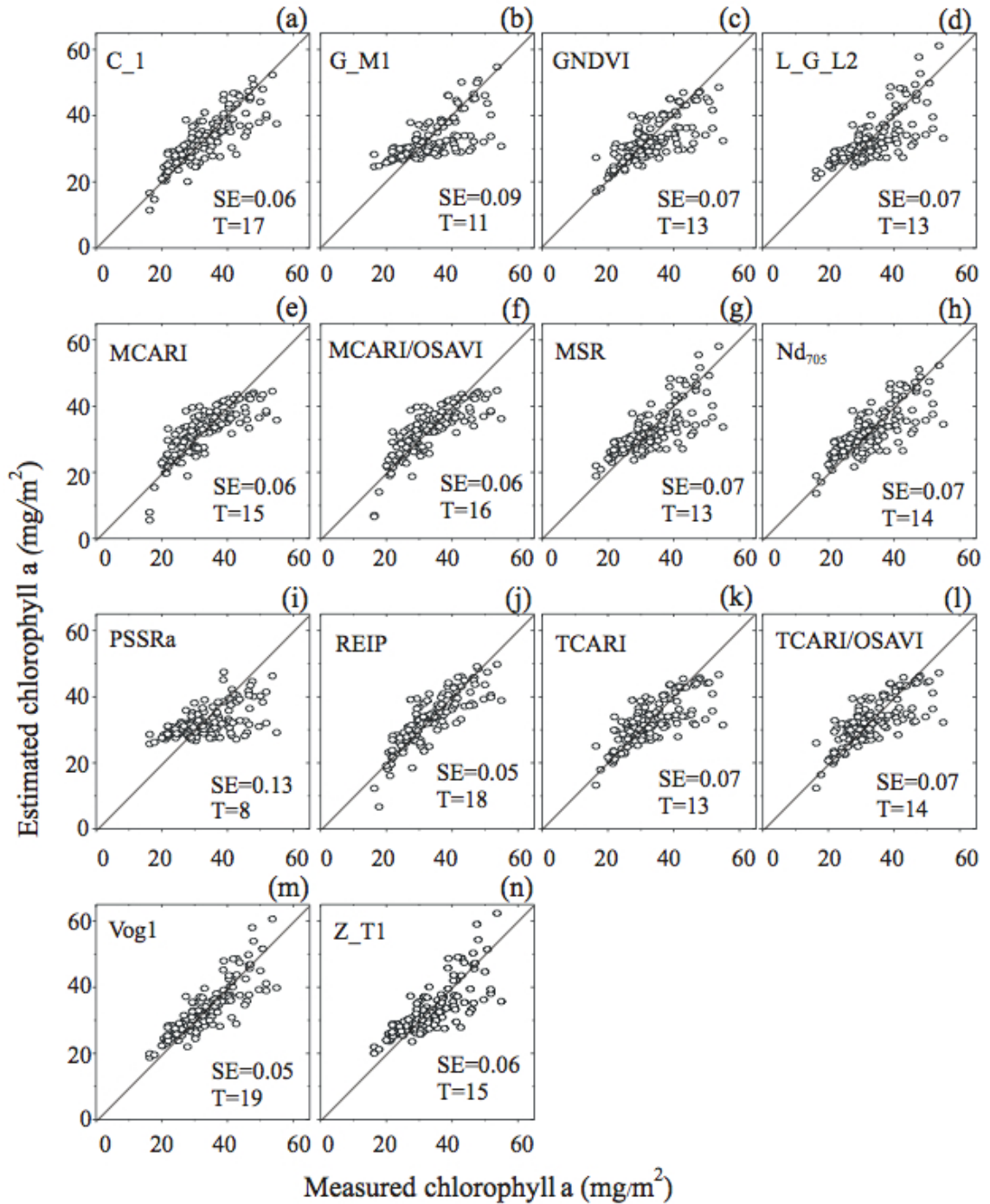


Figure 4.2: Predicted Chla content during the rainy season (October), based on the regression equations from Table 4.4. T-observed value (T), standard error of estimate (SE). Data plotted along a 1:1 line

Among the 14 VIs that were significant estimators for leaf Chla content only the G_M1 and the PSSR_a showed poor estimations of leaf Chla content for both seasons. The Vog1 had the highest recorded R² and T-observed values for the dry season (R²=0.8 and T=28) which is consistent with the study conducted in 2009 by Zhang et al. (2012). With regards to the rainy season, the REIP showed the highest R² (0.73), followed by the MCARI/OSAVI (0.70) and then the Vog1 (0.68).

4.4 Discussion

With the aim to understand which of the published VIs would be associated with Chla content during the dry and rainy seasons I believe that the multivariate statistical analysis that I employed does provide a more than adequate means for examining ability of a given VI to predict Chla content in mangrove leaves. An important observation in this study was the *a priori* multivariate PCA utilized on both seasons datasets for analyzing multiple co-variability between VI and the Chla content. As a result, the PCA process simplifies an *a posteriori* linear analysis between just those VI that have better co-variability and the leaf Chla content.

For this investigation, it is evident that the accuracy in estimating mangrove leaf Chla content does vary between the two seasons even when considering the same VI for the same trees. Specifically, these results would indicate that remote sensing estimations of Chla are most accurate when carried out during the dry season for these sub-tropical mangrove forests. It is plausible that higher moisture content in the mangrove leaves during the rainy season and the increase in leaf Chla content (Flores-de-Santiago et al. 2012) could be influencing the ability of the VI to predict leaf Chla content. Consequently, for separating the condition of stressed mangrove forests hyperspectral measurements should ideally be taken in the dry season.

With regards to the study conducted in the dry season by Zhang et al (2012), I obtained similar results for the optimal VI with a PCA process and a more limited hyperspectral data range. In my study I used 450-1000 nm as compared to 350-2500 nm from Zhang et al (2012). Although I could not use some of the VI that required wavelengths from 1000-2500 nm, the ASD HandHeld unit used in my study showed to

be as useful for leaf mangrove hyperspectral estimations of leaf Chla content. Moreover, while the current study demonstrates that hyperspectral estimation of leaf Chla content on mangrove forest greatly depends on the season, I am unsure as to how well these algorithms will perform at the canopy level. Consequently, it is suggested that further studies be extended to include the canopy spectra.

In regards to the VI themselves, a common observation in this study was the variation observed in regards to the predicting abilities of the many VI used for mangrove leaf Chla estimation. Although the equations for each of the 14 VI that successfully predict leaf Chla content were very different, the selection of wavebands used in such algorithms was limited. For example, the G_M1, L_G_12, MCARI/OSABI, MSR, ND₇₀₅, TCARI/OSAVI, and Z_T1 included just the 550, 700, 705, 710, and 750 nm. The C_1, GNDVI, MCARI, PSSR_a, REIP, and TCARI included 670 or 800 nm, and finally the Vog1 was based on the 720 and 740 nm wavebands.

It is important to note that the VI which had its absorption center wavebands between 670-780 nm (the red-edge position) had the highest R² and T-observed values. In contrast, VI that included just the 680 nm region and above 780 nm such as the LCI, NPCI, PSRI, PSSR_a, and the SIPI appear to quickly saturate at low Chla levels (Wu et al. 2008) and therefore become insensitive to high Chla content. The aforementioned pattern has been described by Wang and Souza (2009) for the same three mangrove species but within tropical Panama. They found that stress sensitivity was greater for wavelengths at 605, 695, 710, and 760 nm where absorption by Chla is relatively weak. At these wavelengths, even a slight drop in leaf Chla content caused by adverse environmental factors results in a large increase in leaf reflectance.

With the exception of the PSSR_a, these VI were not significant with Chla content. The PSSR_a has been previously shown to have an extremely strong relationship with the concentration per unit area of Chla (Blackburn 1998). However, for this sub-tropical mangrove forest the low T-observed values calculated (15 in dry season, 8 in rainy season) would suggest a poor estimation of leaf Chla content as compared to other VI. Additionally, Blackburn (1999) found that the PSSR_a remains sensitive to Chla over a

wide range of concentrations in deciduous trees but in my study heteroscedasticity was evident as scatter about the regression model increased with pigment content. Consequently, the use of the $PSSR_a$ in estimating mangrove leaf Chla content decreases during the rainy season when an increase in leaf Chla content occurs for this type of forest.

In the case of the traditional and most widely used VI for vegetation assessment, namely the NDVI and the SR, I found a consistently poor ability to predict mangrove leaf Chla for both the dry and rainy seasons. This could be explained by the fact that the NDVI and SR are based on the contrast between the maximum absorption in the red due to chlorophyll pigments and the maximum reflection in the infrared caused by leaf cellular structure (Jordan 1969). Therefore, improved indices such as the G_M1 , L_G_I2 , $MCARI/OSABI$, MSR , ND_{705} , $TCARI/OSAVI$, and Z_T1 have been developed in order to linearize their relationships with vegetation biophysical variables. The good results from the aforementioned VI can be explained by the integration in their equation of ratios that have maximum sensitivity and are highly correlated to leaf Chla content (R_{500} , R_{700} , and R_{750}) (Gitelson and Merzlyak 1996; Haboudane et al. 2004). It has been reported that VI that integrate reflectance ratios around R_{500} , R_{700} , and R_{750} may reduce the effect of disturbances such as the non-photosynthetic material (Wu et al. 2008), and are relatively less insensitive to leaf biophysical factors and structure variations (Sims and Gamon 2002). In addition, such wavebands can estimate Chla content at canopy and leaf level by tracking subtle changes of pigment content variations (Zarco-Tejada et al. 2001). However, for this type of mangrove environment, the ND_{705} was found to be a poorer estimator of Chla content as compared to $MCARI/OSAVI$, $TCARI/OSAVI$, or MSR which also only used the 700 and 750 nm from the red-edge region. The addition of the wavelength at 550 nm (e.g., $MCARI/OSAVI$, $TCARI/OSAVI$) has also been found to be extremely useful in pigment content determination (Wu et al. 2008). The reasons for this could be explained by the similarity of the R_{550} with the red-edge wavelengths (Horler et al. 1983). Furthermore, the R_{550} relies on its location between two wide bands of strong pigment absorption. However, the results from my study suggest that the combination of the R_{550} with the red-edge wavelengths was not as important for mangrove leaf Chla determination.

I have shown that VI that include the R_{500} , R_{700} , and R_{750} wavelengths correlates reasonably well with the Chla content in mangrove leaves. However, it is important to note that wavelengths (R_{670} or R_{800}) included in the C_1, GNDVI, MCARI, PSSR_a, REIP, and TCARI resulted in a lower, but still significant correlation with Chla content. Thus, such potential in estimating Chla content could be explained by the fact that Chla plays a major role in light absorption in the range of 530-570 nm (Gitelson et al. 1996) as well as at longer wavelengths (e.g., 800 nm Gitelson and Merzlyak 1997). Moreover, in a previous study by Wang and Souza (2009) the near-infrared region (780-810 nm) was also considered the most important waveband for discriminating these three mangrove species. However, in my study the link between pigment content and the near infrared reflectance was not of key importance for the accurate estimation of Chla. It has been suggested by Daughtry et al. (2000) that the MCARI holds a great potential for pigments and LAI estimations even though this index does not include a near-infrared wavelength in its equation. Hence, spectral vegetation indices that combine reflectance of near-infrared and other visible bands (e.g., MCARI) are responsible to leaf chlorophyll content (Daughtry et al. 2000). It was not unexpected that the MCARI developed good estimations of Chla content in mangrove leaves, mainly because this index was designed to measure the chlorophyll influence in the red and red-edge regions (Daughtry et al. 2000). In the case of the RDVI, this index resulted in poor leaf Chla estimation that could be explained by the fact that RDVI presents weak linearity and high variability with chlorophyll saturation (Haboudane et al. 2004). In contrast the MTVI and MCARI, developed by Haboudane et al (2004), were designed to be less sensitive to chlorophyll content variations for precision agriculture. In my study MTVI1, MCARI1, MTVI2, and MCARI2 were not good predictors of Chla content. Only the TCARI index, developed by Haboudane et al (2002), was found to be a good estimator for this mangrove forest. Moreover, Broge and Leblanc (2001) reported that the SAVI and the MSAVI can be used to be good indicators of greenness measure and relative insensitivity to low chlorophyll effects. However, in this study both were not found to be suitable for leaf Chla estimation.

According to Zhang et al. (2012), TCARI and Vogelmann's Index (Vog1 in this study) both with green and red-edge wavebands in their equations, recorded the highest potential for predicting Chla content in several species and conditions of mangrove leaves. Even though Vog1 did not present the highest R^2 for the rainy season, the R^2 difference between the Vog1 and the two VIs that presented the highest R^2 (REIP and MCARI/OSAVI) was only of 0.05 and 0.02 respectively (Table 4.4). Consequently, this would support the notion that the Vog1 (R_{740}/R_{720}) is the optimal VI for mangrove leaf Chla estimation for sub-tropical environment. Finally, it is important to note that in order to produce maps of mangrove cover, VI are initially required at the leaf level using hyperspectral data and empirical-derived relationships. Following this leaf-level, the scale can shift up to the canopy-level and eventually towards multispectral imagery. Therefore, there is the continued need to assess the predictive capability of VI across a range of mangrove species and, as shown in this study with seasons, across a variety of environmental conditions.

The results of this investigation indicate that for sub-tropical mangroves of the Pacific coast of Mexico the accuracy of and selection of hyperspectral vegetation indices in estimating leaf Chla content can vary according to the season in which the data are collected. For this particular mangrove system it was found that the dry season was more ideal for estimating leaf Chla content. Moreover, it is suggested that the use of PCA which combines leaf hyperspectral properties with the leaf Chla content can allow scientists to more readily identify the influence of seasonality on the Chla content estimations from the most commonly employed hyperspectral vegetation indices. It is suggested that the results may also be useful for future analysis of interactions between hyperspectral data with mangrove canopy cover. By up-scaling the hyperspectral properties of mangrove leaves, the results from this study could be used to analyze the abilities of other remote sensing sensors for mapping of mangroves across a variety of environmental conditions.

4.5 References

- Biber, P. D. (2007) Evaluating a chlorophyll content meter on three coastal wetland plant species. *Agriculture Food Environmental Science*, 1(2), 1–11.
- Blackburn, G. A. (1998) Quantifying chlorophylls and carotenoids at leaf and canopy scales: an evaluation of some hyperspectral approaches. *Remote Sensing of Environment*, 66, 273-285.
- Blackburn, G. A. (1999) Relationships between spectral reflectance and pigment concentrations in stacks of deciduous broad leaves. *Remote Sensing of Environment*, 70, 224-237.
- Blasco, F., Saenger, P., and Janodet, E. (1996) Mangroves as indicators of coastal change. *Catena*, 27, 167-178.
- Blasco, F., Gauquelin, T., Rasolofoharinoro, M., Denis, J., Aizpuru, M., and Caldaïrou, V. (1998) Recent advances in mangrove studies using remote sensing data. *Marine Freshwater Resources*, 49, 287-296.
- Broge, N. H., and Leblanc, E. (2001). Comparing prediction power and stability of broadband and hyperspectral vegetation indices for estimation of green leaf area index and canopy chlorophyll density. *Remote Sensing of Environment*, 76, 156-172.
- Buschmann, C., and Nagel, E. (1993). In vivo spectroscopy and internal optics of leaves as a basis for remote sensing of vegetation. *International Journal of Remote Sensing*, 14, 711–722.
- Cannicci, S., Burrows, D., Fratini, S., Smith, III. T. J., Offenberg, J., and Dahdouh-Guebas, F. (2008). Faunal impact on vegetation structure and ecosystem function in mangrove forests: a review. *Aquatic Botany*, 89, 186-20.
- Carter, G. A. (1994). Ratios of leaf reflectance in narrow wavebands as indicators of plant stress. *International Journal of Remote Sensing*, 15, 697-703.
- Carter, G. A., and Miller, R. L. (1994). Early detection of plant stress by digital imaging within narrow stress-sensitive wavebands. *Remote Sensing of Environment*, 50, 295-302.
- Carter, G. A. (1998). Reflectance wavebands and indices for remote estimation of photosynthesis and stomatal conductance in pine canopies. *Remote Sensing of Environment*, 63, 61-72.
- Chapelle, E. W., Kim, M. S., and McMurtrey, III. J. E. (1992). Ratio analysis of reflectance spectra (RARS): An algorithm for the remote estimation of the concentrations of chlorophyll A, chlorophyll B, and carotenoids in soybean leaves. *Remote Sensing of Environment*, 39, 239-247.
- Cho, M. A., Sobhan, I. M., and Skidmore, A. K. (2006). Estimating fresh grass/herb biomass from HYMAP data using the red-edge position. *Proceedings of SPIE*, 629805-629809.
- Cliff, N. (1988). The eigenvalues-greater-than-one rule and the reliability of components. *Psychological Bulletin*, 103, 276-279.
- Daughtry, C. S. T., Walthall, C. L., Kim, M. S., De Colstoun, E. B., and McMurtrey, J. E. (2000). Estimating corn leaf chlorophyll concentration from leaf and canopy reflectance. *Remote Sensing of Environment*, 74, 229-239.

- Datt, B. (1999). A new reflectance index for remote sensing of chlorophyll content in higher plants. *Journal of Plant Physiology*, 154, 30-36.
- Duke, N. C., Meynecke, J. O., Dittman, S., Ellison, A. M., Anger, K., Berger, U., Cannicci, S., Diele, K., Ewel, K. C., Field, C. D., Koedam, N., Lee, S. Y., Marchand, C., Nordhaus, I., and Dahdouh-Guebas, F. (2007). A world without mangroves?. *Science*, 317, 41-42.
- Feller, I. C., Whigham, D. F., O'Neill, J. P., and McKee, K. L. (1999). Effects of nutrient enrichment on within-stand cycling in a mangrove forest. *Ecology*, 80, 2193-2205.
- Filella, I., and Peñuelas, J. (1994). The red-edge position and shape as indicators of plant chlorophyll content, biomass and hydric status. *International Journal of Remote Sensing*, 15, 1459-1470.
- Flores-de-Santiago, F., Kovacs, J. M., Flores-Verdugo, F. (2012). Assessing seasonal changes in leaf Chlorophyll-a content and leaf morphology in a sub-tropical mangrove forest of the Mexican Pacific. *Marine Ecology Progress Series*, 444, 57-68.
- Flores-de-Santiago, F., Kovacs, J. M., and Flores-Verdugo, F. (2013). Assessing the utility of a portable pocket instrument for estimating seasonal mangrove leaf chlorophyll contents. *Bulletin of Marine Sciences*, 89(2), 621-633.
- Flores-Verdugo, F., Day, J. W., and Briseño-Dueñas, R. (1987). Structure, litter fall, decomposition, and detritus dynamics of mangroves in a Mexican coastal lagoon with an ephemeral inlet. *Marine Ecology Progress Series*, 35, 83-90.
- Gamon, J. A., Peñuelas, J., and Field, C. B. (1992). A narrow-waveband spectral index that tracks diurnal changes in photosynthetic efficiency. *Remote Sensing of Environment*, 41, 35-44.
- Gilman, E. L., Ellison, J., Duke, N. C., and Field, C. (2008). Threats to mangrove from climate change and adaptation options: A review. *Aquatic Botany*, 89, 237-250.
- Gitelson, A. A., Kaufman, Y. J., Merzlyak, M. N. (1996). Use of a green channel in remote sensing of global vegetation from EOS-MODIS. *Remote Sensing of Environment*, 58, 289-298.
- Gitelson, A. A., and Merzlyak, M. N. (1996). Signature analysis of leaf reflectance spectra: Algorithm development for remote sensing of chlorophyll. *Journal of Plant Physiology*, 148, 494-500.
- Gitelson, A. A., and Merzlyak, M. N. (1997). Remote estimation of chlorophyll content in higher plant leaves. *International Journal of Remote Sensing*, 18, 2691-2697.
- Haboudane, D., Miller, J. R., Tremblay, N., Zarco-Tejada, P. J., and Dextrazel, L. (2002). Integrated narrow-band vegetation indices for prediction of crop chlorophyll content for application to precision agriculture. *Remote Sensing of Environment*, 81, 416-426.
- Haboudane, D., Miller, J. R., Pattey, E., Zarco-Tejada, P. J., and Strachan, I. B. (2004). Hyperspectral vegetation indices and novel algorithms for predicting green LAI of crop canopies: Modeling and validation in the context of precision agriculture. *Remote Sensing of Environment*, 90, 337-352.
- Horler, D. N. H., Dockray, M., and Barber, J. (1983). The red-edge of plant leaf reflectance. *International Journal of Remote Sensing*, 4, 273-288.

- Huete, A. R. (1988). A soil-adjusted vegetation index (SAVI). *Remote Sensing of Environment*, 25, 295-309.
- Jordan, C. F. (1969). Derivation of leaf-area index from quality of light on the forest floor. *Ecology*, 50, 663-666.
- Kamaruzaman, J., and Kasawani, I. (2007). Imaging spectrometry on mangrove species identification and mapping in Malaysia. *WSEAS Transaction in Biological Biomedicine*, 8, 118-126.
- Komiyama, A., Eong, O. J., and Pongparn, S. (2008). Allometry, biomass, and productivity of mangrove forest: a review. *Aquatic Botany*, 89, 128-137.
- Kovacs, J. M., Wang, J., and Flores-Verdugo, F. (2005). Mapping mangrove leaf area index at the species level using IKONOS and LAI-2000 sensors for the Agua Brava Lagoon, Mexican Pacific. *Estuarine Coastal and Shelf Science*, 62, 377-384.
- Kovacs, J. M., King, J. M. L., Flores-de-Santiago, F., and Flores-Verdugo, F. (2009). Evaluating the condition of a mangrove forest of the Mexican Pacific based on an estimated leaf area index mapping approach. *Environmental Monitoring and Assessment*, 157, 137-149.
- Kovacs, J. M., Flores-de-Santiago, F., Bastien, J., and Lafrance, P. (2010). An assessment of mangroves in Guinea, West Africa, using a field and remote sensing based approach. *Wetlands*, 30, 773-782.
- Kovacs, J. M., Liu, Y., Zhang, C., Flores-Verdugo, F., and Flores-de-Santiago, F. (2011). A field based statistical approach for validating a remotely sensed mangrove forest classification scheme. *Wetlands Ecology and Management*, 19, 409-421.
- Kristensen, E., Bouillon, S., Dittmar, T., and Marchand, C. (2008). Organic carbon dynamics in mangrove ecosystems: a review. *Aquatic Botany*, 89, 201-219.
- Lichtenthaler, H. K., and Wellburn, A. R. (1983). Determinations of total carotenoids and chlorophylls a and b in leaf extracts in different solvents. *Biochemical Society Trans*, 11, 591-592.
- Lichtenthaler, H. K., Gitelson, A., and Lang, M. (1996). Non-destructive determination of chlorophyll content of leaves of a green and an aurea mutant of tobacco by reflectance measurements. *Journal of Plant Physiology*, 148, 483-493.
- Lichtenthaler, H. K. (1998). The stress concept in plants: an introduction. *Annals of the New York Academy of Sciences*, 851, 187-198.
- McGarigal, K., Cushman, S., and Stafford, S. (2000). *Multivariate statistics for wildlife and ecology research*. New York: Springer-Verlag.
- Merzlyak, M. N., Gitelson, A. A., Chivkunova, O. B., and Rakitin, V. Y. (1999) Non-destructive optical detection of pigment changes during leaf senescence and fruit ripening. *Physiol Plant*, 106, 135-141.
- Moroyoqui-Rojo, M. (2005). Análisis de la eficiencia en la remoción de nutrientes en un sistema experimental silvo pesquero (manglar-ictiofauna) con recirculación de agua. M.Sc. Dissertation, CIDIR Instituto Politécnico Nacional de México.
- Müller, K., Böttcher, U., Meyer-Schatz, F., and Kage, H. (2008). Analysis of vegetation indices derived from hyperspectral reflection measurements for estimating crop canopy parameters of oilseed rape (*Brassica napus* L.). *Biosystems Engineering*, 101, 172-182.

- Nagelkerken, I., Blaber, S. J. M., Bouillon, S., Green, P., Haywood, M., Kirton, L. G., Meynecke, J. O., Pawlik, J., Penrose, H. M., Sasekumar, A., and Somerfield, P. J. (2008). The habitat function of mangrove for terrestrial and marine fauna: a review. *Aquatic Botany*, 89, 155-185.
- Peñuelas, J., Gamon, J. A., Fredeen, A. L., Merino, J., and Field, C. B. (1994). Reflectance indices associated with physiological changes in nitrogen- and water-limited sunflower leaves. *Remote Sensing of Environment*, 48, 135-146.
- Peñuelas, J., and Inque, Y. (1999). Reflectance indices indicative of changes in water and pigment contents of peanut and wheat leaves. *Photosynthetica*, 36, 355-360.
- Polidoro, B. A., Carpenter, K. E., Collins, L., Duke, N. C., and Ellison, A. M., et al. (2010). The loss of species: Mangrove extinction risk and Geographic areas of global concern. *PLoS ONE*, 5, e10095.
- Qi, J., Chehbouni, A., Huete, A. R., Kerr, Y. H., and Sorooshian, S. (1994). A modified soil adjusted vegetation index. *Remote Sensing of Environment*, 48, 119-126.
- Raven, P. H., Evert, R. F., and Eichhorn, S. E. (1992). *Biology of plants*. New York: Worth Publishers.
- Rock, B. N., Hoshizaki, T., and Miller, J. R. (1988). Comparison of in situ and airborne spectral measurements of the blue shift associated with forest decline. *Remote Sensing of Environment*, 24, 109-127.
- Rondeaux, G., Steven, M., and Baret, F. (1996). Optimization of soil-adjusted vegetation indices. *Remote Sensing of Environment*, 55, 95-107.
- Rougean, J. L., and Breon, F. M. (1995). Estimating PAR absorbed by vegetation from bidirectional reflectance measurements. *Remote Sensing of Environment*, 51, 375-384.
- Rouse, J. W., Haas, R. H., Schell, J. A., and Deering, D. W. (1973). Monitoring vegetation systems in the great plains with ERTS. In: N SP-351, ed. 3rd ERTS symposium. NASA, Washington, pp 309-317.
- Sims, D. A., and Gamon, J. A. (2002). Relationships between leaf pigment content and spectral reflectance across a wide range of species, leaf structure and development stages. *Remote Sensing of Environment*, 81, 337-354.
- Sokal, R. R., and Rohlf, F. J. (1994). *Biometry the principles and practice of statistics in biological research*. San Francisco, Ca.: WH Freeman and Company.
- Uraibi, H. S., Midi, H., Talib, B. A., and Yousif, J. B. (2009). Linear regression model selection based on robust bootstrapping technique. *American Journal of Applied Sciences*, 6, 1191-1198.
- Valiela, I., Bowen, J. L., and York, J. K. (2001). Mangrove forest: One of the worlds threatened major tropical environments. *Biological Sciences*, 51, 807-815.
- Vogelmann, J. E., Rock, B. N., and Moss, D. M. (1993). Red-edge spectral measurements from sugar maple leaves. *International Journal of Remote Sensing*, 14, 1563-1575.
- Walters, B. B., Rönnbäck, P., Kovacs, J. M., Crona, B., Hussain, A., Badola, R., Dahdouh-Guebas, F., and Barbier, E. (2008). Ethnobiology, socio-economics and management of mangrove forests: a review. *Aquatic Botany*, 89, 220-236.
- Wu, C., Niu, Z., Tang, Q., and Huang, W. (2008). Estimating chlorophyll content from hyperspectral vegetation indices: modeling and validation. *Agricultural and forest meteorology*, 148, 1230-1241.

- Zarco-Tejada, P. J., Miller, J. R., Noland, T. L., Mohammed, G. H., Sampson, P. H. (2001). Scaling-up and model inversion methods with narrowband optical indices for chlorophyll content estimation in closed forest canopies with hyperspectral data. *IEEE Trans Geosciences in Remote Sensing*, 39, 1491-1506.
- Zhang, C., Yali, L., Kovacs, J. M., Flores-Verdugo, F., Flores-de-Santiago, F., and Chen, K. (2012). Spectral response to varying levels of leaf pigments collected from a degraded mangrove forest. *Journal of Applied Remote Sensing*, 6, 063501.

Chapter 5

5 An object-oriented classification method for mapping mangroves in Guinea, West Africa, using multipolarized ALOS PALSAR L-band data.⁴

5.1 Introduction

To date, many studies have been conducted to examine the use of remotely sensed data from spaceborne platforms for monitoring mangrove forests. However just a few have assessed the use of these data for estimating and spatially predicting quantitative measurements (e.g. Green et al. 1997, Kovacs et al. 2004, Kovacs et al. 2005, Heumann 2011). In the past, several authors have published positive correlation between in situ biophysical properties (e.g. LAI) and pixel-based remotely estimated vegetation indices derived from optical satellite imagery (e.g. Ramsey and Jensen 1996, Green et al. 1998, Kovacs et al. 2010). They suggest that highly accurate estimated composite maps of biophysical properties can be created from these sensors.

Although there are many advantages of using optical imagery for mapping mangrove forests a major limitation is the availability of cloud-free scenes. In many tropical and subtropical zones, the presence of persistent cloud cover is the norm and thus the availability of useful optical data is limited. Hence, the use of Synthetic Aperture Radar (SAR) could be an alternative to traditional optical data. Unaffected by cloud cover, SAR imagery can provide distinctive information on surface areas based on the interaction between active energy and the variability of geometric properties and the dielectric constant of ground features (Ulaby et al. 1986). Due to the commonly persistent flooded ground and moderately flat terrain of mangrove forests, the backscatter mechanism is enhanced within making it an ideal forest canopy for SAR assessments

⁴ A version of this chapter has been published: **Flores-de-Santiago F.**, Kovacs JM., Lafrance P. (2013). An object-oriented classification method for mapping mangroves in Guinea, West Africa, using multipolarized ALOS PALSAR L-band data. **International Journal of Remote Sensing**. 34(2): 563-586. (<http://dx.doi.org/10.1080/01431161.2012.715773>).

(Hess et al. 1990). One example is provided by Kovacs et al. (2006), in which they showed that spaceborne SAR, specifically fine beam co-polarized HH RADARSAT-1 data, can be used for extracting biophysical parameter data from mangrove forests with some degree of accuracy. In this investigation, Kovacs et al. (2006) were able to discern dead wetland stands from healthy ones due to a significant relationship between LAI and the corresponding RADARSAT-1 fine beam backscatter coefficients. Using coarser spatial resolution but multipolarized ENVISAT C band data, Kovacs et al. (2008a) also showed the importance of multipolarized data for accurate monitoring of these forests.

An important addition to the earth observation systems available for mangrove assessment is the Japan Aerospace Exploration Agency's (JAXA) Advanced Land Observing Satellite (ALOS) Phased Array L-band Synthetic Aperture Radar (PALSAR) (Rosenqvist et al. 2000). In contrast to shorter wavelengths (e.g. X-band, C-band), L-band can penetrate to greater depth in high biomass canopies and thus the backscatter is less likely to saturate in these conditions (Mougin et al. 1999). One of the advantages of the ALOS PALSAR over its predecessors is the dual rather than single polarization data that can be acquired. To date L-band SAR data has shown to be useful for mapping mangrove extent and zonation as a function of structural differences between species and growth stages in Australia, New Guiana, and Malaysia (Lucas et al. 2007). It has been suggested that the inclusion of L-band HV data will provide increased opportunities for differentiating between mangroves zones, including different species, growth stages or biomass levels (Lucas et al. 2006). Despite these many advantages, little research has been conducted using ALOS PALSAR data over large mangrove areas (Heumann 2011). Moreover, there is little information regarding the potential to use these data for other classification methods, particularly object-based classification.

While traditional pixel-based classification have been used for extracting and monitoring mangrove zones (Green et al. 1998, Manson et al. 2001, Kovacs et al. 2005, Kovacs et al. 2009, Kovacs et al. 2010), the development of new techniques such as object-based classification, need to be demonstrated for detailed characterization of mangrove forests (Heumann 2011). Object-based classification is a relative recent technology where textural information is used in addition to spectral information for

classifying data (Blaschke and Hay 2001). It is particularly useful for extracting the image-object relation rather than single pixels, which involves the identification of homogenous groups of pixels called objects which have similar spectral and/or spatial characteristics. As a result, objects (i.e. segments) are created by using different ratios of color-shape, and smoothness-compactness. These newly created objects have additional spectral information as compared to single pixels including mean values, median values, minimum and maximum, and variance per band (Hay and Castilla 2008). In addition, the object-based classification could include a variety of conditions such as spectral/spatial information for each object, texture, context, and shape (Herold and Scepan 2002).

The main purpose of this investigation was to determine the level of accuracy which could be achieved using an OBIA approach to L-band ALOS PALSAR single (HH) and dual (HH+HV) polarized data for classifying different species and conditions of mangrove typical of the west African coast. As a secondary objective, I also attempted to identify the ideal SAR filter for use in this OBIA classification procedure.

5.2 Methods

Guinea possesses a relatively extensive freshwater system with 1161 rivers and drainage basins, ranging in size from five to 99 168 km² (NOAA 2011). The annual rainfall for this region often exceeds two meters, but a distinct dry season extends from December to May (Courtin et al. 2010). In lower-Guinea (Prefecture du Forecariah), the flood plains and tidal areas result in an elaborate estuarine system supporting extensive mangrove forests which are central to the local economy (Kasisi 2002). For this study I focused on the islands of Mabala and Yélitono located at the lower end of the Forecariah, Tana, and Melacore rivers in the southern coastal zone of Guinea, West Africa (Fig. 5.1). The two islands have a terrestrial area of approximately 134.6 km², and the coast is influenced by semidiurnal tides with a range of up to three meters (NOAA 2011). According to Courtin et al. (2010) the local population is represented primarily by the autochthonous Soussou ethnic group, who are located in small and dispersed settlements and whose main activities are agricultural, fishing, and freshwater collection.

According to the FAO (2007) and Kovacs et al. (2010), there are six mangrove species that can be found in the southern coast of Guinea: the red mangroves (*Rhizophora mangle*, *R. racemosa*, *R. harisonii*), the black mangrove (*Avicennia germinans*), the white mangrove (*Laguncularia racemosa*), and the button wood (*Conocarpus erectus*).

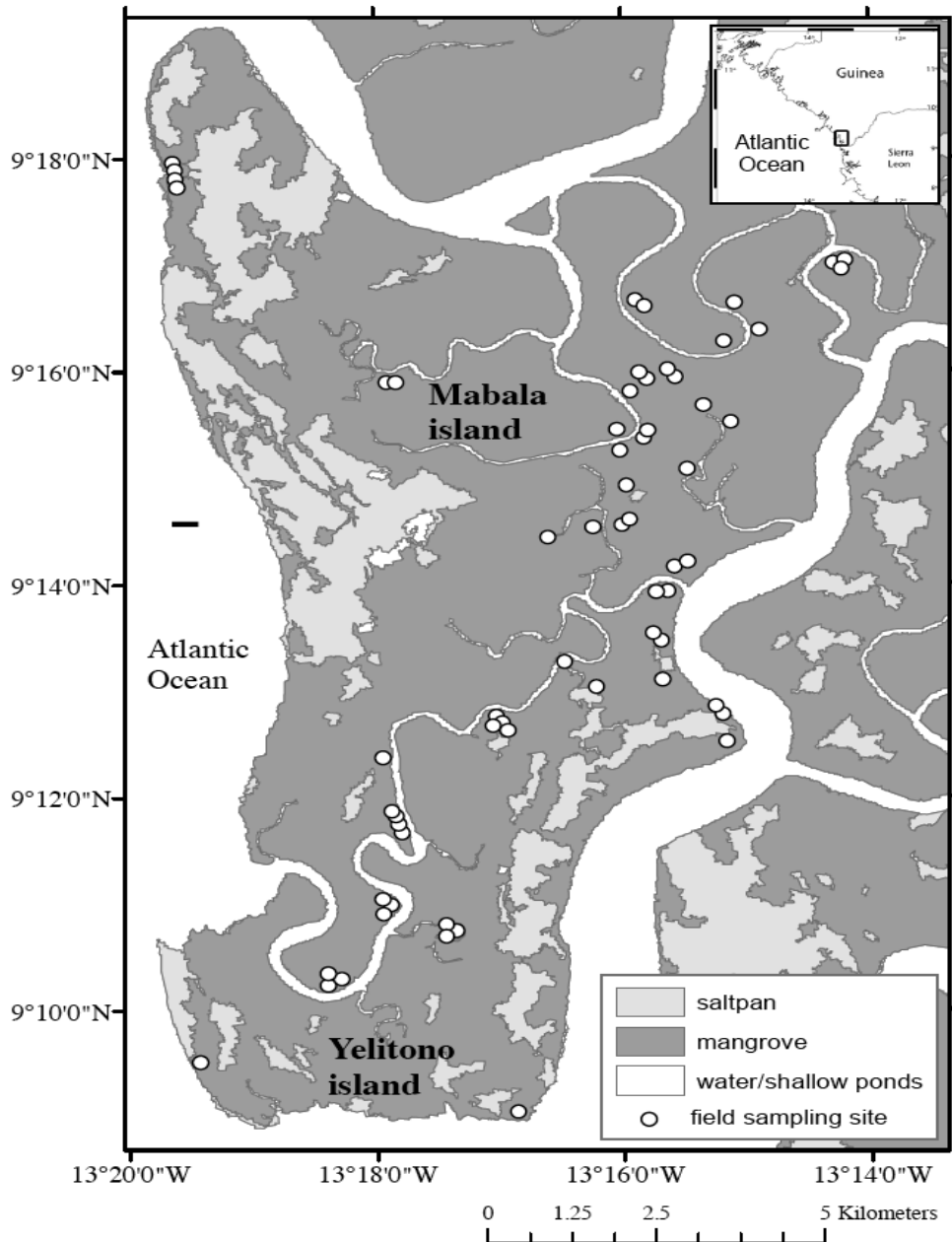


Figure 5.1: Location of the mangrove islands of Guinea, Western Africa

Kovacs et al. (2010) reported that white and button wood mangroves were rarely found and that no uniform stands were encountered in this area. Consequently the mangrove classification that they assessed corresponds to: tall red mangrove (*Rhizophora racemosa*), medium red mangrove (*R. racemosa*), dwarf red mangrove (*R. mangle* and *R. harisonii*), and black mangrove (*Avicennia germinans*).

Given the persistent cloud cover on this tropical zone, two scenes of ALOS PALSAR L-band data were collected for this region: a single polarized (HH) 6.25 m pixel spacing scene dated February 2007, and a dual polarized (HH+HV) 12.5 m pixel spacing scene dated October 2007 (Table 5.1). Both SAR data were spatially corrected by registration to a previously geometrically corrected high spatial resolution scene (Kovacs et al. 2010). In total 20 ground control points were used resulting in an overall root mean square error of 0.68 for the HH and 0.47 for the dual polarized images.

Table 5.1: SAR data collected from the ALOS-PALSAR space-borne sensor

Sensor	ALOS-PALSAR Fine Mode	ALOS-PALSAR Fine Mode
Date of Acquisition	2007-10-14	2007-02-21
Time of Acquisition	23:35:07	23:35:37
Radiometric	16-bit	16-bit
Resolution		
Pixel Spacing	12.5 m	6.25 m
Polarization	HH+HV	HH
Frequency (L-band)	1270 MHz	1270 MHz

The mangrove classification from Kovacs et al. (2010) included four classes that were mapped using a combination of optical data from IKONOS-2, QuickBird, and Airborne (Leica-ADS40) remotely sensed data. However, in this study it was not possible to separate three of the four mangrove classes as there was no difference in the backscatter decibel values between the tall and medium red mangrove which are the same species (*R. racemosa*). The medium red mangrove forms the transition zone between the tall red mangrove and the dwarf red mangrove, the later represented by *R. mangle* and *R. harisonii*. Consequently, for this investigation the classes examined were tall red mangrove (*Rhizophora racemosa*), dwarf red mangrove (*R. mangle* and *R. harisonii*), and black mangrove (*Avicennia germinans*) as shown on figure 5.2. The difference in the

decibels from the mangrove classes was assessed by extracting backscatter information from 63 training sites (Fig. 5.1) on both the single (HH) and dual (HH+HV) polarized scenes. These training sites were selected based on a field campaign carried out from March 13th until April 6th 2008. The sub-meter GPS locations of each of the 63 training sites were found in both the single and the dual polarized scenes and the extraction of the mean values from the decibel were recorded for each of the three mangrove classes.



Figure 5.2: Characterized representation of the land cover classes examined for the classification: (a) Saltpan, (b) Tall Red Mangrove, (c) Dwarf Red Mangrove, (d) Black Mangrove)

The resulting minimum random point number was 557. However, for the accuracy assessment used a value of 598. The first level of classification was performed with three aggregated broad classes (saltpan, mangrove, and water/shallow ponds). A second level of classification was also examined which including the subdivision of the general mangrove class into three new classes: black mangrove, dwarf red mangrove, and tall red mangrove, resulting in a total of five classes.

The accuracy for both classifications was assessed in detail using error matrices and their associated statistics: overall accuracy, class producer accuracy, class user accuracy, and the kappa statistic (Jensen 2005). For the single and dual polarization accuracy assessments, 598 ground truth validation points, selected in a stratified random sample, were used. All points were verified using a high resolution optical airborne false color composite image (NIR, R, G), collected at a 0.5 m spatial resolution, and from the classification maps of Kovacs et al. (2010). In addition, numerous photos and video, taken during the field campaign, were used as reference. The producer and user accuracy were examined for individual class assessments when the overall accuracy was similar amongst the scales at level-1 and level-2 classifications.

All processing of the object-based segmentation and classification was completed using Definiens Professional Earth 7.0 (formerly eCognition) software (Definiens AG, Munich, Germany). Using the multiresolution segmentation process it is possible to create objects using information about the spatial relations existing between the SAR pixels, and analyzing the spectral reflection depending on the ratios between shape (compactness and smoothness) and color (spectral information) all of which can be weighted by the user (Laliberte et al. 2004). There is little knowledge about object-based classification on mangrove forests. However, the flooded terrain and different mangrove classes used made it possible to assess the shape and color criteria based on a relatively simple routine for both scenes (Figs.5.3 and 5.4).

I used several trial and error procedures to first understand how the segmentation process could be affected by changes in the shape and color relationship. Following the trial and error nature of this test, the shape/color ratio was kept at the “best” visual

interpretation from the SAR image. The next step consisted of altering only the smoothness/compactness ratios from the optimal shape/color relation in order to assess which parameter settings best captures the objects of interest (Figs. 5.3 and 5.4).

Once the optimal shape/color and compactness/smoothness ratios were selected to represent the “optimal” image objects conditions, the scale parameter was tested. The key parameter in multiresolution segmentation is a unitless variable of scale that is related to the image’s pixel size (Dingle and King 2011). In principle, there are unlimited choices of scale parameter during the multiresolution segmentation stage. The final decision of the scale parameter is, however, often made by an interpreter based on the visual inspection of the image, rather than quantitative criteria (Wang et al. 2004a). In this study, I used several series of scales for the single (HH) polarized (Fig.5.3), and the dual (HH+HV) polarized data (Fig.5.4). The first hierarchical level of classification (i.e. level-1) corresponded to three land cover classes (saltpan, mangrove, and water/shallow ponds). To date, the scale parameter selection for this type of segmentation has been done mostly by trial and error (e.g. error assessment). In this study after each classification at the level-1 I used the 598 random reference points to identify the optimal scale.

During the classification at level-1, the first rule-base consisted of a separation between water/shallow ponds from land using training data generated by the mean backscatter values from the representative objects. The second rule-base included a separation between saltpan and mangrove from the previous land class area using specific mangrove and saltpan site locations from the field work. This resulted in a relatively easy classification process between the three classes in part due to the clear separation in the decibels from the water, saltpan, and mangrove forests within the single (HH) polarized scene (Fig.5.3). For the dual (HH+HV) polarized scene, I used a series of steps in which the first rule was the application of the decision tree from the HH data for the three general classes (Fig.5.3) which was then followed by the additional rules for the HV data (Fig.5.4).

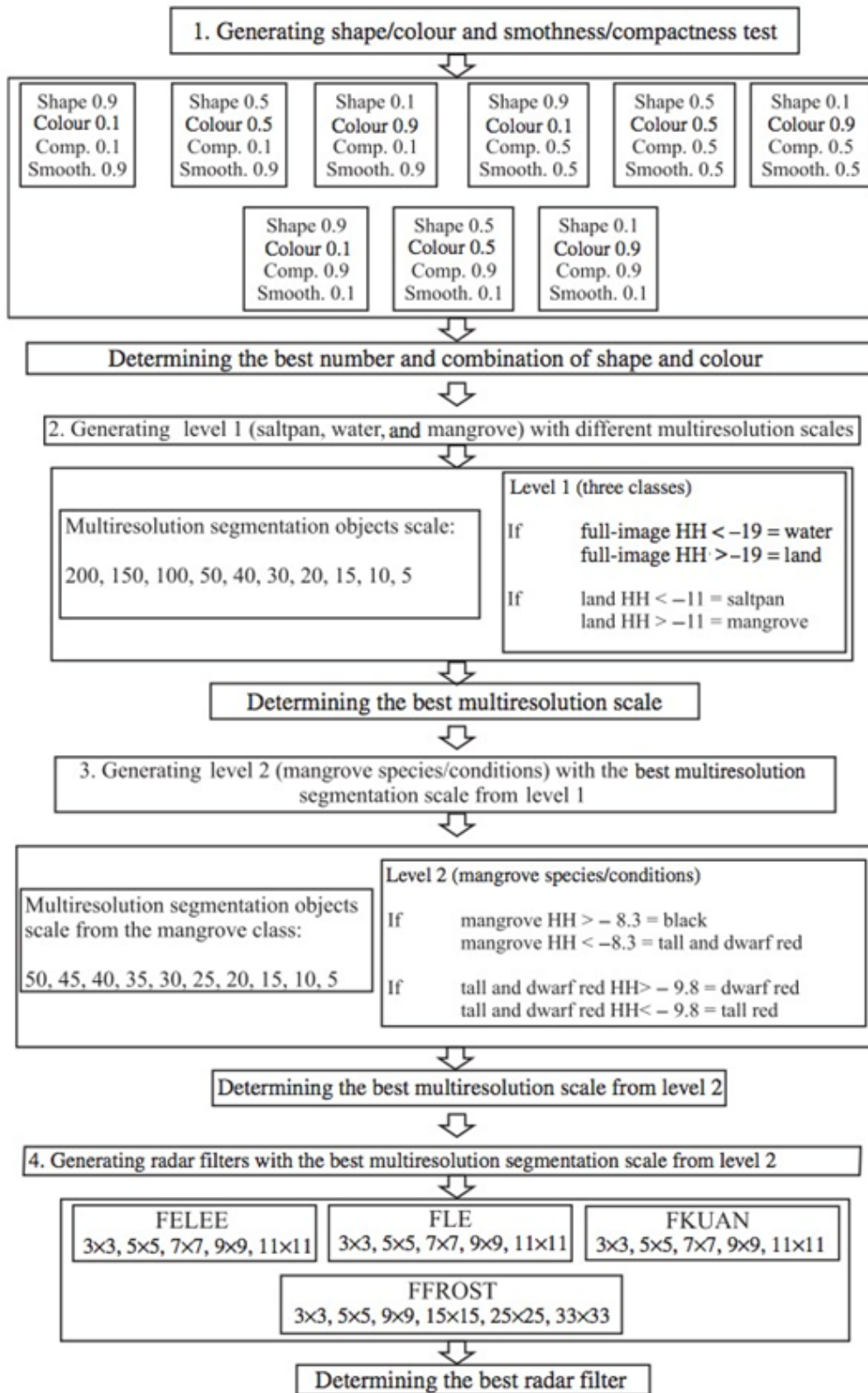


Figure 5.3: Flowchart for the HH L=band ALOS PALSAR data

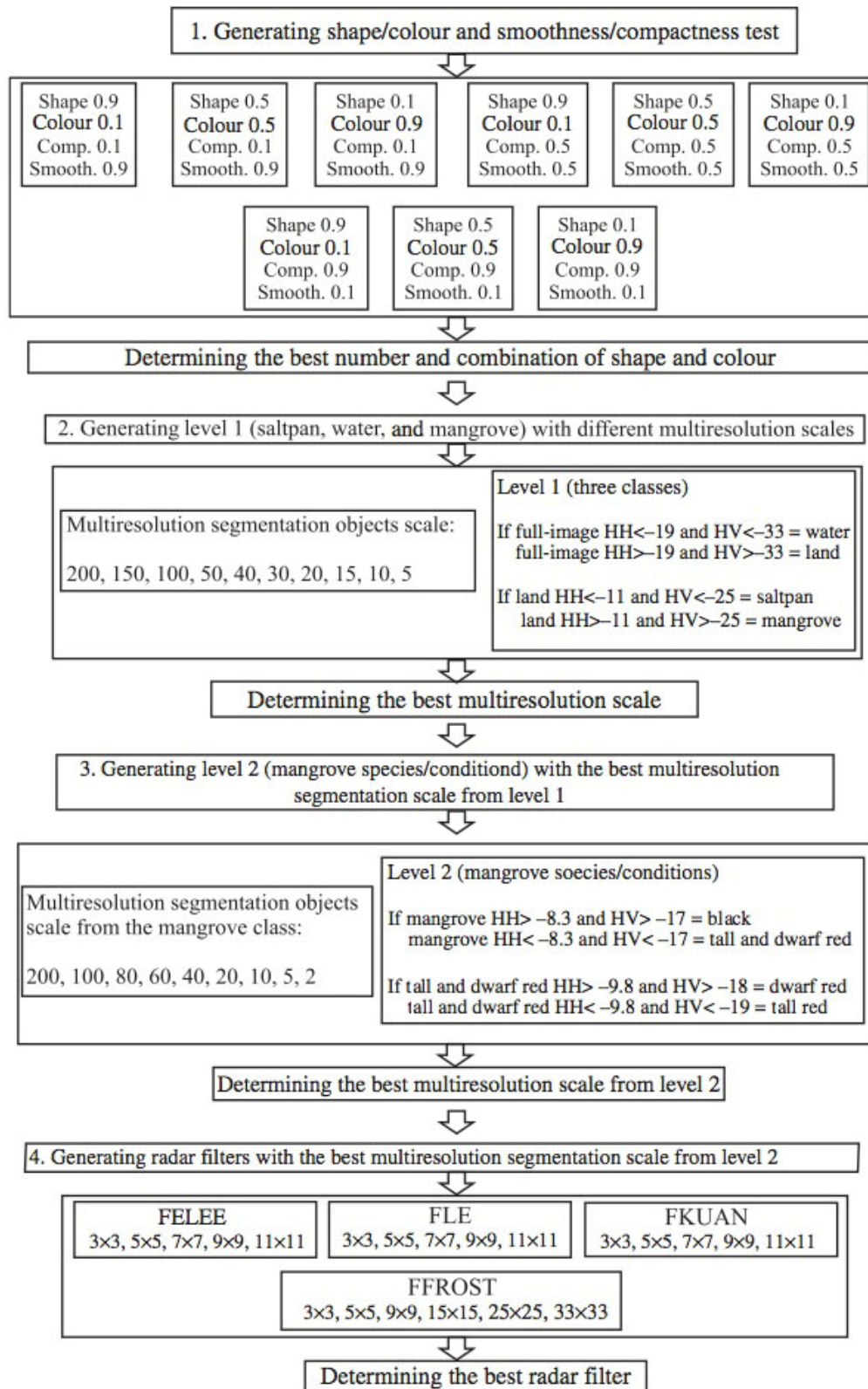


Figure 5.4: Flowchart for the HH+HV L-band ALOS PALSAR data

Once the optimal multiresolution scale at level-1 was selected, I proceeded to create the second level of classification (level-2), which corresponded to the three more refined mangrove classes (tall red, dwarf red, and black mangrove). In this cycle, I merged the objects from the previous mangrove class, and a second multiresolution segmentation was performed only within the mangrove class from level-1. A similar process from level-1 was employed in level-2 where several values for the objects' scales were tested in order to evaluate their impact on the classification accuracy. From the 598 random points from level-1, I subdivided the mangrove points into three mangrove classes in order to obtain five new aggregated random points for the accuracy assessments. Classification was conducted first on the single HH polarized image using only the rule-base of backscatter information for each object depicted on figure 5.3. The HH+HV data classification was followed using the rule-based calculations from the HH data with additional information from the HV band (Fig.5.4). A decision rule based classifier (Jensen 2005, Lillesand et al. 2008) was then applied to both images using the classification hierarchy for both segmented scenes.

Once the optimal scale was selected from level-2, I tested if the accuracy from the level-1 and level-2 classification object scenes could be improved by analyzing several filters and filter sizes. Many adaptive filters have been developed specifically for speckle reduction. Specifically, I tested the best known and the most commonly used digital speckle filters, which remove high frequency noise while preserving high frequency features (i.e. edges). Specifically, I examined the Lee Speckle Filter (FLE) (Lopes et al. 1990), the Enhanced Lee Speckle Filter (FELEE) modified by Lopes et al. (1990), the Kuan Speckle Filter (FKUAN) (Kuan et al. 1985) and the Frost Adaptive Filter (FFROST) (Frost et al. 1982) for both the single and dual polarized scenes.

The FKUAN filter is based on a Minimum Mean Square Error (MMSE) criterion (Gagnon and Jouan 1997). The MMSE is applied to the multiplicative model, and then a signal-dependent additive noise model is applied under the form of a linear filter (Shi and Fung 1994). Therefore the FKUAN filter is optimal when both the scene and the detected intensities are Gaussian distributed. The FLE filter is a particular case of the FKUAN filter when the multiplicative model is first approximated by a linear model (Shi and

Fung 1994) and then the MMSE criterion is applied to this linear model. The FELEE filter, modified by Lopes et al. (1990), introduces a hyperbolic function in the multiplicative model and thus could satisfy the requirement that the more heterogeneous the area is, the less it has to be smoothed. The FFROST filter differs from the FLE and the FKUAN filters in that the scene backscatter is estimated by converting the observed image into an exponential impulse response (Gagnon and Jouan 1997). The resulting filter response is obtained by minimizing the mean square error between the observed image and the multiplicative model (Shi and Fung 1994).

5.3 Results and discussion

Table 5.2 presents a summary of the accuracy statistics from the object-based classification for both SAR scenes at the level-1 segmentation. Accuracy assessments were not performed for the shape/color of 0.9/0.1 and the shape/color of 0.5/0.5 ratios due to obvious poor object scene multiresolution segmentation (Figs. 5.5 b, 5.5 c, and 5.6 b, 5.6 c). For the single and the dual polarized scenes, the shape/color 0.1/0.9 ratio showed a better visually object segmentation (Figs. 5.5 d, and 5.6 d), with overall accuracies of 86.7 % and 91.0 % respectively (Table 5.2). It is clearly evident that color does play a key role in the objects' formation for this type of environment. As previously reported by Thiel et al. (2008), SAR scenes over forested areas are strongly affected by the color (i.e. tone) of the image rather than the shape in which bright objects typically represent forested areas and dark tones represents non forested objects. Moreover, clear-cuts or young forest stands typically possess a middle grey tone. In addition, according to the Definiens's manual (2008), in images with high variability such as SAR scenes the color criterion minimizes the standard deviation of the pixel values within the image objects, and thus the multiresolution segmentation stage is improved.

There was little observed difference between the accuracy assessments from the smoothness and compactness ratios as this relationship typically depends on the weight from the shape criterion (e.g. Lewinski and Zaremski 2004) and, for this investigation, the color parameter had the higher influence. Based on the aforementioned results and the highest accuracy assessment from the relationships (Table 5.2), I then selected a shape/color ratio of 0.1/0.9 with a compactness/smoothness ratio of 0.1/0.9 (Fig. 5.5 f) as

the optimal relationship for the single polarized multiresolution segmentation. For the dual polarized scene, I found an optimal relationship in both the shape/color and the compactness/smoothness ratio of 0.1/0.9 (Fig. 5.6 e).

Table 5.2: Single (HH), and dual (HH+HV) polarization modes accuracy assessment at level 1 (saltpan, mangrove, water), using a combination of shape/color and compactness/smoothness multiresolution segmentation approach

	Shape	Color	Compactness	Smoothness	No. objects	Overall accuracy (%) level 1
HH Scale 100	0.9	0.1	0.5	0.5	447	86.7
	0.5	0.5	0.5	0.5	316	
	0.1	0.9	0.5	0.5	152	
	0.1	0.9	0.1	0.9	133	
	0.1	0.9	0.9	0.1	183	
HH+HV Scale 20	0.9	0.1	0.5	0.5	2369	91.0
	0.5	0.5	0.5	0.5	1660	
	0.1	0.9	0.5	0.5	766	
	0.1	0.9	0.1	0.9	696	
	0.1	0.9	0.9	0.1	929	

As expected there was an inverse relationship between the number of objects and the scale parameter for both images (Figs. 5.7 a, 5.7 b). For both SAR data, the overall accuracy increases up to a scale of approximately 50 beyond which it decreased. For the single (HH) data, the optimal scale was 40 with an overall accuracy of 91.1 %. With an average object area of 130 ha for this level, the objects often merged several mangrove species. Moreover, bigger objects often separated large areas of saltpan and water. According to Table 5.3, using this scale results in a classification where the mangrove and water classes have higher producer and user accuracies than the saltpan class and where most of the error is due to mangrove misclassified as saltpan. From Fig. 5.7 c, it is also apparent that this misclassification only increases with an increased scale.

Table 5.3: The error matrix for the single pol (HH) data at level-1 using a multiresolution segmentation scale of 40

Class	Reference data			User's accuracy (%)
	Saltpan	Mangrove	Water	
Saltpan	65	8	6	82.3
Mangrove	29	308	5	90.1
Water	1	4	172	97.2
Producer's accuracy (%)	68.4	96.3	94	
Overall accuracy (%)	91.1			
Overall Kappa statistic (%)	0.84			

For the dual (HH+HV) data, I found the optimal scale at a level of 20 which produced an overall accuracy of 92.3 % (Table 5.4) and an average object area of 130 ha. With regards to increasing scale and overall accuracy, a similar pattern to HH was found (Fig. 5.7). However, the overall accuracy of the dual polarized was consistently higher. Consequently, it is apparent that even with a coarser spatial resolution and higher average object area, the addition of the HV helps to improve the classification of the mangrove at this level. Lucas et al. (2007) had also suggested that L-band HV data could be used as a reliable source for delineating different mangrove zones in Australia and Malaysia based on the species stage. The producer and user accuracies for the three classes were higher when compared to the single polarized data. There was little difference in the user accuracy with an increase in scale (Fig. 5.7 f). However, the saltpan class once again indicated the lowest producer accuracy (81.1 %) with the misclassification of mangrove (Table 5.4). The misclassification of mangrove as saltpan may have resulted from sparse mangrove stands where little backscatter occurs (i.e. dark tones) in contrast to healthy mangrove ones with higher backscatter (i.e. lighter grey tones, Kovacs et al. (2006, 2008b)).

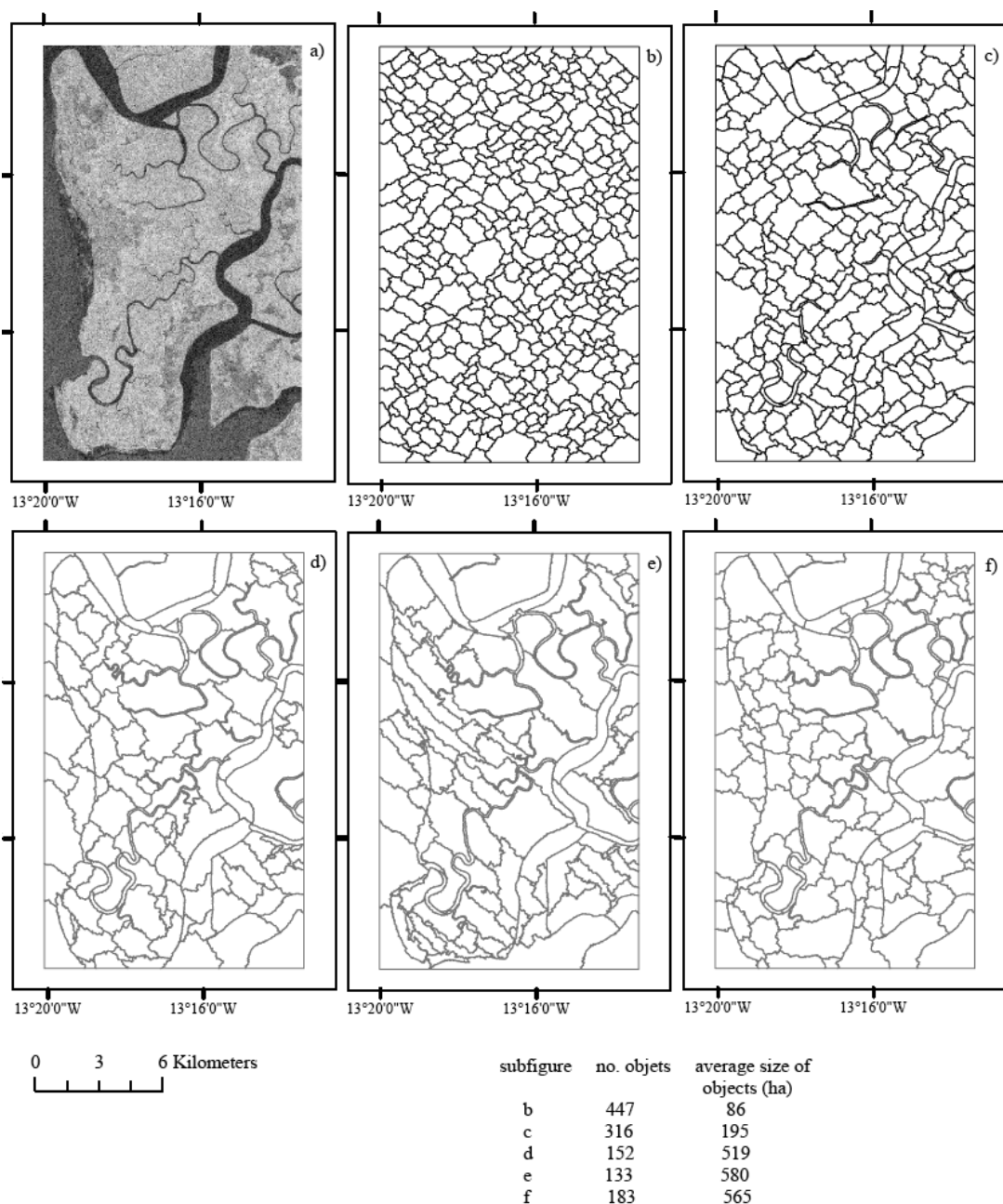


Figure 5.5: Multiresolution segmentation objects. HH L-band ALOS PALSAR data
(a). Objects for: (b) shape=0.9, compactness=0.5; (c) shape=0.5, compactness=0.5;
(d) shape=0.1, compactness=0.5; (e) shape=0.1, compactness=0.1; (f) shape=0.1,
compactness=0.9

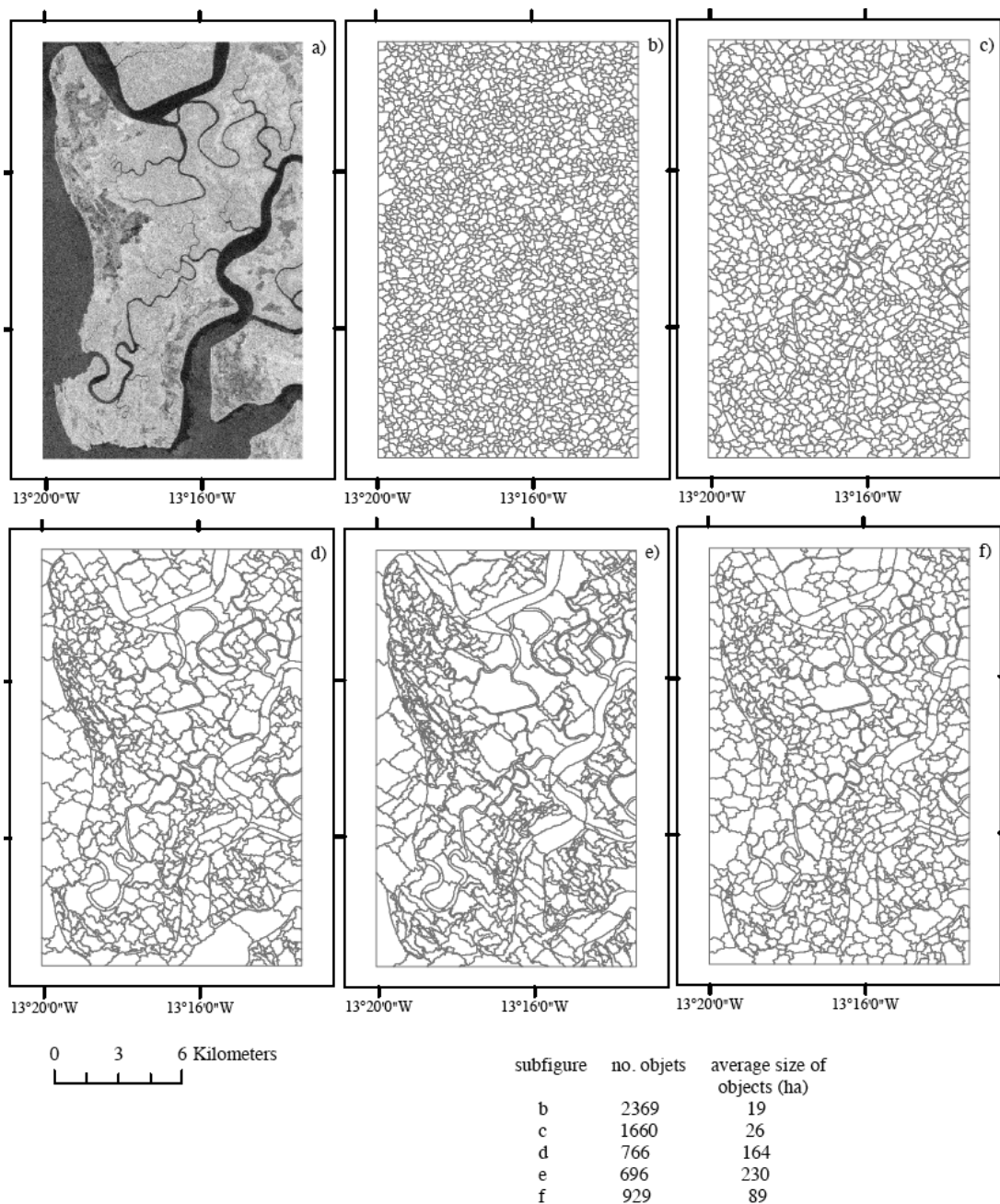


Figure 5.6: Multiresolution segmentation objects. HH+HV L-band ALOS PALSAR data (a). Objects for: (b) shape=0.9, compactness=0.5; (c) shape=0.5, compactness=0.5; (d) shape=0.1, compactness=0.5; (e) shape=0.1, compactness=0.1; (f) shape=0.1, compactness=0.9

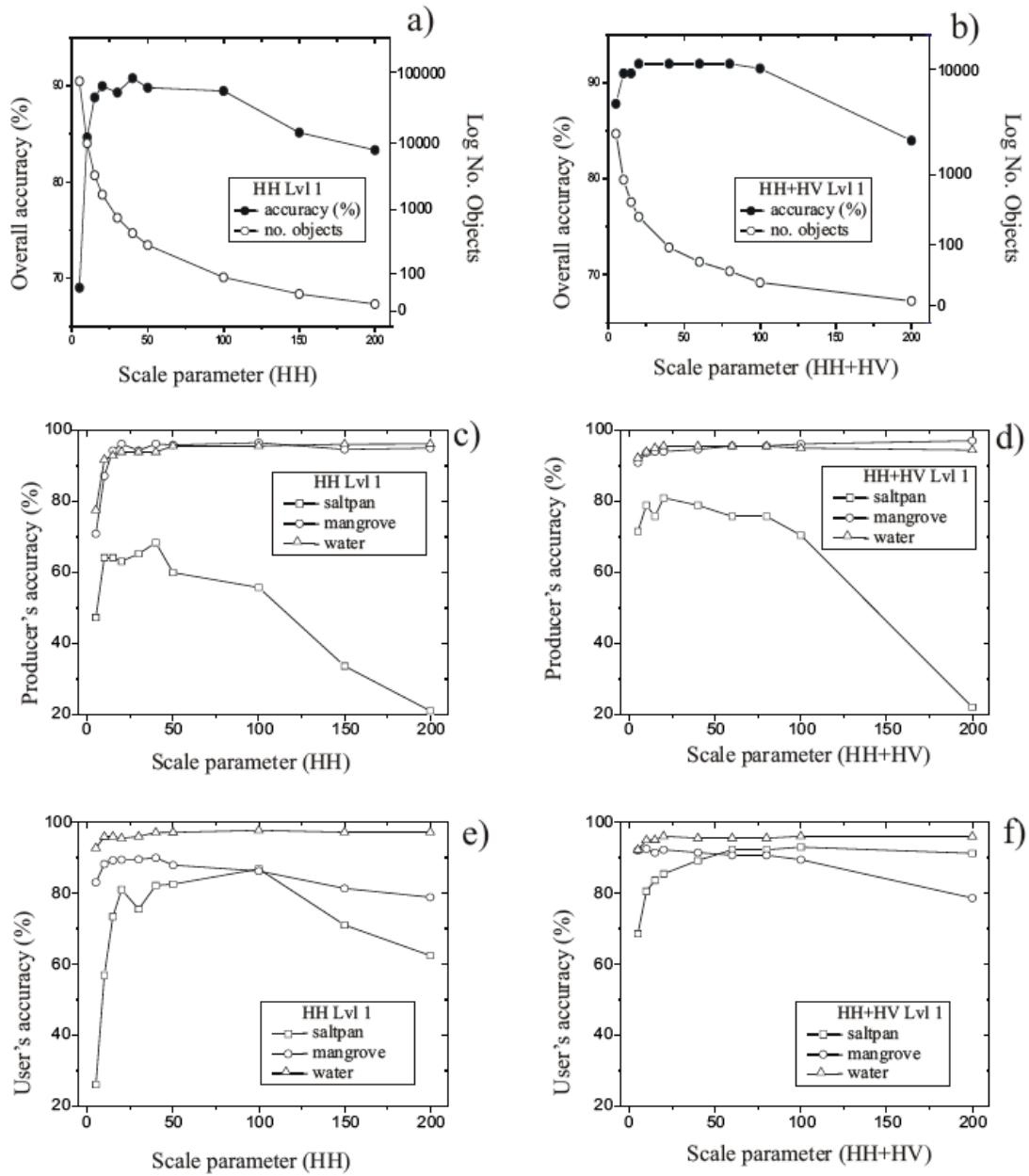


Figure 5.7: Accuracy assessment for the HH and HH+HV L-band using different scales at level 1

Table 5.4 The error matrix for the dual pol (HH + HV) data at level-1 using a multiresolution segmentation scale of 20

Class	Reference data			
	Saltpan	Mangrove	Water	User's accuracy (%)
Saltpan	77	12	1	85.6
Mangrove	18	301	7	92.3
Water	0	7	174	96.1
Producer's accuracy (%)	81.1	94.1	95.6	
Overall accuracy (%)	92.3			
Overall Kappa statistic (%)	0.87			

The highest overall accuracy for the single polarized data was found at a scale of 15 (Fig. 5.8). However, I selected an optimal scale of 10 because the producer accuracy of the black mangrove decreases at a scale of 15. Unlike the level-1 classification, the overall accuracy of the optimal scale for the single polarized was quite poor at 57.4 % with an average object area of 15 ha. The object size for this scale separates patches of forest within the species. In particular, the producer accuracy for black mangrove and dwarf red mangrove were very low and the user accuracy for tall red mangrove as well (Table 5.5). For the HH data, it was evident that at higher scales many of the small black mangrove areas were incorporated into larger areas of adjacent dwarf red and tall red mangroves. As the segmentation becomes coarser, each object will tend to incorporate a wider range of image brightness values (Kim et al. 2008). Therefore, a general trend of increasing average variance of the objects is expected with coarse scale (i.e. decreasing number of objects) and each segment will tend to include more pixels from high similar class such as black mangrove into less similar classes like dwarf red and tall red mangrove.

Table 5.5: The error matrix for the single pol (HH) data at level-2 using a multiresolution segmentation scale of 10 within the mangrove area

Class	Reference data					User's accuracy
	Saltpan	Black	Dwarf red mangrove	Tall red mangrove	Water	
Saltpan	45	1	3	3	1	84.9
Black mangrove	3	35	16	5	0	59.3
Dwarf red mangrove	4	37	43	12	1	44.3
Tall red mangrove	22	46	75	41	2	22.0
Water	19	2	1	2	179	88.2
Producer's accuracy	48.4	28.9	31.2	65.1	97.8	
Overall accuracy (%)	57.4					
Overall Kappa	0.46					

For the dual polarized I chose an optimal scale of five with an average object area of 1.5 ha (Fig. 5.8 b). The object area for this scale was much lower compared with the HH data. The user and producer accuracies from the saltpan and water remained constant with an increase in the scale thus suggesting that most of the discrepancy was due in part to the three mangrove classes. According to table 5.6, it is apparent that the misclassification occurs amongst the various mangrove classes. Poor levels of accuracy, both producer and users, were found for all three mangrove classes. The poorest classification was observed for the red mangrove with a producer accuracy for the dwarf variant on only 32 % and a user's accuracy for the tall variant of 20 %. This source of classification errors could be explained by the omission of fringe mangrove (i.e. tall red mangrove) that are less than the pixel size from the coarse dual polarized scene, resulting in mixed classes (Manson et al. 2001). As an example, Souza-Filho and Paradella (2003) were not able to perform a difference between mangroves based exclusively on pixel RADARSAT backscatter.

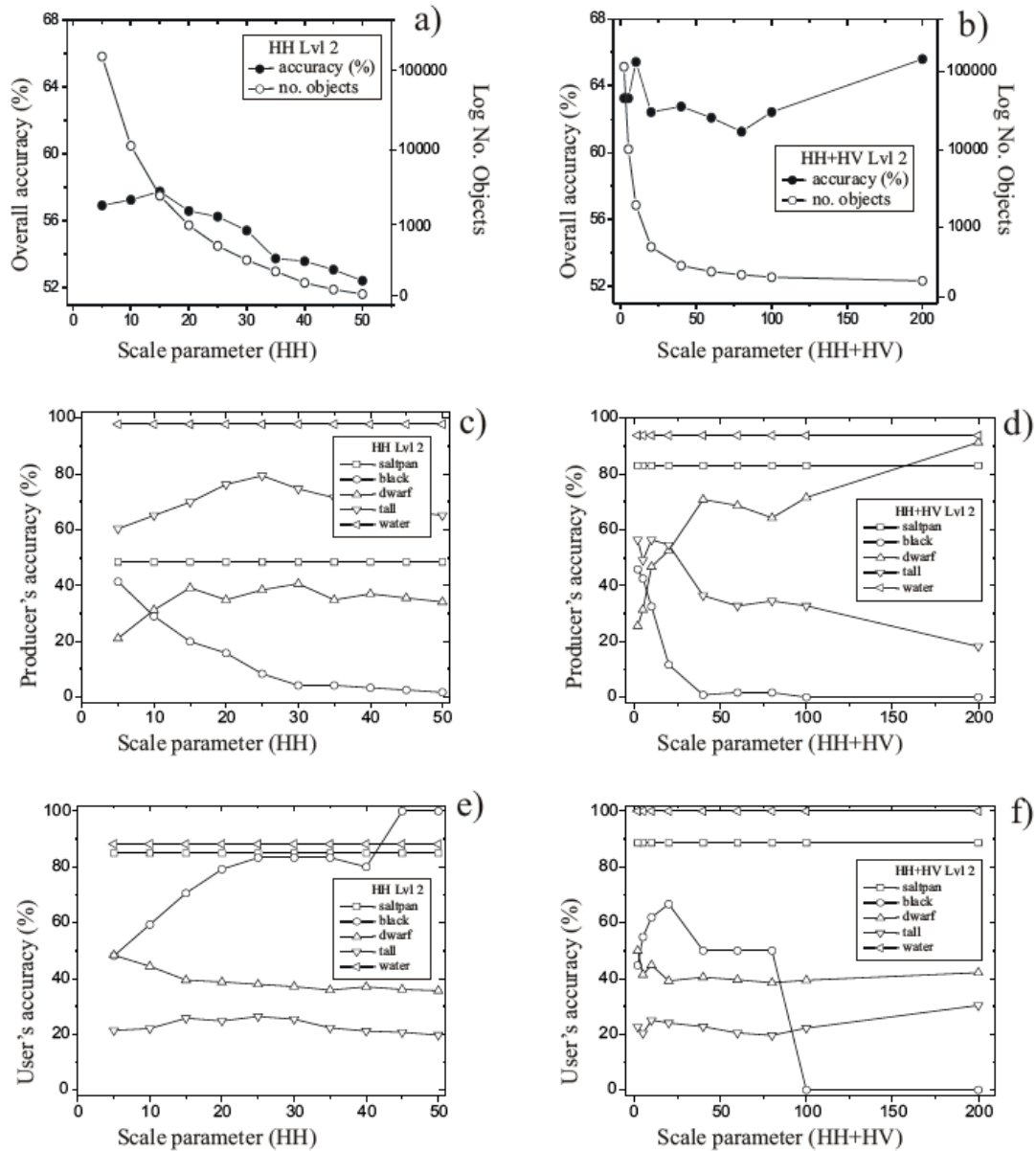


Figure 5.8: Accuracy assessment for the HH and HH+HV L-band using different scales at level 2

Table 5.6: The error matrix for the dual pol (HH+HV) data at level-2 using a multiresolution segmentation scale of 5 within the mangrove area

Class	Reference data					User's accuracy
	Saltpan	Black mangrove	Dwarf red mangrove	Tall red mangrove	Water	
Saltpan	78	3	4	2	1	88.6
Black mangrove	4	51	30	6	2	54.8
Dwarf red mangrove	2	35	43	20	4	41.4
Tall red mangrove	10	31	60	27	5	20.3
Water	0	0	0	0	180	100
Producer's accuracy	83	42.5	31.4	49.1	93.8	
Overall accuracy	63.4					
Overall Kappa	0.54					

According to tables 5.5 and 5.6 the overall accuracies improve within the HH+HV data. However it is important to mention that the major contribution in the overall accuracy between both data was a better classification of saltpan (48.4 % to 83 % producer's accuracy, and 84.9 % to 88.6 % user's accuracy) as well as water (97.8 % to 93.8 % producer's accuracy, and 88.2 % to 100 % user's accuracy). The producers and users accuracies for the mangrove forest decreased slightly from the HH to the HH+HV data in particular with the black (59.3 % to 54.8 % user's accuracy) and the dwarf red mangrove (44.3 % to 41.4 %).

According to figure 5.9, the various SAR filters applied to the single polarized scene at a segmentation scale of 20 at level-1 did not improve the overall accuracy. The same outcome, although worse, was found at the level-2 classification at a segmentation scale of 10 (Fig. 5.9 c). Moreover, it was deemed that none of the filters, at any size, could be used to improve the classification of the mangroves.

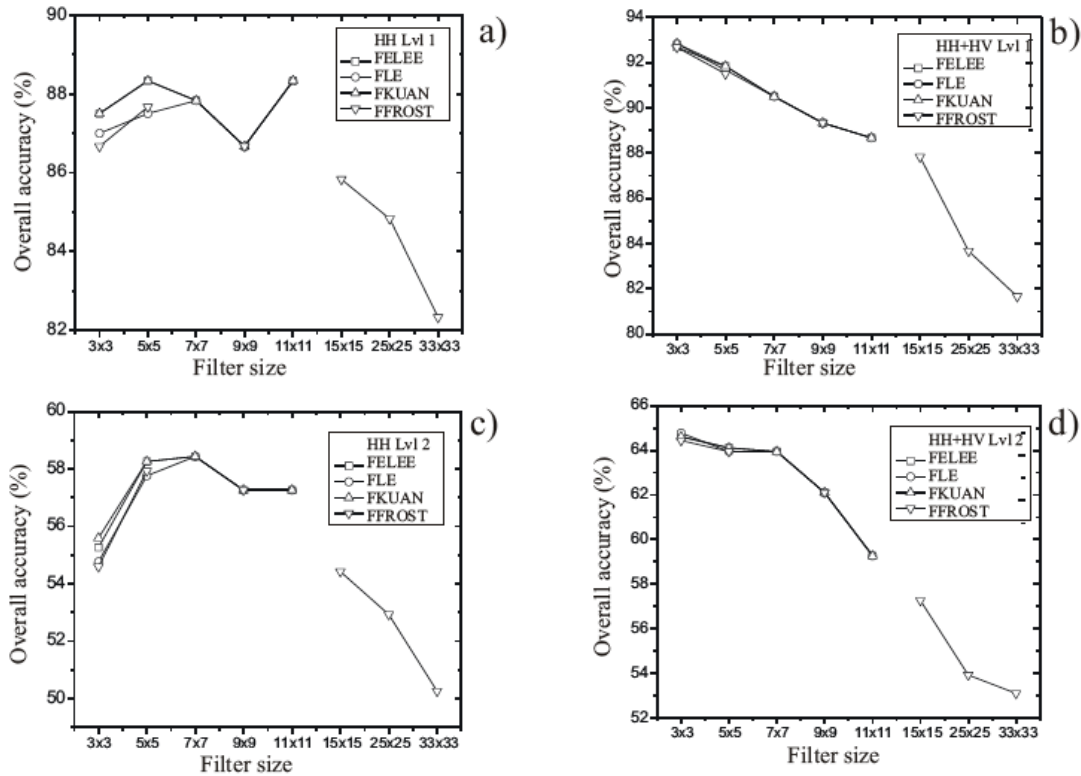


Figure 5.9: Accuracy assessment using different SAR filters from the optimal HH and HH+HV multiresolution scale at levels 1-2. a = HH level 1; b = HH+HV level 1; c = HH level 2; d = HH+HV level 2

When the filters were applied to the dual polarized data, only a very slight increase in accuracy was observed at the 3x3 size for both levels of classification. Beyond this filter size, the filters actually decreased the classification accuracies. A comparison of the error matrices of all the single and dual polarized approaches before and after filtering also reveals very little change in the patterns of producer and user accuracies (Tables 5.5, 5.6, 5.7, 5.8).

Table 5.7: The error matrix for the dual pol (HH+HV) data at level-1 using a Lee 3x3 filter with a multiresolution segmentation scale of 20

Class	Reference data			User's accuracy (%)
	Saltpan	Mangrove	Water	
Saltpan	77	12	5	81.9
Mangrove	18	303	1	94.1
Water	0	5	177	97.3
Producer's accuracy (%)	81.1	94.7	96.7	
Overall accuracy (%)	93.1			
Overall Kappa statistic (%)	0.88			

Table 5.8: The error matrix for the dual pol (HH+HV) data at level-2 using a Lee 3x3 filter with a multiresolution segmentation scale of 5

Class	Reference data					User's accuracy
	Saltpan	Black mangrove	Dwarf red mangrove	Tall red mangrove	Water	
Saltpan	77	2	5	3	7	81.9
Black mangrove	5	43	11	6	1	65.2
Dwarf red mangrove	2	45	57	13	2	47.9
Tall red mangrove	10	30	62	32	3	23.4
Water	0	0	2	1	179	98.4
Producer's accuracy	81.9	35.8	41.6	58.2	93.2	
Overall accuracy	64.9					
Overall Kappa	0.55					

For the single polarized data at a segmentation scale of 40, a shape and color ratio of 0.1/0.9, and a compactness/smoothness ratio of 0.9/0.1, the number of objects classified is 895. For the dual polarized data at a segmentation scale of 20, a shape and color ratio of 0.1/0.9, compactness and smoothness ratio of 0.1/0.9 and using a Lee filter of 3x3 the number of objects is 695. The main difference between the single and dual polarized scenes is misclassification between the saltpan and water classes as observed in the north east corner of the eastern island and the north western area (Fig. 5.10). It is

evident that the inclusion of the HV in the multiresolution segmentation from the dual polarized data improves the classification of saltpan.

The number of objects in the optimal scale parameters is higher on the dual polarized scene as compared to the single polarized data (Fig. 5.10) increasing the definition of the mangrove classes on the dual polarized. The results show that the incorporation of the rule-based classifications within the HH band, and a second level decision-tree based on the HV data, improves the separation of classes with each level of classification. For example, as reported by Krause et al. (2004) using optical data, lower-level objects could represent individual trees (e.g. sparse dwarf red and black mangrove), mid-level objects could represent a group of tree crowns of the same species and age (e.g. tall red mangrove), and high-level objects could represent a mangrove forest patch, such as the level-1 classification in this study.

The results from my best classification, dual polarized at 64.9 %, would indicate a relatively comparable approach to optical mangrove endeavors. For example, Kovacs et al. (2010) reported an overall accuracy of 78 % with four mangrove species/conditions and four non-mangrove features, using IKONOS, Quickbird and airborne multispectral data for this particular mangrove forest. Another study using only mangrove classes (i.e. no other land cover/use) reported an overall classification accuracy of nearly 75 % using Quickbird or IKONOS data (Wang et al. 2004b). More recently, Neukermans et al. (2008) report an overall accuracy of 72 % with four mangrove species using Quickbird multispectral imagery and a fuzzy classification scheme.

Within the object-based classification stage, black mangrove objects were located more in-land as reported by Kovacs et al. (2010). Tall red mangroves were located along the channels in fringe zones while dwarf red mangrove in the transition zones between tall red and black mangrove. Some of the misclassification between the tall and the dwarf red mangrove objects could be due to the later being found in close proximity to saltpans and with limited leaf coverage. In these sparsely, dispersed canopies, the radar signal may not be attenuated by a thick canopy and thus double-bounce may prevail resulting in an

enhanced backscatter which may be similar to the healthy tall red mangrove canopies (Kovacs et al. 2006, Kovacs et al. 2008a, Kovacs et al. 2008b).

For comparative sake, a series of photos and optical imagery were used to identify key patterns in the classification procedure. For example, figure 5.11 a shows a fringe black mangrove area close to the saltpan, followed by tall red mangrove in the distance. This pattern describes the zonation of the mangrove common to this study area. Black mangrove (*A. germinans*), is known to tolerate extremely high salinity levels and thus commonly associated with saltpans at some distance from the tidal channel's influence (Bertrand 1999, Wilkie and Fortuna 2003). In figure 5.11 b, taken in the middle of the channel, it is possible to differentiate the tall red mangrove on the right side from the dwarf red mangrove on the left. This particular pattern was common along the channels and may result from the geomorphological characteristics of the system. The mixing regime of these frequently flushed sites may change depending on the tide and the slope of the adjacent banks (Bertrand 1999, Anthony 2004). As a consequence, one side of the tidal channel is at higher elevation with little tidal flushing (dwarf areas) as compared to the tall red mangrove that developed well in low sloped high tidal influenced areas (Kovacs et al. 2010). Figure 5.11 c shows a fringe of dwarf red mangrove along the saltpan with tall red mangrove in the distance. These red dwarf mangroves are typically found in relatively higher soil salinities. Figure 5.11 d again shows a sharp zonation pattern. In this case, black mangrove is at a higher elevation near the saltpan with the tall healthy red mangrove adjacent at a lower elevation.

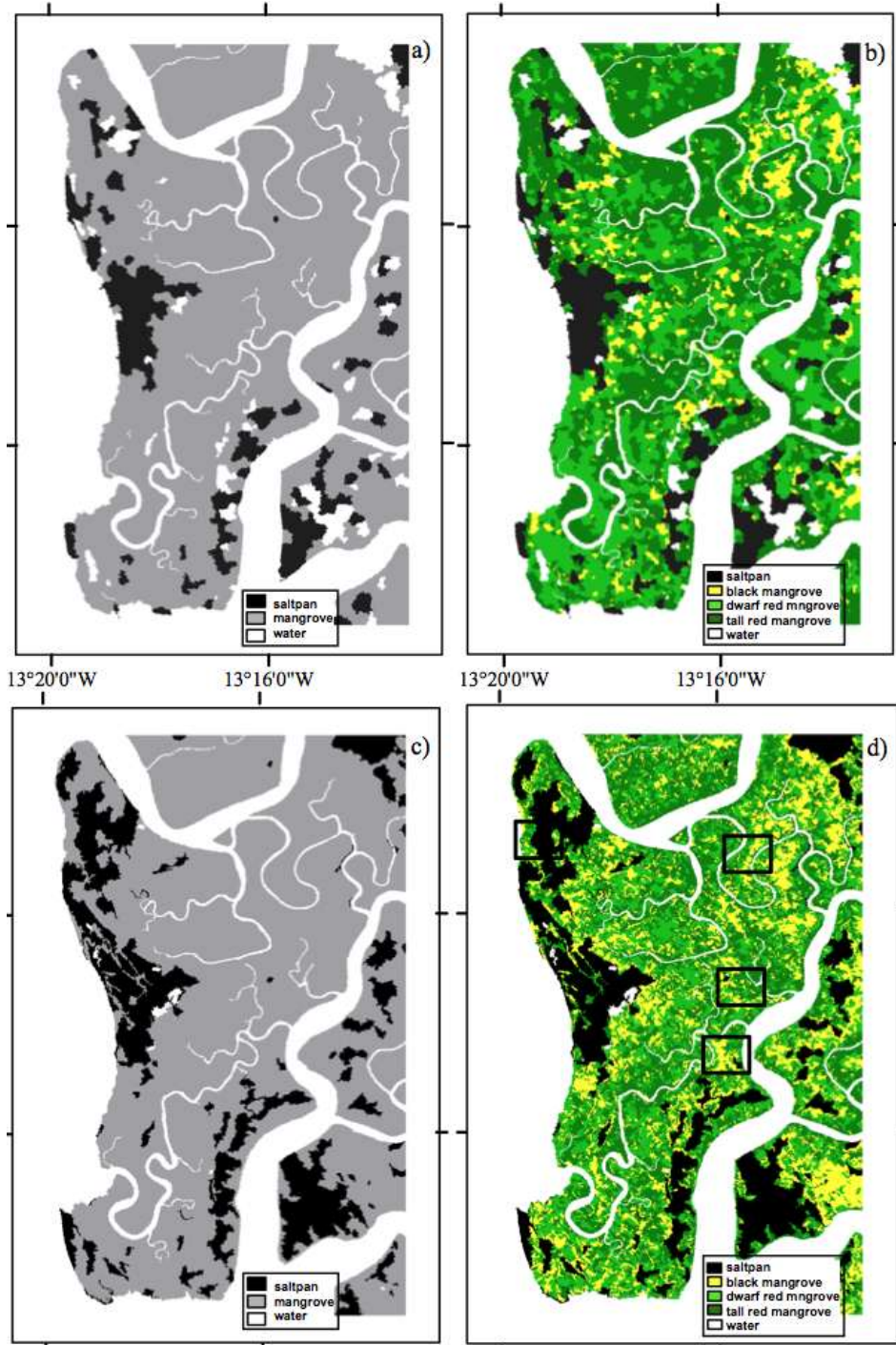


Figure 5.10: Object-based classification of L-band ALOS PALSAR. HH level 1 segmentation scale of 40 (a); HH level 2 segmentation scale of 10 (b); HH+HV level 1 segmentation scale of 20 using a 3x3 Lee filter (c); HH+HV level 2 segmentation scale of 5 using a 3x3 Lee filter. Black rectangles represent locations for figure 5.11

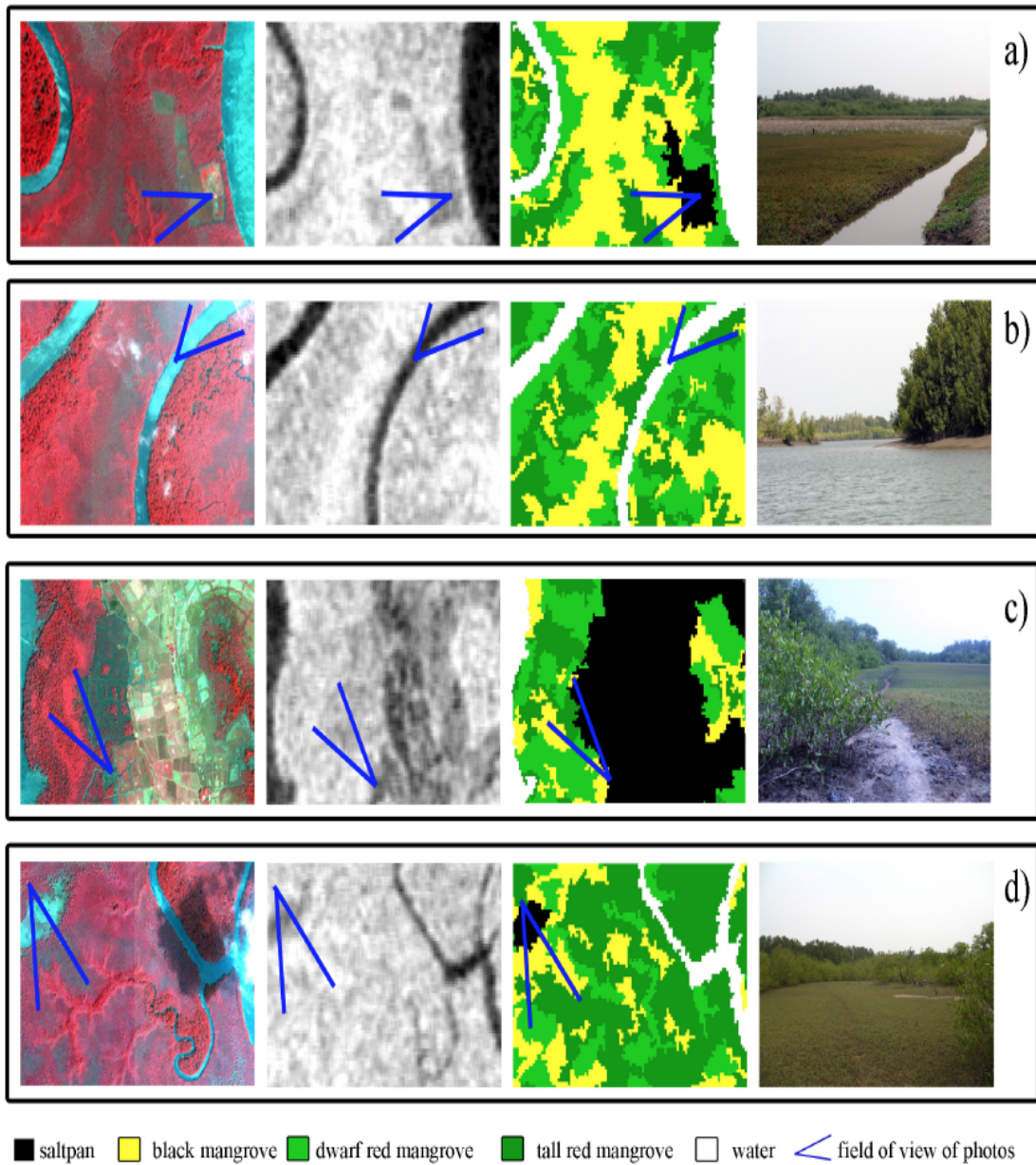


Figure 5.11: Examples of mangrove species mapping using a HH+HV ALOS PALSAR data object-based classification with a 3x3 Lee filter. From left to right: enhanced false color IKONOS composite (NIR, R, G); original ALOS HH+HV data; Object-oriented classification; Field photograph

5.4 Conclusions

The results of this investigation indicate that a multiresolution segmentation and object-based classification approach to ALOS PALSAR L-band SAR data can be used to provide an accurate assessment of mangrove forests. Both the single polarized (HH) and dual polarized (HH+HV) data were shown to be useful in separating mangrove from non-mangrove areas using a rule-based process. At this level, the overall accuracy assessments for the single and dual polarized scenes were quite high at 91.1% and 92.3%, respectively. At the second level of classification, the overall accuracy was highest for the HH+HV data but major problems remained in separating the three mangrove classes. The accuracy assessments for the three mangrove classes were much lower with the highest overall accuracy being 64.9% for a 3x3 Lee filter applied to the dual polarized scene at a multiresolution scale of 5 and a shape/color ratio of 0.1/0.9. Depending on the mangrove species present, their zonation pattern, and the surrounding land use, it is suggested that including relations to object features such as shape area or object length may improve classification using these SAR data. For example, in other regions of the world where the primary agriculture activity adjacent to the mangroves may be coconut plantations, rather than rice patties as in Guinea, considerable confusion may occur in regards to the amount of backscatter relative to the surrounding mangroves. In such cases, object asymmetry, for example, may help separate the mangrove trees from the coconut trees. As for the type of mangrove forests examined, it is suggested that the results of this study would be most applicable to estuarine mangrove forests of western Africa and the Americas where similar species (e.g. *A. germinans*, *R. mangle*, *R. racemosa*, *R. harisonii*) and a similar low number of mangrove species can be found.

5.5 References

- Anthon, E. J. (2004). Sediment dynamics and morphological stability of estuarine mangrove swamps in Sherbro Bay, West Africa. *Marine Geology*, 208, 207-224.
- Blaschke, T., and Hay, G. (2001). Object-oriented image analysis and scale-space: theory and methods for modeling and evaluating multi-scale landscape structure. *International Archives in Photogrammetry Remote Sensing*, 34, 22-29.
- Bertrand, F. (1999). Mangrove dynamics in the Rivières du Sud area, West Africa: an ecogeographic approach. *Hydrobiologia*, 413, 115-126.
- Congalton, R., and Green, K. (1999). *Assessing the accuracy of remotely sensed data: principles and practices*. Florida: CRC/LEWIS Press.

- Courtin, F., Jambonneau, V., Camara, M., Camara, O., Coulibaly, B., and others. (2010). A geographical approach to identify sleeping sickness risk factors in a mangrove ecosystem. *Tropical Medicine International Health*, 15(8), 881-889.
- Definiens. (2008). Developer 7 user guide. Germany: Definiens AG.
- Dingle, R. L., and King, D. J. (2011). Comparison of pixel- and object-based classification in land cover change mapping. *International Journal of Remote Sensing*, 32(6), 1505-1529.
- FAO. (2007). *The world's mangroves 1980-2005*. In FAO Forestry Paper 153, Food and Agricultural Organization, 77.
- Frost, V. S., Stiles, J. A., Shanmugan, K. S., and Holtzman, J. C. (1982). A model for radar images and its application to adaptive digital filtering of multiplicative noise. *IEEE Transactions on Pattern Analysis and Machine Intelligence*, 4(2), 157-166.
- Gagnon, L., and Jouan, A. (1997). Speckle filtering of SAR images – A comparative study between complex-wavelength-based and standard filters. *Proceedings of SPIE*, San Diego.
- Green, E. P., Mumby, P. J., Alasdair, E. J., Clark, C. D., and Ellis, A. C. (1997). Estimating leaf area index of mangroves from satellite data. *Aquatic Botany*, 58, 11-19.
- Green, E. P., Clark, C. D., Mumby, P. J., Edwards, A. J., and Ellis, A. C. (1998). Remote sensing techniques for mangrove mapping. *International Journal of Remote Sensing*, 19, 935-956.
- Hay, G. J., and Castilla, G. (2008). Geographic Object-Based Image Analysis (GEOBIA): A new name for a new discipline. In: *Lecture Notes in Geoinformation and Cartography*. 75-89.
- Herold, M., and Scepan, J. (2002). Object-oriented mapping and analysis of urban land use/cover using IKONOS data. In: *Proceedings of 22nd EARSEL symposium geoinformation for European-wide integration*, Prague.
- Hess, L. L., Melack, J. M., and Simonett, D. S. (1990). Radar detection of flooding beneath the forest canopy: a review. *International Journal of Remote Sensing*, 11, 1313-1325.
- Heumann, B. W. (2011). Satellite remote sensing of mangrove forests: recent advances and future opportunities. *Progress in Physical Geography*, 35(1), 87-108.
- Jensen, J. R. (2005). *Introductory digital image processing a remote sensing perspective*. New York: Pearson Prentice Hall.
- Kasisi, R. (2002). Volume 1: National strategy for conservation regarding biological diversity and the sustainable use of these resources. In: National strategy and action plan for biological diversity, Ministry of mines geology and the environment: 64.
- Kim, M., Madden, M., and Warner, T. (2008). Estimation of optimal image object size for the segmentation of forest stands with multispectral IKONOS imagery. In: Blaschke, T., LANG, S. and HAY, G.J., (2008). *Object-based image analysis. Spatial concepts or knowledge-driven remote sensing applications*. Lecture notes in Geoinformation and cartography.

- Kovacs, J. M., Flores-Verdugo, F., Wang, J., Aspen, L. P. (2004). Estimating leaf area index of a degraded mangrove forest using high spatial resolution satellite data. *Aquatic Botany*, 80, 13-22.
- Kovacs, J. M., Wang, J., and Flores-Verdugo, F. (2005). Mapping mangrove leaf area index at the species level using IKONOS and LAI-2000 sensors for the Agua Brava Lagoon, Mexican Pacific. *Estuarine, Coastal and Shelf Science*, 62, 377-384.
- Kovacs, J. M., Vandenberg, C. V., Flores-Verdugo, F. (2006). Assessing fine beam RADARSAT-1 backscatter from a white mangrove (*Laguncularia racemosa* (Gaertner)) canopy. *Wetlands, Ecology and Management*, 14, 401-408.
- Kovacs, J. M., Zhang, C., and Flores-Verdugo, F. (2008a). Mapping the condition of mangroves of the Mexican Pacific using C-band ENVISAT ASAR and Landsat optical data. *Ciencias Marinas*, 34, 407-418.
- Kovacs, J. M., Vandenberg, C. V., Wang, J., and Flores-Verdugo, F. (2008b). The use of multipolarized spaceborne SAR backscatter for monitoring the health of a degraded mangrove forest. *Journal of Coastal Research*, 24, 248-254.
- Kovacs, J. M., King, J. M. L., Flores-de-Santiago, F., and Flores-Verdugo, F. (2009). Evaluating the condition of a mangrove forest of the Mexican Pacific based on an estimated leaf area index mapping approach. *Environmental Monitoring and Assessment*, 157, 137-149.
- Kovacs, J. M., Flores-de-Santiago, F., Bastien, J., and Lafrance, P. (2010). An assessment of mangroves in Guinea, West Africa, using a field and remote sensing based approach. *Wetlands*, 30, 773-782.
- Krause, G., Bock, M., Weiers, S., and Braun, G. (2004). Mapping land-cover and mangrove structures with remote sensing techniques: A contribution to a synoptic GIS in support of coastal management in North Brazil. *Environmental Management*, 34, 429-440.
- Kuan, D. T., Sawchuk, A. A., Strand, T. C., and Chavel, P. (1985). Adaptive noise smoothing filter for images with signal-dependent noise. *IEEE Transactions on Pattern Analysis and Machine Intelligence*, 7(2), 165-177.
- Laliberte, A. S., Rango, A., Havstad, K. M., Paris, J. F., Beck, R. F., and others. (2004). Object-oriented image analysis for mapping shrub encroachment from 1937 to 2003 in southern New Mexico. *Remote Sensing of Environment*, 93, 198-210.
- Lewinski, S., and Zaremski, K. (2004). Examples of object-oriented classification performed on high-resolution satellite images. *Miscellanea Geographical*, 11, 349-358.
- Lillesand, T. M., Kiefer, R. W., and Chapman, J. W. (2008). *Remote Sensing and Image Interpretation*. New York: John Wiley & Sons, Inc.
- Lopes, A., Touzi, R., Nezry, E. (1990). Adaptive speckle filters and scene heterogeneity. *IEEE Transactions on Geoscience and Remote Sensing*, 28(6), 992-1000.
- Lucas, R. M., Cronin, N., Lee, A., Witte, C., and Moghaddam, M. (2006). Empirical relationships between AIRSAR backscatter and LiDAR-derived forest biomass, Queensland, Australia. *Remote Sensing of Environment*, 100, 388-406.
- Lucas, R. M., Mitchell, A. L., Rosenqvist, A., Proisy, C., Melius, A., and Ticehurst, C. (2007). The potential of L-band SAR for quantifying mangrove characteristics

- and change: case studies from the tropics. *Aquatic Conservation Marine and Freshwater Ecosystems*, 17, 245–264.
- Manson, F. J., Loneragan, N. R., McLeod, I. M., Kenyon, R. A. (2001). Assessing techniques for estimating the extent of mangroves: Topographic maps, aerial photographs and Landsat TM images. *Marine Freshwater Research*, 52, 787–792.
- Mougin, E., Proisy, C., Marty, G., Fromard, F., Puig, H., Betoulle, J. L., Rudant, J. P. (1999). Multifrequency and multipolarisation radar backscattering from mangrove forests. *IEEE Transactions Geosciences Remote Sensing*, 37, 94–102.
- Neukermans, G., Dahdouh-Guebas, F., Kairo, J. G., and Koedam, N. (2008). Mangrove species and stand mapping in Gazi bay (Kenya) using Quickbird satellite imagery. *Journal of Spatial Sciences*, 53, 75–86.
- NOAA. (2011). Tide Tables: Europe and West Coast of Africa. 220. USA: North Wind Publishing.
- Ramsey, E., and Jensen, J. R. (1996). Remote sensing of mangrove wetlands: relating canopy spectra to site specific data. *Photogrammetric Engineering Remote Sensing*, 62, 939-948.
- Rosenqvist, A., Shimada, M., Chapman, B., Freeman, A., De Grandi, G., Saatchi, S., and Rauste, Y. (2000). The Global Rain Forest Mapping project: a review. *International Journal of Remote Sensing*, 21, 1375–1387.
- Shi, Z., and Fung, K. B. (1994). A comparison of digital speckle filters. *Proceedings of IGRASS*, 94, 2129-2133.
- Souza-Filho, P. W. M., and Paradella, W. R. (2003). Use of synthetic aperture radar for recognition of Coastal Geomorphological Features, land-use assessment and shoreline changes in Braganca coast, Para, Northern Brazil. *Anais da Academia Brasileira de Ciencias*, 75, 341–356.
- Thiel, C., Thiel, C., Riedel, T., and Schullius, C. (2008). Object-based classification of SAR data for the delineation of forest cover maps and the detection of deforestation – a viable procedure and its application in GSE Forest Monitoring. In: Blaschke, T., Lang, S., and Hay, G. J. (2008). *Object-based image analysis. Spatial concepts or knowledge-driven remote sensing applications. Lecture notes in Geoinformation and cartography*.
- Ulaby, F. T., Moore, R. K., and Fung, A. K. (1986). Volume scattering and emission theory, advanced systems and applications. In: *Microwave remote sensing: active and passive*. Dedham: Artech House, Inc.
- Wang, L., Sousa, W. P., and Gong, P. (2004a). Integration of object-based and pixel-based classification for mapping mangroves with IKONOS imagery. *International Journal of Remote Sensing*, 25, 5655-5668.
- Wang, L., Sousa-Filho, W. P., Gong, P., and Biging, G. S. (2004b). Comparison of IKONOS and QuickBird images for mapping mangrove species on the Caribbean coast of Panama. *Remote Sensing of Environment*, 91, 432–440.
- Wilkie, M. L., and Fortuna, S. (2003). *Status and Trends in Mangrove Area Extent Worldwide*. Available online at: <http://www.fao.org/docrep/007/j1533e/j1533e00.HTM> accessed April 20, 2009.

Chapter 6

6 Discussion and Conclusions

6.1 Summary and general discussion

Mangrove forests provide direct and indirect ecological support for many terrestrial and aquatic species in the tropics and sub-tropics (Cannicci et al. 2008). They are considered one of the most important ecosystems for carbon balance, input of nutrients to the ocean, and as a support for fisheries and local communities (Komiya et al. 2008; Nagelkerken et al. 2008; Walters et al. 2008). Despite their major ecologic and economic importance, it is recognized that mangrove forests are under considerable degradation because of hydrological changes and anthropogenic impacts (Polidoro et al. 2010). Due to the alarming worldwide loss of mangrove areas, biophysical information at leaf and canopy level is critically needed for monitoring environmental changes. Results from my investigation provide key elements and methodology for future research including seasonal environmental assessment, carbon balance models, primary productivity estimation, and remote sensing assessments over inaccessible large areas using hyperspectral and SAR data.

Many authors have studied large areas of mangrove forests, however only a few used *in situ* biophysical variables and non-optical data, such as SAR, for monitoring species of mangrove under conditions of stress. Furthermore, prior to this study no research has been conducted on assessing seasonal variability on leaf pigment content using absorbance and reflectance devices over different species of mangrove. Temporal variability regarding leaf pigment content was assessed using information from the end of the dry season, and the end of the rainy season in a sub-tropical mangrove forest of the Pacific coast of Mexico. Despite the fact that mangroves are considered an evergreen forest with a constant litter fall rate throughout the year (Arreola-Lizárraga et al. 2004), results from my investigation indicate that the lack of fresh water availability and the increase of soil salinity during the dry season affected leaf pigment content and hyperspectral reflectance.

Chapter 2 assessed the seasonality of leaf Chla content within three major mangrove species of the Americas. Results showed a marked seasonality among the poor/dwarf mangrove classes, presenting a significant increase in leaf Chla during the rainy season in all three species. It is important to mention that the poor/dwarf classes were located away from the main channel with no apparent tidal circulation and were close to the drier saltpan area. On the contrary, the healthy stands located along the fringe of the main tidal channel did not present change in Chla content between the dry and rainy seasons. These results from Chapter 2 have particular importance in monitoring seasonal development of mangrove species and conditions in a mixed sub-tropical environment. The observed differences between the seasons would indicate a clear pattern that basin mangroves from the sub-tropics of Mexico depend primarily on fresh water availability. Consequently, knowing the seasonal changes in pigments would allow future remote sensing studies to identify the optimal time to acquire imagery for accurate biomass or LAI mapping and monitoring.

There has been recent interest in using quick and relatively non-expensive devices to monitor leaf pigments in the field (Biber 2007). Absorbance instruments such as the CCM-200 measure the beam of light that pass through the leaf in a close chamber (Opti-Sciences 2002). On the other hand, reflectance devices such as the ASD field Handheld spectrometer measure the reflected energy from the leaf in many consecutive wavelengths. Results from Chapters 3 and 4 showed a significant linear association between the CCI from the CCM-200, and the 14 vegetation indices from the ASD field HandHeld unit for the accurate estimation of Chla in mangrove leaves. Although both units are reliable for Chla quantification, differences between the two units are evident in the field. The CCM-200 is much easier to use and carry, while the ASD FieldSpec HandHeld unit requires external batteries, a fiber optic wire to attach the plant probe unit, and in some cases a laptop computer, making data acquisition extremely difficult in any mangrove environment. However, the information provided by the CCM-200 could not be used at canopy level. On the contrary, the hyperspectral data from the ASD spectrometer could be applied to airborne or spaceborne hyperspectral sensors in mangrove ecology. The principal objective of Chapter 4 was to use hyperspectral data from the ASD FieldSpec HandHeld spectrometer to assess the estimation accuracy of

Chla during two seasons (dry and rainy). Results from this chapter are of utmost importance for future remote sensing applications such as mapping of mangrove areas using seasonal information from spaceborne or airborne optical sensors in large areas of mangrove forests.

Multi-polarized SAR data are becoming more available for tropical areas where the persistent cloud cover is a major problem for optical data (Heumann 2011). However, most current SAR satellite sensors do not provide full polarized data. One alternative to improve the analysis of SAR data consists of processing the single and dual polarized sets of data using OBIA. However, little research has been conducted on mangrove forest classification using both sets of polarized images. A single (HH) and a dual (HH+HV) polarized imagery from the spaceborne ALOS PALSAR L-band data were acquired for the same area of Guinea, Africa in order to assess the most optimal set of data for mangrove classification at species level using OBIA. A detailed decision rule-based procedure was developed in Chapter 5 to incorporate OBIA to the SAR imagery over mangrove areas. In this study, color/shape ratios, scale parameters, and SAR filters were analyzed on the backscatter data and used in the object-based classification.

In Chapter 5, the determination of the optimal scale parameter during the segmentation process was a major problem for both sets of SAR data. However, the proposed processing procedure in Chapter 5 was based on multiple tests using the overall accuracy for each scale and the number of objects produced by the segmentation process. The results showed that it is possible to select an optimal scale for each level of segmentation based on a quantified category rather than a subjective scale randomly chosen by the researcher. Another problem presented in this study was the different spatial resolution scenes between the single (HH) and the dual (HH+HV) polarized imagery. The scales varied from image to image depending on the number of objects created by the segmentation process. The single polarized imagery with higher spatial resolution (6.25 m) was more difficult and less accurate (57%) compared to the dual polarized data when objects were separated from mangrove classes at level 2. The dual polarized scene with coarse spatial resolution (12.5 m) presented a more detailed object segmentation and accuracy at the same level 2 (65%) compared with the single polarized

scene. The results showed that the classification accuracies between the single and dual polarized scenes varied considerably. Moreover, the use of SAR filters did not improve the overall accuracy of the SAR classification. However, overall accuracies from the OBIA classification at level 1 (mangrove and non-mangrove) were high for both SAR scenes with 92% and 93% for the single and dual polarized scenes respectively. Consequently, the L-band from the single and dual polarized ALOS PALSAR sensor and the object-based classification provided a reliable assessment of mangrove and non-mangrove classification on nearly permanent cloudy region of the tropics.

It is important to note that this is the first study regarding mangrove classification using SAR data and OBIA. However, every mangrove environments depends on species composition and local environmental factors. As a consequence, the methodology applied in this study could be used in other tropical and sub-tropical latitudes, however calibration for the rule based classification have to be consider depending on the local mangrove species and classification scheme.

6.2 Conclusion

This thesis has developed and evaluated a number of useful techniques with the objective of improve ecological assessments of mangrove forests from the tropics and sub-tropics. Using multiple *in situ* approaches based on multivariate statistics analysis, the overall assessment of seasonal mangrove forests pigments and biophysical variables were possible for sub-tropical environments. Although the results from the SAR classification were not performed for the same sub-tropical area, OBIA showed potential application for mangrove forests mapping for study areas where optical data are not available. In general, this research demonstrated the successful application of optical *in situ* data for future mapping of mangrove areas using hyperspectral spaceborne sensors. However, OBIA classification using SAR data over mangrove areas is still largely affected by the spatial resolution and object backscatter variability.

The seasonal analysis of leaf pigments in this thesis showed that Chla content variability in sub-tropical basin mangroves depends on the fresh water availability during the rainy season. On the contrary, fringe red and black mangroves were not affected by

seasonality in leaf Chla content. However, the estimation of leaf pigments using CCI and hyperspectral spectrometer varied considerably between the seasons. As a result, rapid devices such as the CCM-200 unit could be used for Chla content estimation in sub-tropical mangroves. However, Chlb was not possible to estimate in most of the mangrove classes. The preprocessing PCA method for a large number of VI during the hyperspectral estimation of seasonal Chla content proved to be of utmost importance for the accurate and fast separation of those VI that presented a significant co-variability with Chla. Interestingly, the VI that presented the optimal mangrove leaf Chla estimation for sub-tropical environment was the Vogelmann Index (R_{740}/R_{720}) during the dry season. Mapping mangrove areas of the tropics of Guinea using SAR data at species level were not as high as expected using an OBIA process. However, the separation of mangrove and non-mangrove areas was quite high using the HH (92%) and HH+HV (93%) data. Although results from the ALOS L-band classification of mangrove areas at level 2 presented low accuracies, this thesis is the first to provide a detailed method for decision rule-based classification of mangrove forests using information from SAR data.

6.3 Future directions

Based on the results of this thesis it is suggested that frequent on-going data acquisitions of both biophysical and biochemical variables are necessary for effective ecological assessments and monitoring of mangroves. Future research could include a more detailed assessment of the inter-annual variability of mangrove leaf Chla content in tropical and sub-tropical environments. The results from such a study could help in determining whether the rainy season alone affects the observed increase in leaf Chla content over an entire year. Although the CCM-200 unit was shown to be a good predictor of mangrove Chla content, the feasibility of using such unit in other mangrove areas of the tropics and sub-tropics remains unanswered. Consequently, it is suggested that the unit be assessed for other species of mangrove that are more common to other regions of the world.

The results from the Chla content estimation using close-range hyperspectral data could also be tested at the canopy level using information derived from airborne or spaceborne data (e.g. Hyperion). However, the results from this chapter of my thesis were

based on a pooled sample of mangrove hyperspectral data. As a consequence, the inter-species hyperspectral variability may also be worth investigating in order to determine to which degree each mangrove species and condition (fringe/basin) can affect the Chla content estimations. Moreover, future assessments of the inter-species hyperspectral signature separability would be of utmost importance for ascertaining the optimal bands for future mapping of mangrove areas at species level from airborne or spaceborne hyperspectral data.

Finally, it is suggested that the SAR classification of mangrove areas should be examined using information derived from the grey-level co-occurrence matrix (GLCM). When possible, higher spatial resolution data from SAR sensors such as RADARSAT-2 or the yet to be launched ALOS-2 could be an option for improving the biophysical estimation and mapping of mangrove areas using an OBIA classification.

6.4 References

- Arreola-Lizárraga, J. A., Flores-Verdugo, F., and Ortega-Rubio, A. (2004). Structure and litterfall of an arid mangrove stand on the Gulf of California, Mexico. *Aquatic Botany*, 79, 137-143.
- Biber, P. D. (2007). Evaluating a chlorophyll content meter on three coastal wetland plant species. *Agriculture Food Environment Sciences*, 1(2), 1-11.
- Cannicci, S., Burrows, D., Fratini, S., Smith, T. J. III., Offenber, J., and Dahdouh-Guebas, F. (2008). Faunal impact on vegetation structure and ecosystem function in mangrove forests: a review. *Aquatic Botany*, 89, 186–200.
- Heumann, B. W. (2011). Satellite remote sensing of mangrove forests: recent advances and future opportunities. *Progress Physical Geography*, 35(1), 87-108.
- Komiyama, A., Eong, O. J., and Pongpan, S. (2008). Allometry, biomass, and productivity of mangrove forest: a review. *Aquatic Botany*, 89, 128–137.
- Nagelkerken, I., Blaber, S. J. M., Bouillon, S., Green, P., and others. (2008). The habitat function of mangrove for terrestrial and marine fauna: a review. *Aquatic Botany*, 89, 155–185.
- Opti-Sciences. (2002). CCM-200 Chlorophyll Content Meter. Available online at www.optisciences.com
- Peñuelas, J., and Fillela, I. (1998). Visible and near-infrared reflectance techniques for diagnosing plant physiological status. *Trends in Plant Sciences*, 3, 151-156.
- Polidoro, B. A., Carpenter, K. E., and others. (2010). The loss of species: Mangrove extinction risk and Geographic areas of global concern. *PLoS ONE*, 5(4), e10095.
- Walters, B. B., Rönnbäck, P., Kovacs, J. M., Crona, B., and others. (2008). Ethnobiology, socio-economics and management of mangrove forests: a review. *Aquatic Botany*, 89, 220–236.

Appendices

Appendix A: List of abbreviations

ANCOVA	Analysis of co-variance
ANOVA	Analysis of variance
CCI	Chlorophyll Content Index
CCM	Chlorophyll Content Meter
Chla	Chlorophyll-a
Chlb	Chlorophyll-b
FELEE	Enhanced Lee Speckle Filter
FFROST	Frost Adaptive Filter
FKUAN	Kuan Speckle Filter
FLE	Lee Speckle Filter
GNDVI	Green normalized difference vegetation index
LAI	Leaf Area Index
LCI	Leaf chlorophyll index
MCARI	Modified chlorophyll absorption ratio index
MMSE	Minimum Mean Square Error
MSR	Modified simple ratio
NDI	Normalized vegetation index
NDVI	Normalized difference vegetation index
NPCI	Normalized pigment chlorophyll ratio index
OBIA	Object-based Image Analysis
OSAVI	Optimized soil-adjusted vegetation index
PAR	Photosynthetically Active Radiation
PCA	Principal Component Analysis
PRI	Photochemical reflectance index
PSRI	Plant senescence reflectance index
PSSRa	Pigment specific simple ratio
RARSa	Ratio analysis of reflectance spectra
RDVI	Renormalized difference vegetation index
REIP	Red-edge inflection point
SAR	Synthetic Aperture Radar
SAVI	Soil adjusted vegetation index
SE	Standard Error
SIPI	Structural independent pigment index
SR	Simple ratio
TCARI	Transformed chlorophyll absorption ratio index
TChl	Total chlorophyll
TVI	Triangular vegetation index
VI	Vegetation Indices
Vogl	Vogelmann's Index

Appendix B: Permission letter from Marine Ecology Progress Series

Dear Francisco

You may include the paper Flores de Santiago et al. (2012) Mar Ecol Prog Ser 444:57–68 in your PhD thesis to be submitted to the University of Western Ontario, provided the original source of publication is clearly acknowledged at the start of the chapter or section.

With best wishes
Ian Stewart
Permissions Manager
Inter-Research

On 4 Apr 2013, at 17:09, Francisco Javier Flores De Santiago wrote:

Dear Editor-in-chief Otto Kinne, Marine Ecology Progress Series
I am a PhD student at the University of Western Ontario and the author of the manuscript entitled “Flores-de-Santiago F., Kovacs J.M., Flores-Verdugo F. (2012). Seasonal changes in leaf chlorophyll a content and morphology in a sub-tropical mangrove forest of the Mexican Pacific. Marine Ecology Progress Series 444: 57-68.
(<http://dx.doi.org/10.3354/meps09474>)”.

My thesis is “manuscript format” and the aforementioned article is part of one chapter. Therefore, I am wondering if I have permission to include the article as a thesis chapter?

Best regards
Francisco Flores de Santiago
PhD candidate
Department of Geography
University of Western Ontario

Ian Stewart
Production Manager – Marine Ecology Progress Series

Inter-Research Science Center

Appendix C: Permission letter from Bulletin of Marine Sciences

Dear Francisco,

The inclusion of the article as a dissertation chapter is permitted under BMS guidelines. Please make sure that in your inclusion the journal and reference is included. The Bulletin still owns the copyright to the published article so for other uses please check with us before proceeding.

Best,

--

Rafael J Araujo
Assistant Editor (Bulletin of Marine Science) and
Senior Research Associate (Division of Marine Biology and Fisheries)
Rosenstiel School of Marine & Atmospheric Science
University of Miami

From: Francisco Javier Flores De Santiago

Date: Thursday, April 4, 2013 11:13 AM

To: Rafael Araujo

Subject: Question about copyright

Dear Editor-in-chief Rafael J Araujo, Bulletin of Marine Science,
I am a PhD student at the University of Western Ontario and the author of the manuscript entitled "Flores-de-Santiago F., Kovacs J.M., Flores-Verdugo F. (2013). Assessing the utility of a portable pocket instrument for estimating seasonal mangrove leaf chlorophyll contents. Bulletin of Marine Science (<http://dx.doi.org/10.5343/bms.2012.1032>)".
My thesis is "manuscript format" and the aforementioned article is part of one chapter. Therefore, I am wondering if I have permission to include the article as a thesis chapter?

Best regards

Francisco Flores de Santiago
PhD candidate
Department of Geography
University of Western Ontario

Appendix D: Permission letter from Wetlands, Ecology and Management

Dear Dr. Flores de Santiago,

Please open your accepted paper in www.springer.com and you can find an option "Reprints and Permissions" in the right pane. Please use the same for obtaining the appropriate permission.

Thank you very much.
Best regards,
Gayathri

Gayathri Balasubramanian
Springer
Journals Editorial Office (JEO)
JEO Assistant

From: Francisco Javier Flores De Santiago
Sent: 04 April 2013 20:45:37
To: Balasubramanian, Gayathri
Subject: Question about copyright

Dear Editor-in-chief E Wolanski, Wetlands, Ecology and Management,
I am a PhD student at the University of Western Ontario and the author of the manuscript entitled "Flores-de-Santiago F., Kovacs J.M., Flores-Verdugo F. (in press). The influence of seasonality in estimating mangrove leaf chlorophyll-a content from hyperspectral data. Wetland, Ecology and Management. (<http://dx.doi.org/10.1007/s11273-013-9290-x>)".
WETL-D-12-00756R1

My thesis is "manuscript format" and the aforementioned article is part of one chapter. Therefore, I am wondering if I have permission to include the article as a thesis chapter?

Best regards

Francisco Flores de Santiago
PhD candidate
Department of Geography
University of Western Ontario

RightsLink



Thank You For Your Order!

Dear Mr. Francisco Flores,

Thank you for placing your order through Copyright Clearance Center's RightsLink service. Springer has partnered with RightsLink to license its content. This notice is a confirmation that your order was successful.

Your order details and publisher terms and conditions are available by clicking the link below:
<http://s100.copyright.com/CustomerAdmin/PLF.jsp?ref=1843a818-66bd-4366-afc3-f823fdb01754>

Order Details

Licensee: Francisco Flores

License Date: Apr 18, 2013

License Number: 3132000221704

Publication: Wetlands Ecology and Management

Title: The influence of seasonality in estimating mangrove leaf chlorophyll-a content from hyperspectral data

Type Of Use: Thesis/Dissertation

Total: 0.00 CAD

To access your account, please visit <https://myaccount.copyright.com>.

Please note: Online payments are charged immediately after order confirmation; invoices are issued daily and are payable immediately upon receipt.

To ensure we are continuously improving our services, please take a moment to complete our [customer satisfaction survey](#).

B.1:v4.2

[+1-877-622-5543](tel:+18776225543) / Tel: [+1-978-646-2777](tel:+19786462777)
customercare@copyright.com
<http://www.copyright.com>



Appendix E: Permission letter from International Journal of Remote Sensing

Dear Francisco,

That's fine, do go ahead. You will simply need to add an acknowledgement and full reference to the paper as a footnote to the relevant section of your thesis.

Best wishes,

Louise

From: Francisco Javier Flores De Santiago

Sent: 22 April 2013 23:02

To: Glenn, Louise

Subject: IJRS copyright

Dear Louise Gleen, Managing Editor, International Journal of Remote Sensing, I am a PhD student at the University of Western Ontario and the author of the manuscript entitled "Flores-de-Santiago F., Kovacs J.M., Lafrance P. (2013). An object-oriented classification method for mapping mangroves in Guinea, West Africa, using multipolarized ALOS PALSAR L-band data. International Journal of Remote Sensing 34(2), 563-586. (<http://dx.doi.org/10.1080/01431161.2012.715773>)".

My thesis is "manuscript format" and the aforementioned article is part of one chapter. Therefore, I am wondering if I have permission to include the article as a thesis chapter?

Best regards

Francisco Flores de Santiago
PhD candidate
Department of Geography
University of Western Ontario

Curriculum Vitae

Name: Francisco Javier Flores de Santiago

Post-secondary Education and Degrees: Universidad Autónoma de Baja California
Facultad de Ciencias Marinas
Ensenada, Baja California, Mexico
2000-2005 B.Sc. Oceanography.

Universidad Autónoma de Baja California
Facultad de Ciencias Marinas
Ensenada, Baja California, Mexico
2005-2007 M.Sc. Coastal Oceanography.

The University of Western Ontario
London, Ontario, Canada
2009-2013 Ph.D. Geography

Publications:

- Kovacs J.M., Jiao X., **Flores-de-Santiago F.**, Zhang C., Flores-Verdugo F. (*in press*). Assessing relationships between Radarsat-2 C-band and structural parameters of a degraded mangrove forest. *International Journal of Remote Sensing* 34(20), 7003-7020. (<http://dx.doi.org/10.1080/01431161.2013.813090>).
- Kovacs J.M., Lu X.X., Flores-Verdugo F., Zhang C., **Flores-de-Santiago F.**, Jiao X. (2013). Applications of ALOS PALSAR for monitoring biophysical parameters of a degraded black mangrove (*Avicennia germinans*) forest. *ISPRS Journal of Photogrammetry and Remote Sensing* 82, 102-111. (<http://dx.doi.org/10.1016/j.isprsjprs.2013.05.004>)
- Flores-de-Santiago F.**, Kovacs J.M., Flores-Verdugo F. (2013). The influence of seasonality in estimating mangrove leaf chlorophyll-a content from hyperspectral data. *Wetlands, Ecology and Management* 21(3), 193-207 (<http://dx.doi.org/10.1007/s11273-013-9290-x>).
- Flores-de-Santiago F.**, Kovacs J.M., Lafrance P. (2013). An object-oriented classification method for mapping mangroves in Guinea, West Africa, using multipolarized ALOS PALSAR L-band data. *International Journal of Remote Sensing* 34(2), 563-586 (<http://dx.doi.org/10.1080/01431161.2012.715773>).
- Flores-de-Santiago F.**, Kovacs J.M., Flores-Verdugo F. (2013). Assessing the utility of a portable pocket instrument for estimating seasonal mangrove leaf chlorophyll contents. *Bulletin of Marine Science* 89(2), 621-633. (<http://dx.doi.org/10.5343/bms.2012.1032>).
- Flores-de-Santiago F.**, Kovacs J.M., Flores-Verdugo F. (2012). Seasonal changes in leaf chlorophyll a content and morphology in a sub-tropical mangrove forest of the Mexican Pacific. *Marine Ecology Progress Series* 444, 57-68. (<http://dx.doi.org/10.3354/meps09474>).
- Zhang C., Liu Y., Kovacs J.M., Flores-Verdugo F., **Flores-de-Santiago F.**, Chen K. (2012). Spectral response to varying levels of leaf pigments collected from a degraded mangrove forest. *Journal of Applied Remote Sensing* 6(1), 063501. (<http://dx.doi.org/10.1117/1.JRS.6.063501>).

- Kovacs J.M., Liu Y., Zhang C., Flores-Verdugo F., **Flores-de-Santiago F.** (2011). A field based statistical approach for validating a remotely sensed mangrove forest classification scheme of Isla La Palma, Sinaloa, Mexico. *Wetlands, Ecology and Management* 19, 409-421. (<http://dx.doi.org/10.1007/s11273-011-9225-3>).
- Kovacs J.M., **Flores-de-Santiago F.**, Bastien J., Lafrance P. (2010). An assessment of mangroves in Guinea, West Africa, using a field and remote sensing based approach. *Wetlands* 30, 773-782. (<http://dx.doi.org/10.1007/s13157-010-0065-3>).
- Kovacs, J.M., King, J.M.L., **Flores-de-Santiago, F.**, Flores-Verdugo F. (2009). Evaluating the condition of a mangrove forest of the Mexican Pacific based on an estimated leaf area index mapping approach. *Environmental Monitoring and Assessment* 157, 137-149. (<http://dx.doi.org/10.1007/s10661-008-0523-z>).
- Flores-de-Santiago, F.**, Santamaría-del-Ángel, E., González-Silvera, A., Martínez-Díaz-de-León, A., Millán-Núñez, R., and Kovacs J.M. (2007). Assessing dynamic micro-regions in the Great Islands of the Gulf of California based on MODIS aqua imagery products. *Proceedings of the Society of Photo-Optical Instrumentation Engineers*. Vol. 6680, 668010 (<http://dx.doi.org/10.1117/12.732574>).